January / February 2024
Volume 53, Number 1

Applied Radiology

Applied Radiology®

YEARS

The Journal of Practical Medical Imaging and Management

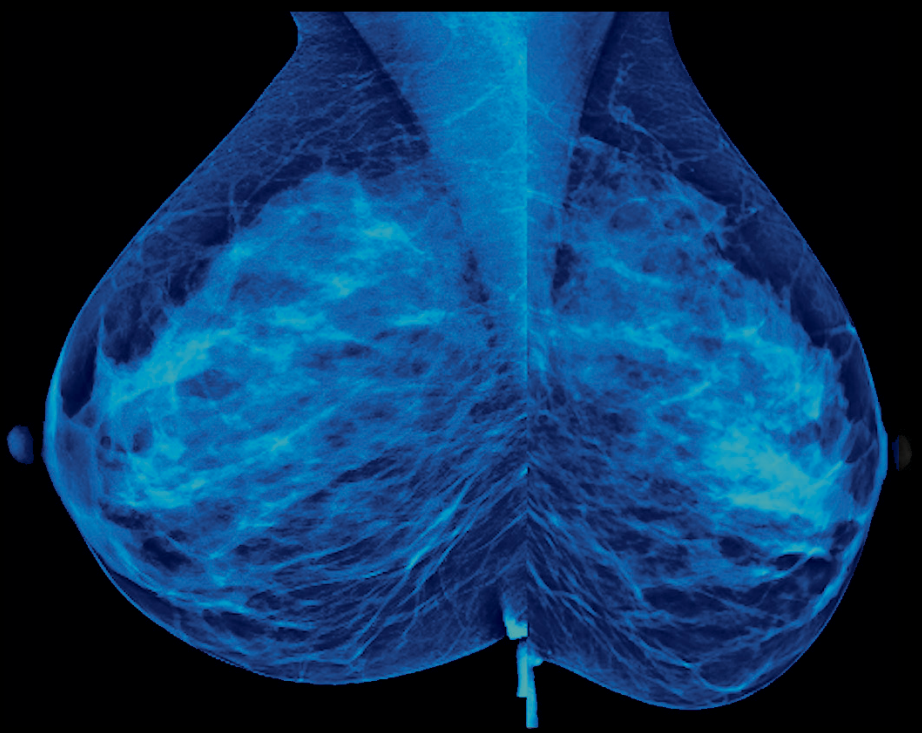

CME Next Top Model: An Overview of Breast Cancer Risk Assessment Models

Extracorporeal Membrane Oxygenation

Minimizing the Pain of Local Anesthetic Injection

AI's Diversity Problem in Radiology

The Compounded Value of AI Beyond Radiology

January / February 2024 Volume 53, Number 1

www.appliedradiology.com

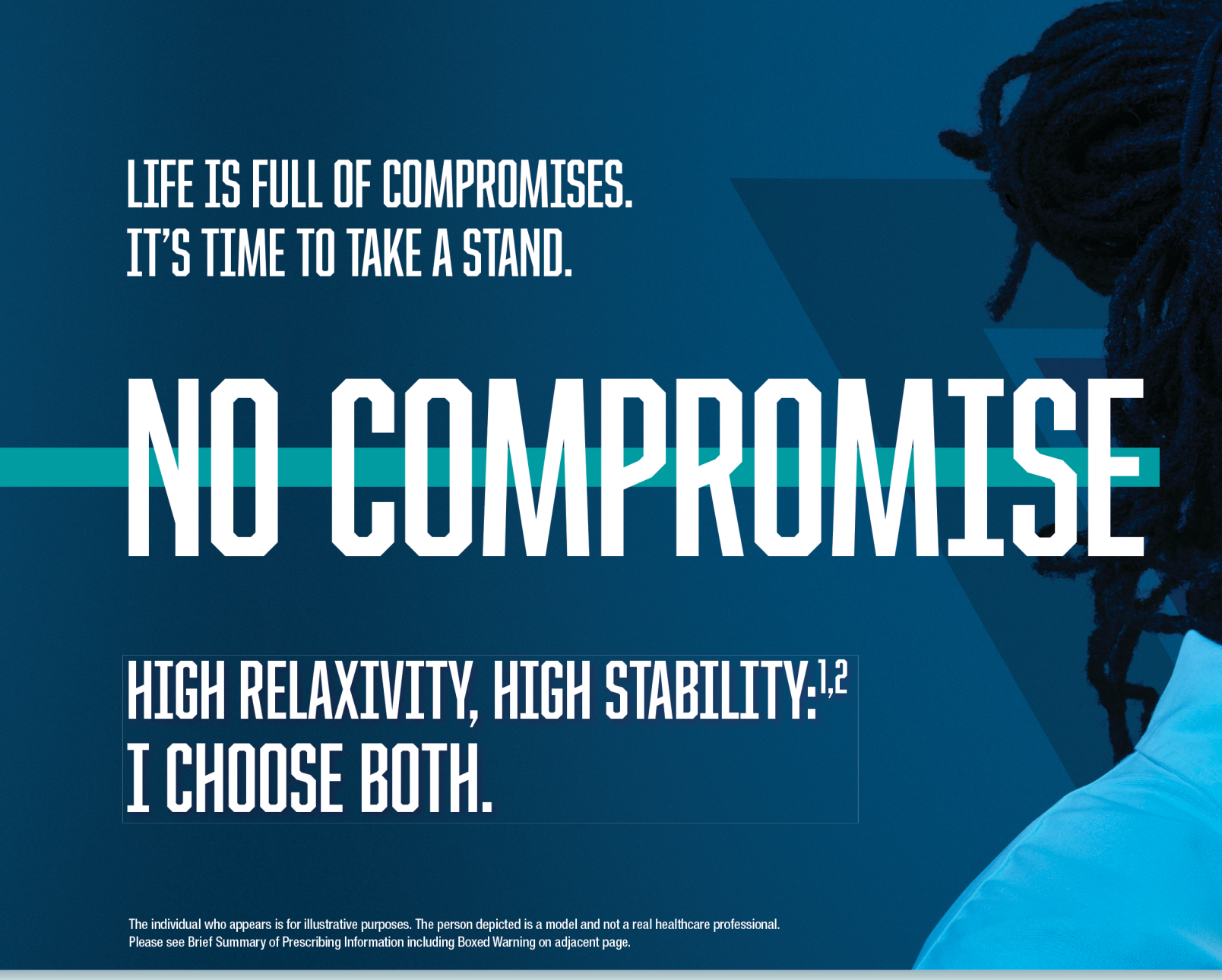

LIFE IS FULL OF COMPROMISES. IT'S TIME TO TAKE A STAND.

NO COMPROMISE

HIGH RELAXIVITY, HIGH STABILITY:[1,2] I CHOOSE BOTH.

The individual who appears is for illustrative purposes. The person depicted is a model and not a real healthcare professional.
Please see Brief Summary of Prescribing Information including Boxed Warning on adjacent page.

VUEWAY™ (gadopiclenol) solution for injection

Indications
VUEWAY injection is indicated in adults and children aged 2 years and older for use with magnetic resonance imaging (MRI) to detect and visualize lesions with abnormal vascularity in:

- the central nervous system (brain, spine and surrounding tissues),
- the body (head and neck, thorax, abdomen, pelvis, and musculoskeletal system).

IMPORTANT SAFETY INFORMATION

WARNING: NEPHROGENIC SYSTEMIC FIBROSIS (NSF)

Gadolinium-based contrast agents (GBCAs) increase the risk for NSF among patients with impaired elimination of the drugs. Avoid use of GBCAs in these patients unless the diagnostic information is essential and not available with non-contrasted MRI or other modalities. NSF may result in fatal or debilitating fibrosis affecting the skin, muscle and internal organs.

- **The risk for NSF appears highest among patients with:**
  - **Chronic, severe kidney disease (GFR <30 mL/min/1.73 m^2), or**
  - **Acute kidney injury.**
- **Screen patients for acute kidney injury and other conditions that may reduce renal function. For patients at risk for chronically reduced renal function (e.g. age >60 years, hypertension, diabetes), estimate the glomerular filtration rate (GFR) through laboratory testing.**
- **For patients at highest risk for NSF, do not exceed the recommended VUEWAY dose and allow a sufficient period of time for elimination of the drug from the body prior to any re-administration.**

Contraindications
VUEWAY injection is contraindicated in patients with history of hypersensitivity reactions to VUEWAY.

Warnings
Risk of **nephrogenic systemic fibrosis** is increased in patients using GBCA agents that have impaired elimination of the drugs, with the highest risk in patients chronic, severe kidney disease as well as patients with acute kidney injury. Avoid use of GBCAs among these patients unless the diagnostic information is essential and not available with non-contrast MRI or other modalities.

Hypersensitivity reactions, including serious hypersensitivity reactions, could occur during use or shortly following VUEWAY administration. Assess all patients for any history of a reaction to contrast media, bronchial asthma and/or allergic disorders, administer VUEWAY only in situations where trained personnel and therapies are promptly available for the treatment of hypersensitivity reactions, and observe patients for signs and symptoms of hypersensitivity reactions after administration.

INTRODUCING

Vueway™
(gadopiclenol) injection
485.1 mg/mL

HALF THE GADOLINIUM DOSE COMPARED TO OTHER MACROCYCLIC GBCAS IN APPROVED INDICATIONS.[1,3-6] FROM BRACCO, YOUR TRUSTED PARTNER IN MRI.

BRACCO
LIFE FROM INSIDE

Gadolinium retention can be for months or years in several organs after administration. The highest concentrations (nanomoles per gram of tissue) have been identified in the bone, followed by other organs (brain, skin, kidney, liver and spleen). Minimize repetitive GBCA imaging studies, particularly closely spaced studies, when possible.

Acute kidney injury requiring dialysis has occurred with the use of GBCAs in patients with chronically reduced renal function. The risk of acute kidney injury may increase with increasing dose of the contrast agent.

Ensure catheter and venous patency before injecting as **extravasation** may occur, and cause tissue irritation.

VUEWAY may **impair the visualization of lesions** seen on non-contrast MRI. Therefore, caution should be exercised when Vueway MRI scans are interpreted without a companion non-contrast MRI scan.

The most common adverse reactions (incidence ≥ 0.5%) are injection site pain (0.7%), and headache (0.7%).

You are encouraged to report negative side effects of prescription drugs to the FDA. Visit www.fda.gov/medwatch or call 1-800-FDA-1088.

Please see BRIEF SUMMARY of Prescribing Information for VUEWAY, including BOXED WARNING on Nephrogenic Systemic Fibrosis.

Manufactured for Bracco Diagnostics Inc. by Liebel-Flarsheim Company LLC - Raleigh, NC, USA 27616.

VUEWAY is a trademark of Bracco Imaging S.p.A.

References: 1. Vueway™ (gadopiclenol) Injection Full Prescribing Information. Monroe Twp., NJ: Bracco Diagnostics Inc.; September 2022. **2.** Robic C, Port M, Rousseaux O, et al. Physicochemical and Pharmacokinetic Profiles of Gadopiclenol: A New Macrocyclic Gadolinium Chelate With High T1 Relaxivity. *Invest Radiol.* 2019 Aug;54: 475–484. **3.** GADAVIST® (gadobutrol) Injection. Full Prescribing Information. Bayer HealthCare Pharmaceuticals Inc. Whippany, NJ; April 2022. **4.** DOTAREM® (gadoterate meglumine) Injection. Full Prescribing Information. Guerbet LLC. Princeton, NJ; April 2022. **5.** CLARISCAN™ (gadoterate meglumine) injection for intravenous use. Full Prescribing Information. GE Healthcare. Marlborough, MA; February 2020. **6.** ProHance® (Gadoteridol) Injection. Full Prescribing Information and Patient Medication Guide. Monroe Twp., NJ: Bracco Diagnostics Inc.; December 2020.

VISIT VUEWAY.COM FOR MORE INFORMATION

Bracco Diagnostics Inc.
259 Prospect Plains Road, Building H
Monroe Township, NJ 08831 USA
Phone: 609-514-2200
Toll Free: 1-877-272-2269 (U.S. only)
Fax: 609-514-2446

Bracco Diagnostics Inc.

LIFE FROM INSIDE

Vueway™

(gadopiclenol) injection, for intravenous use

BRIEF SUMMARY: Please see package insert of full prescribing information.

WARNING: NEPHROGENIC SYSTEMIC FIBROSIS (NSF)

Gadolinium-based contrast agents (GBCAs) increase the risk for NSF among patients with impaired elimination of the drugs. Avoid use of GBCAs in these patients unless the diagnostic information is essential and not available with non-contrasted MRI or other modalities. NSF may result in fatal or debilitating fibrosis affecting the skin, muscle and internal organs.

- **The risk for NSF appears highest among patients with:**
  - **Chronic, severe kidney disease (GFR <30 mL/min/1.73 m^2), or**
  - **Acute kidney injury.**
- **Screen patients for acute kidney injury and other conditions that may reduce renal function. For patients at risk for chronically reduced renal function (e.g. age >60 years, hypertension, diabetes), estimate the glomerular filtration rate (GFR) through laboratory testing.**
- **For patients at highest risk for NSF, do not exceed the recommended Vueway dose and allow a sufficient period of time for elimination of the drug from the body prior to any re-administration *[see Warnings and Precautions (5.1) in the full Prescribing Information]*.**

INDICATIONS AND USAGE

Vueway™ (gadopiclenol) is a gadolinium-based contrast agent indicated in adult and pediatric patients aged 2 years and older for use with magnetic resonance imaging (MRI) to detect and visualize lesions with abnormal vascularity in:

- the central nervous system (brain, spine, and associated tissues),
- the body (head and neck, thorax, abdomen, pelvis, and musculoskeletal system).

CONTRAINDICATIONS

Vueway is contraindicated in patients with history of hypersensitivity reactions to gadopiclenol.

WARNINGS AND PRECAUTIONS

Nephrogenic Systemic Fibrosis Gadolinium-based contrast agents (GBCAs) increase the risk for nephrogenic systemic fibrosis (NSF) among patients with impaired elimination of the drugs. Avoid use of GBCAs among these patients unless the diagnostic information is essential and not available with non-contrast MRI or other modalities. The GBCA-associated NSF risk appears highest for patients with chronic, severe kidney disease (GFR <30 mL/min/1.73 m^2) as well as patients with acute kidney injury. The risk appears lower for patients with chronic, moderate kidney disease (GFR 30-59 mL/min/1.73 m^2) and little, if any, for patients with chronic, mild kidney disease (GFR 60-89 mL/min/1.73 m^2). NSF may result in fatal or debilitating fibrosis affecting the skin, muscle, and internal organs. Report any diagnosis of NSF following Vueway administration to Bracco Diagnostics Inc. (1-800-257-5181) or FDA (1-800-FDA-1088 or www.fda.gov/medwatch).

Screen patients for acute kidney injury and other conditions that may reduce renal function. Features of acute kidney injury consist of rapid (over hours to days) and usually reversible decrease in kidney function, commonly in the setting of surgery, severe infection, injury or drug-induced kidney toxicity. Serum creatinine levels and estimated GFR may not reliably assess renal function in the setting of acute kidney injury. For patients at risk for chronically reduced renal function (e.g., age >60 years, diabetes mellitus or chronic hypertension), estimate the GFR through laboratory testing.

Among the factors that may increase the risk for NSF are repeated or higher than recommended doses of a GBCA and the degree of renal impairment at the time of exposure. Record the specific GBCA and the dose administered to a patient. For patients at highest risk for NSF, do not exceed the recommended Vueway dose and allow a sufficient period of time for elimination of the drug prior to re-administration. For patients receiving hemodialysis, physicians may consider the prompt initiation of hemodialysis following the administration of a GBCA in order to enhance the contrast agent's elimination *[see Use in Specific Populations (8.6) and Clinical Pharmacology (12.3) in the full Prescribing Information]*. The usefulness of hemodialysis in the prevention of NSF is unknown.

Hypersensitivity Reactions With GBCAs, serious hypersensitivity reactions have occurred. In most cases, initial symptoms occurred within minutes of GBCA administration and resolved with prompt emergency treatment.

- Before Vueway administration, assess all patients for any history of a reaction to contrast media, bronchial asthma and/or allergic disorders. These patients may have an increased risk for a hypersensitivity reaction to Vueway.
- Vueway is contraindicated in patients with history of hypersensitivity reactions to Vueway *[see Contraindications (4) in the full Prescribing Information]*.
- Administer Vueway only in situations where trained personnel and therapies are promptly available for the treatment of hypersensitivity reactions, including personnel trained in resuscitation.
- During and following Vueway administration, observe patients for signs and symptoms of hypersensitivity reactions.

Gadolinium Retention Gadolinium is retained for months or years in several organs. The highest concentrations (nanomoles per gram of tissue) have been identified in the bone, followed by other organs (e.g. brain, skin, kidney, liver, and spleen). The duration of retention also varies by tissue and is longest in bone. Linear GBCAs cause more retention than macrocyclic GBCAs. At equivalent doses, gadolinium retention varies among the linear agents with gadodiamide causing greater retention than other linear agents such as gadoxetate disodium, and gadobenate dimeglumine. Retention is lowest and similar among the macrocyclic GBCAs such as gadoterate meglumine, gadobutrol, gadoteridol, and gadopiclenol.

Consequences of gadolinium retention in the brain have not been established. Pathologic and clinical consequences of GBCA administration and retention in skin and other organs have been established in patients with impaired renal function *[see Warnings and Precautions (5.1) in the full Prescribing Information]*. There are rare reports of pathologic skin changes in patients with normal renal function. Adverse events involving multiple organ systems have been reported in patients with normal renal function without an established causal link to gadolinium.

While clinical consequences of gadolinium retention have not been established in patients with normal renal function, certain patients might be at higher risk. These include patients requiring multiple lifetime doses, pregnant and pediatric patients, and patients with inflammatory conditions. Consider the retention characteristics of the agent when choosing a GBCA for these patients. Minimize repetitive GBCA imaging studies, particularly closely spaced studies, when possible.

Acute Kidney Injury In patients with chronically reduced renal function, acute kidney injury requiring dialysis has occurred with the use of GBCAs. The risk of acute kidney injury may increase with increasing dose of the contrast agent. Do not exceed the recommended dose.

Extravasation and Injection Site Reactions Injection site reactions such as injection site pain have been reported in the clinical studies with Vueway *[see Adverse Reactions (6.1) in the full Prescribing Information]*. Extravasation during Vueway administration may result in tissue irritation *[see Nonclinical Toxicology (13.2) in the full Prescribing Information]*. Ensure catheter and venous patency before the injection of Vueway.

Interference with Visualization of Lesions Visible with Non-Contrast MRI As with any GBCA, Vueway may impair the visualization of lesions seen on non-contrast MRI. Therefore, caution should be exercised when Vueway MRI scans are interpreted without a companion non-contrast MRI scan.

ADVERSE REACTIONS

The following serious adverse reactions are discussed elsewhere in labeling:

- Nephrogenic Systemic Fibrosis *[see Warnings and Precautions (5.1) in the full Prescribing Information]*
- Hypersensitivity Reactions *[see Contraindications (4) and Warnings and Precautions (5.2) in the full Prescribing Information]*

Clinical Trials Experience Because clinical trials are conducted under widely varying conditions, adverse reaction rates observed in the clinical trials of a drug cannot be directly compared to rates in the clinical trials of another drug and may not reflect the rates observed in clinical practice.

The safety of Vueway was evaluated in 1,047 patients who received Vueway at doses ranging from 0.025 mmol/kg (one half the recommended dose) to 0.3 mmol/kg (six times the recommended dose). A total of 708 patients received the recommended dose of 0.05 mmol/kg. Among patients who received the recommended dose, the average age was 51 years (range 2 years to 88 years) and 56% were female. The ethnic distribution was 79% White, 10% Asian, 7% American Indian or Alaska native, 2% Black, and 2% patients of other or unspecified ethnic groups.

Overall, approximately 4.7% of subjects receiving the labeled dose reported one or more adverse reactions.

Table 1 lists adverse reactions that occurred in >0.2% of patients who received 0.05 mmol/kg Vueway.

TABLE 1. ADVERSE REACTIONS REPORTED IN >0.2% OF PATIENTS RECEIVING VUEWAY IN CLINICAL TRIALS

Adverse Reaction	Vueway 0.05 mmol/kg (n=708) (%)
Injection site pain	0.7
Headache	0.7
Nausea	0.4
Injection site warmth	0.4
Injection site coldness	0.3
Dizziness	0.3
Local swelling	0.3

Adverse reactions that occurred with a frequency ≤ 0.2% in patients who received 0.05 mmol/kg Vueway included: maculopapular rash, vomiting, worsened renal impairment, feeling hot, pyrexia, oral paresthesia, dysgeusia, diarrhea, pruritus, allergic dermatitis, erythema, injection site paresthesia, Cystatin C increase, and blood creatinine increase.

Adverse Reactions in Pediatric Patients

One study with a single dose of Vueway (0.05 mmol/kg) was conducted in 80 pediatric patients aged 2 years to 17 years, including 60 patients who underwent a central nervous system (CNS) MRI and 20 patients who underwent a body MRI. One adverse reaction (maculopapular rash of moderate severity) in one patient (1.3%) was reported in the CNS cohort.

USE IN SPECIFIC POPULATIONS

Pregnancy Risk Summary There are no available data on Vueway use in pregnant women to evaluate for a drug-associated risk of major birth defects, miscarriage or other adverse maternal or fetal outcomes. GBCAs cross the human placenta and result in fetal exposure and gadolinium retention. The available human data on GBCA exposure during pregnancy and adverse fetal outcomes are limited and inconclusive *(see Data)*. In animal reproduction studies, there were no adverse developmental effects observed in rats or rabbits with intravenous administration of Vueway during organogenesis *(see Data)*. Because of the potential risks of gadolinium to the fetus, use Vueway only if imaging is essential during pregnancy and cannot be delayed. The estimated background risk of major birth defects and miscarriage for the indicated population(s) are unknown. All pregnancies have a background risk of birth defect, loss, or other adverse outcomes. In the U.S. general population, the estimated background risk of major birth defects and miscarriage in clinically recognized pregnancies is 2% to 4% and 15% to 20% respectively. Data *Human Data* Contrast enhancement is visualized in the placenta and fetal tissues after maternal GBCA administration. Cohort studies and case reports on exposure to GBCAs during pregnancy have not reported a clear association between GBCAs and adverse effects in the exposed neonates. However, a retrospective cohort study comparing pregnant women who had a GBCA MRI to pregnant women who did not have an MRI reported a higher occurrence of stillbirths and neonatal deaths in the group receiving GBCA MRI. Limitations of this study include a lack of comparison with non-contrast MRI and lack of information about the maternal indication for MRI. Overall, these data preclude a reliable evaluation of the potential risk of adverse fetal outcomes with the use of GBCAs in pregnancy.

Animal Data Gadolinium Retention: GBCAs administered to pregnant non-human primates (0.1 mmol/kg on gestational days 85 and 135) result in measurable gadolinium concentration in the offspring in bone, brain, skin, liver, kidney, and spleen for at least 7 months. GBCAs administered to pregnant mice (2 mmol/kg daily on gestational days 16 through 19) result in measurable gadolinium concentrations in the pups in bone, brain, kidney, liver, blood, muscle, and spleen at one-month postnatal age.

Reproductive Toxicology: Animal reproduction studies conducted with gadopiclenol showed some signs of maternal toxicity in rats at 10 mmol/kg and rabbits at 5 mmol/kg (corresponding to 52 times and 57 times the recommended human dose, respectively). This maternal toxicity was characterized in both species by swelling, decreased activity, and lower gestation weight gain and food consumption.

No effect on embryo-fetal development was observed in rats at 10 mmol/kg (corresponding to 52 times the recommended human dose). In rabbits, a lower mean fetal body weight was observed at 5 mmol/kg (corresponding to 57 times the recommended human dose) and this was attributed as a consequence of the lower gestation weight gain.

Lactation Risk Summary There are no data on the presence of gadopiclenol in human milk, the effects on the breastfed infant, or the effects on milk production. However, published lactation data on other GBCAs indicate that 0.01% to 0.04% of the maternal gadolinium dose is excreted in breast milk. Additionally, there is limited GBCA gastrointestinal absorption in the breast-fed infant. Gadopiclenol is present in rat milk. When a drug is present in animal milk, it is likely that the drug will be present in human milk *(see Data)*. The developmental and health benefits of breastfeeding should be considered along with the mother's clinical need for Vueway and any potential adverse effects on the breastfed infant from Vueway or from the underlying maternal condition. Data In lactating rats receiving single intravenous injection of [^{153}Gd]-gadopiclenol, 0.3% and 0.2% of the total administered radioactivity was transferred to the pups via maternal milk at 6 hours and 24 hours after administration, respectively. Furthermore, in nursing rat pups, oral absorption of gadopiclenol was 3.6%.

Pediatric Use The safety and effectiveness of Vueway for use with MRI to detect and visualize lesions with abnormal vascularity in the CNS (brain, spine, and associated tissues), and the body (head and neck, thorax, abdomen, pelvis, and musculoskeletal system) have been established in pediatric patients aged 2 years and older.

Use of Vueway in this age group is supported by evidence from adequate and well-controlled studies in adults with additional pharmacokinetic and safety data from an open-label, uncontrolled, multicenter, single dose study of Vueway (0.05 mmol/kg) in 80 pediatric patients aged 2 to 17 years. The 80 patients consisted of 60 patients who underwent a CNS MRI and 20 patients who underwent a body MRI *[see Adverse Reactions (6.1) and Clinical Pharmacology (12.3) in the full Prescribing Information]*.

The safety and effectiveness of Vueway have not been established in pediatric patients younger than 2 years of age.

Geriatric Use Of the total number of Vueway-treated patients in clinical studies, 270 (26%) patients were 65 years of age and over, while 62 (6%) patients were 75 years of age and over. No overall differences in safety or efficacy were observed between these subjects and younger subjects.

This drug is known to be substantially excreted by the kidney, and the risk of adverse reactions to this drug may be greater in patients with impaired renal function. Because elderly patients are more likely to have decreased renal function, it may be useful to monitor renal function.

Renal Impairment In patients with renal impairment, the exposure of gadopiclenol is increased compared to patients with normal renal function. This may increase the risk of adverse reactions such as nephrogenic systemic fibrosis (NSF). Avoid use of GBCAs among these patients unless the diagnostic information is essential and not available with non-contrast MRI or other modalities. No dose adjustment of Vueway is recommended for patients with renal impairment. Vueway can be removed from the body by hemodialysis *[see Warnings and Precautions (5.1, 5.3, 5.4) and Clinical Pharmacology (12.3) in the full Prescribing Information]*.

OVERDOSAGE

Among subjects who received a single 0.3 mmol/kg intravenous dose of gadopiclenol (6 times the recommended dose of Vueway), headache and nausea were the most frequently reported adverse reactions. Gadopiclenol can be removed from the body by hemodialysis *[see Clinical Pharmacology (12.3) in the full Prescribing Information]*.

PATIENT COUNSELING INFORMATION Advise the patient to read the FDA-approved patient labeling (Medication Guide).

Nephrogenic Systemic Fibrosis Inform the patient that Vueway may increase the risk for NSF among patients with impaired elimination of the drugs and that NSF may result in fatal or debilitating fibrosis affecting the skin, muscle and internal organs.

Instruct the patients to contact their physician if they develop signs or symptoms of NSF following Vueway administration, such as burning, itching, swelling, scaling, hardening and tightening of the skin; red or dark patches on the skin; stiffness in joints with trouble moving, bending or straightening the arms, hands, legs or feet; pain in the hip bones or ribs; or muscle weakness *[see Warnings and Precautions (5.1) in the full Prescribing Information]*.

Gadolinium Retention Advise patients that gadolinium is retained for months or years in brain, bone, skin, and other organs following Vueway administration even in patients with normal renal function. The clinical consequences of retention are unknown. Retention depends on multiple factors and is greater following administration of linear GBCAs than following administration of macrocyclic GBCAs *[see Warnings and Precautions (5.3) in the full Prescribing Information]*.

Injection Site Reactions Inform the patient that Vueway may cause reactions along the venous injection site, such as mild and transient burning or pain or feeling of warmth or coldness at the injection site *[see Warnings and Precautions (5.5) in the full Prescribing Information]*.

Pregnancy Advise pregnant women of the potential risk of fetal exposure to Vueway *[see Use in Specific Populations (8.1) in the full Prescribing Information]*.

Rx only

US Patent No. 10,973,934

Manufactured for Bracco Diagnostics Inc. by Liebel-Flarsheim Company LLC - Raleigh, NC, USA 27616.

Toll Free: 1-877-272-2269 (U.S. only)

Revised November 2022

AppliedRadiology®

The Journal of Practical Medical Imaging and Management

Anderson Publishing, Ltd
180 Glenside Avenue,
Scotch Plains, NJ 07076
Tel: 908-301-1995
Fax: 908-301-1997
info@appliedradiology.com

Editorial Advisory Board

Applied Radiology®

The Journal of Practical Medical Imaging and Management

January / February 2024
Vol 53 No 1

Applied Radiology (ISSN 0160-9963, USPS 943180) is published in print 6 times a year, January, March, May, July, September, and November, by Anderson Publishing Ltd at 180 Glenside Ave., Scotch Plains NJ 07076. Periodicals postage paid at Scotch Plains, NJ and additional mailing offices. Free subscriptions for US-based qualified radiology professionals. Subscriptions for the US and its territories and possessions: $115 per year, $225 for two years. Foreign and Canadian subscriptions $215 for one year payable in US funds, international money orders, or by credit card only. Postmaster: Please send address changes to Applied Radiology, PO Box 317, Lincolnshire, IL 60069-0317 (847-564-5942) or email AppliedRadiology@Omeda.com.

Congratulations to our 2023 Leaders on the Horizon Residents' Program Winners

AppliedRadiology®

The Journal of Practical Medical Imaging and Management

Leaders on the Horizon Residents' Program 2023

Tej I. Mehta, MD
The Johns Hopkins Hospital

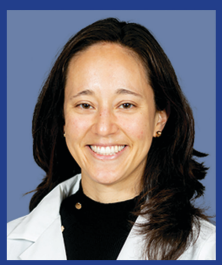

Monica M. Matsumoto, MD
University of Pennsylvania

Peterson Chang, MD
West Visayas State University Medical Center

Helena Bentley, MD
University of British Columbia

William Raynor, MD
Rutgers Robert Wood Johnson Medical School

Sherif B. Elsherif, MD
University of Florida, College of Medicine Jacksonville

Supported by Bracco Diagnostics, Inc.

appliedradiology.com/leaders

Dr Schwartz is the Editor-in-Chief of *Applied Radiology*. She is the chief of the Division of Neuroradiology and holds the Robert A. Zimmerman Chair in Pediatric Neuroradiology in the Department of Radiology at The Children's Hospital of Philadelphia. She is also a professor of radiology, Perelman School of Medicine, University of Pennsylvania. Dr Schwartz can be reached at erin@appliedradiology.com.

New Year, New Section

Erin Simon Schwartz, MD

At the risk of repeating myself,[1] I am excited to introduce another new section of the Editorial Advisory Board of *Applied Radiology* called, "Global Radiology." This section will be under the direction of Associate Editor **Pradnya Mhatre, MD, MRMD (MRSC)**, who is transitioning from our Advocacy/Governmental Affairs section. Dr Mhatre is an assistant professor of Radiology and Imaging Sciences at the Emory University School of Medicine, as well as the Program Manager of Radiology Safety/Quality Assurance for RAD-AID International. Dr Mhatre has skillfully developed and led the Global Health Imaging department, and we are thrilled to have a new board section dedicated to medical imaging issues of worldwide relevance.

Joining Dr Mhatre in this section is **Reed Omary, MD, MS,** the Carol D. and Henry P. Pendergrass Professor of Radiology & Radiological Sciences and a professor of Biomedical Engineering at the Vanderbilt University Medical Center. Dr Omary also recently stepped away from his longtime position as the institution's chair of radiology (2012-2023) to undertake a year-long sabbatical focusing on climate change and sustainability. Dr Omary intends to bring an environmental impact perspective to our global section.

Yet another new Associate Editor, **K. Elizabeth Hawk, MS, MD, PhD,** will lead our newly renamed Nuclear and Molecular Imaging section. By replacing the section's previous name, Nuclear Medicine, we believe the section will more accurately reflect the nature of this important and rapidly evolving field.

Please also join me in thanking **Blake Johnson, MD,** as he transitions off the editorial advisory board. Dr. Johnson was the longest-serving member of our Neuroradiology section, and we will miss his lively participation in our editorial board meetings.

And we're still not finished. Our Radiological Cases, Body Imaging, Emergency Imaging, Musculoskeletal Imaging, and Neuroradiology sections would all be well served by more members eager to share their expertise with readers of *Applied Radiology*. If you're interested, please don't hesitate to send me your CV!

Reference

1) Schwartz ES. Call for service. *Appl Radiol.* 2023; 52(1):6.

Next Top Model: An Overview of Breast Cancer Risk Assessment Models

Description

Numerous risk assessment models are available to calculate a woman's lifetime risk of developing and/or carrying a gene mutation that may predispose her to developing breast cancer. Knowledge of risk may help to inform individual screening practices. Further understanding and evaluation of risk assessment models are needed to increase their utilization.

The purpose of this activity is to 1) introduce breast cancer risk assessment models for estimating an individual's risk of developing breast cancer or risk for carrying a gene mutation that may predispose to developing breast cancer, 2) review the strengths and limitations of each model and the model's applicability to underrepresented populations, and 3) provide an example that demonstrates the use of risk assessment models.

Learning Objectives

Upon completing this activity, the reader should be able to:

- Identify the available breast cancer risk assessment models.
- Describe the strengths and limitations of each model.
- Explain each model's applicability to underrepresented populations.

Target Audience

- Radiologists
- Related Imaging Professionals

Authors

Pooja Agrawal, MD; Carolyn M. Audet, PhD; Laura L. Ernst, BA; Katie Lang, MS; Sonya A. Reid, MD, MPH; Katie M. Davis, DO; Rebecca Selove, PhD, MPH; Maureen Sanderson, PhD; Lucy B. Spalluto, MD, MPH

Affiliations: Department of Radiology, Baylor College of Medicine, Houston, TX (Dr Agrawal); Department of Health Policy, Vanderbilt University Medical Center, Nashville, Tennessee (Dr Audet); Vanderbilt University School of Medicine, Nashville, Tennessee (Ms Ernst); Division of Genetic Medicine, Vanderbilt University Medical Center, Nashville, Tennessee (Ms. Lang); Vanderbilt-Ingram Cancer Center, Nashville, Tennessee (Drs Reid, Sanderson, Spalluto); Division of Hematology and Oncology, Vanderbilt University Medical Center, Nashville, Tennessee (Drs Reid); Department of Radiology, Vanderbilt University Medical Center, Nashville, Tennessee (Drs Davis, Spalluto); Center for Prevention Research, Tennessee State University, Nashville, Tennessee (Dr Selove); Department of Family and Community Medicine, Meharry Medical College, Nashville, Tennessee (Dr Sanderson); Veterans Health Administration-Tennessee Valley Health Care System Geriatric Research, Education and Clinical Center (GRECC), Nashville, Tennessee (Dr Spalluto).

Commercial Support

None

Accreditation/ Designation Statement

This activity has been planned and implemented in accordance with the accreditation requirements and policies of the Accreditation Council for Continuing Medical Education (ACCME) through the joint providership of IAME and Anderson Publishing.

IAME is accredited by the ACCME to provide continuing medical education for physicians. IAME designates this enduring material for a maximum of 1 AMA PRA Category 1 Credits™. Physicians should claim only the credit commensurate with the extent of their participation in the activity.

Instructions

This activity is designed to be completed within the designated time period. To successfully earn credit, participants must complete the activity during the valid credit period. To receive CME credit, you must:

1. Review this article in its entirety.
2. Visit *appliedradiology.org/SAM2*.
3. Log into your account or create an account (new users).
4. Complete the post-test and review the discussion and references.
5. Complete the evaluation.
6. Print your certificate.

Estimated time for completion: 1 hour

Date of release and review: January 1, 2024

Expiration date: December 30, 2024

Disclosures

Planner: Erin Simon Schwartz, MD, discloses no relevant financial relationships with any ineligible companies.

Authors: Pooja Agrawal, MD, discloses no relevant financial relationships with ineligible companies. Carolyn M. Audet, PhD, discloses no relevant financial relationships with ineligible companies. Laura L. Ernst, BA, discloses no relevant financial relationships with ineligible companies. Katie Lang, MS, discloses no relevant financial relationships with ineligible companies. Sonya A. Reid, MD, MPH, discloses no relevant financial relationships with ineligible companies. Katie M. Davis, DO, discloses no relevant financial relationships with ineligible companies. Rebecca Selove, PhD, MPH, discloses no relevant financial relationships with ineligible companies. Maureen Sanderson, PhD, discloses no relevant financial relationships with ineligible companies. Lucy B. Spalluto discloses no relevant financial relationships with ineligible companies.

IAME has assessed conflict of interest with its faculty, authors, editors, and any individuals who were in a position to control the content of this CME activity. Any identified relevant conflicts of interest have been mitigated. IAME's planners, content reviewers, and editorial staff disclose no relationships with ineligible entities.

Next Top Model: An Overview of Breast Cancer Risk Assessment Models

Pooja Agrawal, MD; Carolyn M. Audet, PhD; Laura L. Ernst, BA; Katie Lang, MS; Sonya A. Reid, MD, MPH; Katie M. Davis, DO; Rebecca Selove, PhD, MPH; Maureen Sanderson, PhD; Lucy B. Spalluto, MD, MPH

In 2023, an estimated 298,000 women in the United States were diagnosed with breast cancer.[1] Incidence rates for breast cancer have been increasing by approximately 0.5% per year since the mid-2000s.[2] Significant racial disparities in breast cancer mortality exist, with mortality rates in Black women being approximately 40% higher than those for White women, despite similar incidence rates.[1] Disparities are also prominent among young women. When comparing Black women age ≤50 years to White women in the same age group, mortality rates were 1.9-2.6 times higher in Black women versus 1.1-1.2 times higher in the groups aged ≥70 years.[3]

Identifying a diverse population of young women at high risk for breast cancer with dedicated risk assessment models can help to address these existing disparities in mortality. Clinicians perform breast cancer risk assessment by asking a series of questions about such characteristics as family and breast health history and inputting the answers into an electronic tool, which calculates a woman's risk for breast cancer. Women identified as being at high risk (lifetime risk ≥20%) can be offered guideline-based early screening mammography and supplemental screening with MRI. This early or supplemental screening in high-risk women can identify cancers at earlier stages, prevent delays in diagnosis, and initiate earlier treatment. Ultimately, identification of a diverse population of young, high-risk women has the potential to improve mortality and address existing breast cancer disparities.

While numerous risk assessment models have been developed to identify women at high risk for developing breast cancer, these models remain underutilized in the clinical setting. The purpose of this activity is to

1) introduce breast cancer risk assessment models for estimating an individual's risk of developing breast cancer or risk for carrying a gene mutation that may predispose to developing breast cancer,
2) review the strengths and limitations of each model and the model's applicability to underrepresented populations, and
3) provide a case study that demonstrates the use of risk assessment models.

Risk Factors for Breast Cancer

Many risk factors can increase an individual's likelihood of developing breast cancer (Figure 1).[4] Nonmodifiable risk factors include increasing age, being born female, personal or family history of breast cancer, and inherited genetic changes in breast cancer susceptibility genes.[4] Hormonal and reproductive risk factors include long menstrual history and having children later in life.[4] Breastfeeding for at least one year can serve as a protective factor and decrease risk.[4] Potentially modifiable risk factors include excess body weight, menopausal hormone therapy, physical inactivity, and excess alcohol consumption.[4] Medical risk factors include high breast tissue density and history of radiation to

Affiliations: Department of Radiology, Baylor College of Medicine, Houston, Texas (Dr Agrawal); Department of Health Policy, Vanderbilt University Medical Center, Nashville, Tennessee (Dr Audet); Vanderbilt University School of Medicine, Nashville, Tennessee (Ms Ernst); Division of Genetic Medicine, Vanderbilt University Medical Center, Nashville, Tennessee (Ms Lang); Vanderbilt-Ingram Cancer Center, Nashville, Tennessee (Drs Reid, Sanderson, Spalluto); Division of Hematology and Oncology, Vanderbilt University Medical Center, Nashville, Tennessee (Dr Reid); Department of Radiology, Vanderbilt University Medical Center, Nashville, Tennessee (Drs Davis, Spalluto); Center for Prevention Research, Tennessee State University, Nashville, Tennessee (Dr Selove); Department of Family and Community Medicine, Meharry Medical College, Nashville, Tennessee (Dr Sanderson); Veterans Health Administration-Tennessee Valley Health Care System Geriatric Research, Education and Clinical Center (GRECC), Nashville, Tennessee (Dr Spalluto).
Conflict of Interest Statement:The authors report no relevant conflicts of interest.
Keywords: breast imaging, breast cancer risk assessment models, breast cancer screening

Figure 1. Breast cancer risk factors include personal characteristics, hormonal/reproductive factors, personal breast history, family history.

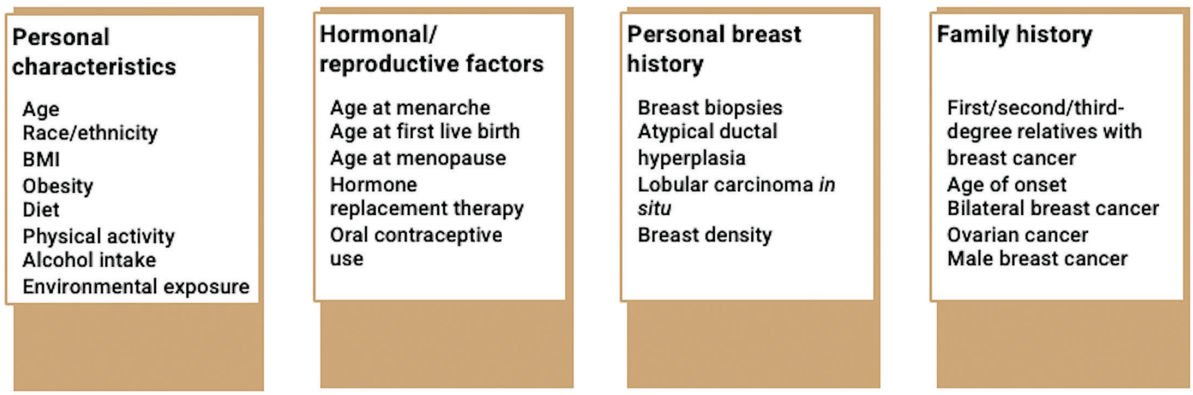

the chest.[4] Additional factors that can increase risk include history of breast biopsies and diagnosis of atypical hyperplasia or lobular carcinoma *in situ* (LCIS).[4]

Screening Guidelines Based on Calculated Lifetime Risk

The American College of Radiology (ACR) and Society of Breast Imaging (SBI) recommend risk assessment no later than age 25.[5] For those at average risk, annual screening with mammography is recommended starting at age 40. If a patient is found to have a lifetime risk ≥20%, ACR guidelines recommend annual screening beginning at age 30 and annual breast MRI beginning at age 25-30. More specific guidelines are available for women with other factors that may increase personal risk for breast cancer (eg, history of chest radiation therapy; genetics-based increased risk; personal histories of breast cancer and dense breast tissue; family history of breast cancer at a young age; personal history of atypical ductal hyperplasia (ADH), atypical lobular hyperplasia, or LCIS).

National Comprehensive Cancer Network (NCCN) guidelines also recommend screening mammography for high-risk women at younger ages and supplemental screening with contrast-enhanced breast MRI.[6,7] Specifically, patients with a lifetime risk ≥20% should receive an annual screening mammogram beginning either at age 40 or 10 years prior to when the youngest family member was diagnosed with the disease, but not prior to age 30 (whichever comes first). Tomosynthesis is recommended. Additionally, patient with a lifetime risk ≥20% should either undergo annual breast MRI beginning at age 40 or 10 years prior to when the youngest family member was diagnosed with breast cancer, but not prior to age 25 (whichever comes first). If a patient cannot undergo MRI, then contrast-enhanced mammography or whole breast ultrasound should be considered. Additional guidelines are available for women with other high-risk factors (eg, those with thoracic radiation between ages 10 and 30, increased 5-year risk of invasive breast cancer, ADH and ≥20% lifetime risk, lobular neoplasia and ≥20% lifetime risk, or pedigree suggestive of genetic predisposition).

Overview of Risk Assessment Models

Gail Model

The Gail model is one of the earliest models of breast cancer risk assessment, first published in 1989.[8] The data was derived from 243,221 White women in the Breast Cancer Detection Demonstration Project (BCDDP), a screening program conducted between 1973 and 1980 in the United States.[9] This model was modified in 1992 by the National Surgical Adjuvant Breast and Bowel Project (NSABP) to estimate the absolute risk of developing *only* invasive breast cancer.[10] Researchers have made additional updates to the model to provide more accurate estimates for Black women, Asian and Pacific Islander women, and Hispanic women. The modified model is used in the National Cancer Institute's (NCI) Breast Cancer Risk Assessment Tool. It estimates a patient's 5-year and lifetime risk of developing invasive breast cancer and is available at https://bcrisktool.cancer.gov/.[11]

Factors included in the Gail model are age, race/ethnicity, age at menarche, age at first live birth, number of previous breast biopsies, presence of atypical hyperplasia on biopsy, and number of affected first-degree relatives.

While easily accessible, well-calibrated to provide moderate discriminatory accuracy in studies of predominantly White women, and updated to provide more accurate estimates among different populations, the Gail model may underestimate risk in certain populations, such as Black women with previous biopsies and Hispanic women born outside the United States.[12-17] Additionally, owing to a lack of data, the model may be inaccurate among Native American and Alaskan Native women.

The Gail model has additional weaknesses that should be considered.

For example, it does not account for family history of breast cancer beyond affected first-degree relatives, thereby excluding paternal family history. For this reason, the NCCN guidelines do not list it as a model that should be used to identify candidates for supplemental screening with breast MRI. Instead, a patient found to have a 5-year risk of invasive breast cancer >1.7% in individuals age >35 per the Gail model should receive an annual screening mammogram (to begin when identified as being at increased risk), with tomosynthesis if available.

Furthermore, the Gail model does not include the age at onset of breast cancer among relatives or family history of other cancers. The model also does not consider variables such as mammographic density and should not be used in women under the age of 35. Additionally, the Gail model should not be used in women with known *BRCA1/BRCA2* mutations, those with a previous history of breast cancer, those with prior treatment of Hodgkin lymphoma with radiation to the chest, or those with breast cancer-causing syndromes, including Li-Fraumeni syndrome.

Table 1: Summary of Risk Assessment Models (selected factors)

	GAIL	TYRER-CUZICK	BCSC	BRCAPRO	CANRISK
Personal characteristics					
Age	X	X	X	X	X
Race/ethnicity	X		X	X	
Body mass index		X			X
Alcohol intake					X
Hormonal/reproductive					
Age at menarche	X	X			X
Age at first live birth	X	X			X
Age at menopause		X			X
Hormone replacement therapy use		X			X
Oral contraceptive use					X
Personal breast history					
Prior breast biopsies	X	X	X		
Atypical hyperplasia	X	X	X		
Lobular carcinoma in situ		X	X		
Breast density		X	X		X
Family history					
Number of affected first-degree relatives	X	X	X	X	X
Number of affected second-degree relatives		X		X	X
Number of affected third-degree relatives		X			X
Age of onset of breast cancer		X		X	X
Bilateral breast cancer		X		X	X
Ovarian cancer		X		X	X
Male breast cancer		X		X	X

International Breast Cancer Intervention Study [IBIS]/Tyrer-Cuzick (version 8)

The Tyrer-Cuzick model, also known as the IBIS model, was developed by scientists at the Wolfson Institute of Preventive Medicine, Queen Mary University of London.[18,19] The Tyrer-Cuzick model was developed using data on first breast cancer diagnoses among women in the United Kingdom (Thames Cancer Registry) between 2005-2009. Familial risk is based on data from a Swedish population-based study.[19] The latest version of the model (version 8) incorporates additional risk factors such as breast density and single nucleotide polymorphisms (SNPs). The model estimates an individual's 10-year and lifetime risk for developing breast cancer, as well as the likelihood of carrying a *BRCA1* or *BRCA2* gene. It is available at https://ibis.ikonopedia.com/ and https://ems-trials.org/riskevaluator/.[20,21]

Factors included in the Tyrer-Cuzick model are age, body mass index, reproductive history (age at menarche, age at first live birth, age at menopause), exogenous hormone exposure (hormone replacement therapy duration), results of previous breast biopsy (hyperplasia, presence of LCIS or atypical hyperplasia), breast density, family history (number and age of onset of first, second, or third-degree relatives with breast cancer, ovarian cancer diagnoses, male breast cancer diagnoses, unaffected relatives), Ashkenazi Jewish origin, and previous genetic test results (*BRCA1/2*).

External validation studies for the current version of the Tyrer-Cuzick model are ongoing. The Tyrer-Cuzick model has been found to be well-calibrated overall in non-Hispanic White women and Black women, with good calibration for Asian/Pacific Islanders and Native Americans, although sample sizes were small.[22] The model may overestimate risk for Hispanic women.[22] The addition of mammographic density was

found to increase the discriminatory accuracy of the model.[23] One study suggests the Tyrer-Cuzick model may overestimate risk for women at the highest-risk decile.[24]

A major strength of the Tyrer-Cuzick model is that it includes a diverse range of risk factors, including breast density and a comprehensive family history. Like the Gail model, it is easily accessible online and has undergone periodic updates to incorporate additional data on breast cancer incidence. Unlike the Gail model, the Tyrer-Cuzick model can be used in women ages <35 years and can calculate the risk for *BRCA1 or BRCA2* mutations.

The Tyrer-Cuzick model should not be used to assess risk in women who have already been diagnosed with breast cancer and may overestimate risk in women with atypical hyperplasia and LCIS.[25,26]

The Breast Cancer Surveillance Consortium (BCSC) Risk Calculator version 2.0

The BCSC Risk Calculator model was developed in 2008 using data from 1,095,484 women in seven mammography registries participating in the NCI-funded BCSC in the United States.[27] The study included women ages ≥35 with at least 1 mammogram with breast density measured using the Breast Imaging Reporting and Data System (BI-RADS) classification system. The model was updated in 2015 (version 2) to include benign breast diagnoses.[28] The BCSC Risk Calculator estimates a patient's 5- and 10-year risk of developing invasive breast cancer and is available at: https://tools.bcsc-scc.org/BC5yearRisk/calculator.htm.[29]

Factors included in the BCSC Risk Calculator are age, race/ethnicity, history of first-degree relatives with breast cancer (yes/no), history of a breast biopsy with benign breast disease diagnoses if known, and BI-RADS breast density.

The original model was externally validated among patients in the Mayo Mammography Health Study (MMHS) cohort.[30] Version 2 of the model was validated in a cohort of women in Chicago and was well-calibrated but found to underestimate risk in younger women, Hispanic and non-Hispanic Black women, and those with almost entirely fat breast density.[28]

The major strengths of the BCSC Risk Calculator are that it incorporates BI-RADS breast density and is easily accessible. This model cannot be used in women with a previous diagnosis of breast cancer or DCIS, prior breast augmentation, prior mastectomy, or those aged <35 or >74. Additionally, it does not account for a family history of breast cancer beyond affected first-degree relatives, thereby excluding paternal family history.

BRCAPRO

The BRCAPRO model was developed in 1997 based on estimates of *BRCA1* mutation frequencies in the general population and age-specific incidence rates of breast and ovarian cancers in carriers and noncarriers of mutations.[31] It was expanded in 1998 to include *BRCA2*.[32] The model uses Mendelian genetics and Bayes' theorem to calculate a patient's likelihood of carrying a germline mutation in the *BRCA1* or *BRCA2* genes, developing invasive breast cancer, or developing contralateral breast cancer. Access to the model can be requested at https://projects.iq.harvard.edu/bayesmendel/bayesmendel-r-package.[33]

Factors included in the BRCAPRO model are age, race/ethnicity, number/age at onset of first or second-degree relatives with breast cancer, family history of bilateral breast cancer or male breast cancer, personal or family history of ovarian cancer, and Ashkenazi Jewish origin.

Validation studies demonstrate variation in the performance of the BRCAPRO model with some studies demonstrating appropriate performance and other studies finding the model to underpredict risk.[34,35]

Like the Tyrer-Cuzick and the CanRisk models, one of the strengths of the BRCAPRO model is its ability to assess the likelihood of carrying a *BRCA1* and/or *BRCA2* gene mutation. The model also considers information about unaffected relatives and is routinely updated.

The BRCAPRO model does not include non-hereditary risk factors, such as age at menarche, age at first live birth, age at menopause, or specific results of prior breast biopsies. It also excludes family history of third-degree relatives.

Additionally, this model may underestimate risk in patients without *BRCA* gene mutations, as well as in families with prostate or ovarian cancer.[36] The model is not immediately accessible; however, it can be requested through an online form.

CanRisk (BOADICEA v5)

The Breast and Ovarian Analysis of Disease Incidence and Carrier Estimation Algorithm (BOADICEA) model calculates the probabilities of carrying rare loss-of-function variants in several breast or ovarian cancer susceptibility genes in addition to estimating the risk of developing breast and ovarian cancer.[37-39] It has undergone numerous updates since its development in 2002 and incorporates the effects of common genetic variants (summarized as polygenic risk scores, PRS), pathogenic variants in other genes, mammographic density, and additional risk factors. The latest version of the model (v6) is available to use via a web tool called CanRisk (https://www.canrisk.org/).[37,38,40-44]

Factors included in the CanRisk Tool for breast cancer risk estimation are age, body mass index, height, daily alcohol intake, age at menarche, age at first live birth, use of menopause hormone therapy, use or oral contraception, parity, mammographic density, family and personal-proband history of breast, ovarian, and pancreatic cancer, rare pathogenic variants in moderate and

high-risk susceptibility genes, age information on unaffected family members, information on year of birth to capture birth cohort, Ashkenazi Jewish origin, and common cancer genetic susceptibility variants (Polygenic Risk Scores).[45]

The model has been validated in several studies, largely consisting of women of European ancestry, and has been found to be well-calibrated.[24,46-48] However, it may not be as reliable in populations at lower risk for breast cancer or those of non-European ancestry.[49]

Like the Tyrer-Cuzick model, the CanRisk Tool includes a diverse range of risk factors, including comprehensive family history. Additionally, this is the only model that includes lifestyle risk factors such as alcohol consumption. The model is easily accessible online but requires the user to create an account for access. Unlike other models, it can be used in patients with a previous diagnosis of breast cancer.

The CanRisk tool should not be used in patients with personal history ductal carcinoma *in situ* (DCIS). Additionally, it will underestimate risk in those with Ataxia-Telangiectasia or homozygous carriers of pathogenic CHEK2 pathogenic truncating variants and should not be used in these patients. The CanRisk tool does not incorporate information on prior breast biopsies (number or result).

Figure 2. A pedigree for case study 1 shows that the patient's mother and sister were diagnosed with breast cancer.

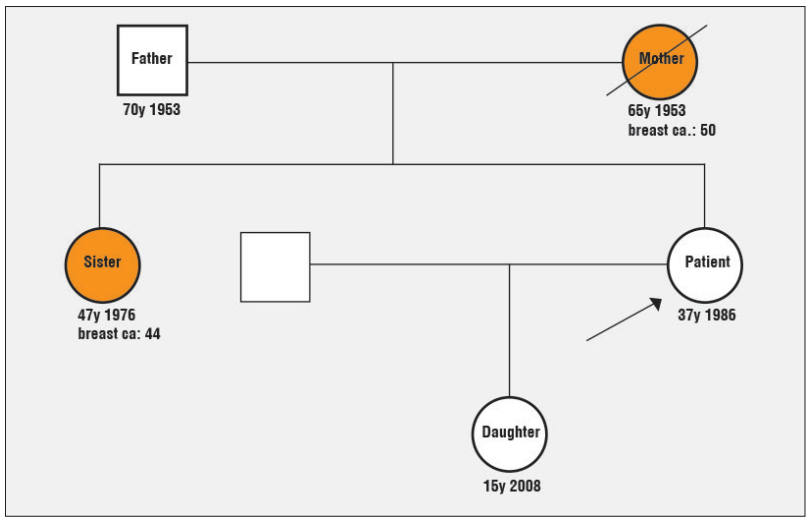

Table 1 provides a summary of the factors included in several risk assessment models.

Case Study

A 37-year-old White female wishes to know her lifetime risk for developing breast cancer. She has no significant medical history and is not Ashkenazi Jewish. She has never been tested for genetic mutations, had a mammogram, or had a breast biopsy. Menarche was at age 14, and she is premenopausal. She had a daughter at the age of 22, who is currently 15 and healthy. The patient's mother (diagnosed at age 50, deceased age 65) and sister (diagnosed at age 44, alive (currently 47) had unilateral breast cancer (Figure 2). Her father is living, age 70, and healthy. There is no family history of ovarian cancer. Genetic testing for the patient's relatives has never been performed. She is 5 foot 4 inches, weighs 150 pounds, and does not drink alcohol. She has never used hormone replacement therapy or oral contraceptives. She has never had an SNP array/PRS calculated.

What is the patient's lifetime risk for developing breast cancer? What are the appropriate breast cancer screening recommendations?

Risk Model Assessment

The Tyrer-Cuzick and CanRisk models calculate the patient's lifetime

Figure 3. Lifetime breast cancer risk as calculated by the Tyrer-Cuzick (21.1%), BRCAPRO (13.0%), and CanRisk (22.3%) models for case study 1.

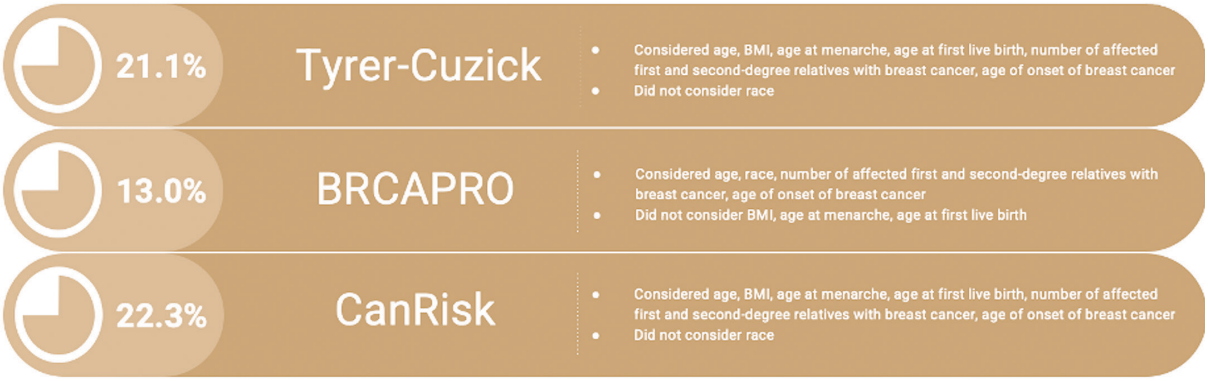

Figure 4. Bilateral craniocaudal (A) and mediolateral oblique screening mammogram (B) from the patient in the case study demonstrates heterogeneously dense breast tissue with no focal abnormality. Bilateral axial MIP images (C,D) demonstrate focal, clumped non-mass enhancement in the left outer breast. Bilateral axial postcontrast subtraction images (E,F) redemonstrate focal clumped non-mass enhancement with initial fast and delayed persistent kinetics in the left outer breast. MRI biopsy of the focal, clumped non-mass enhancement was performed. Pathology demonstrated DCIS with microinvasive component.

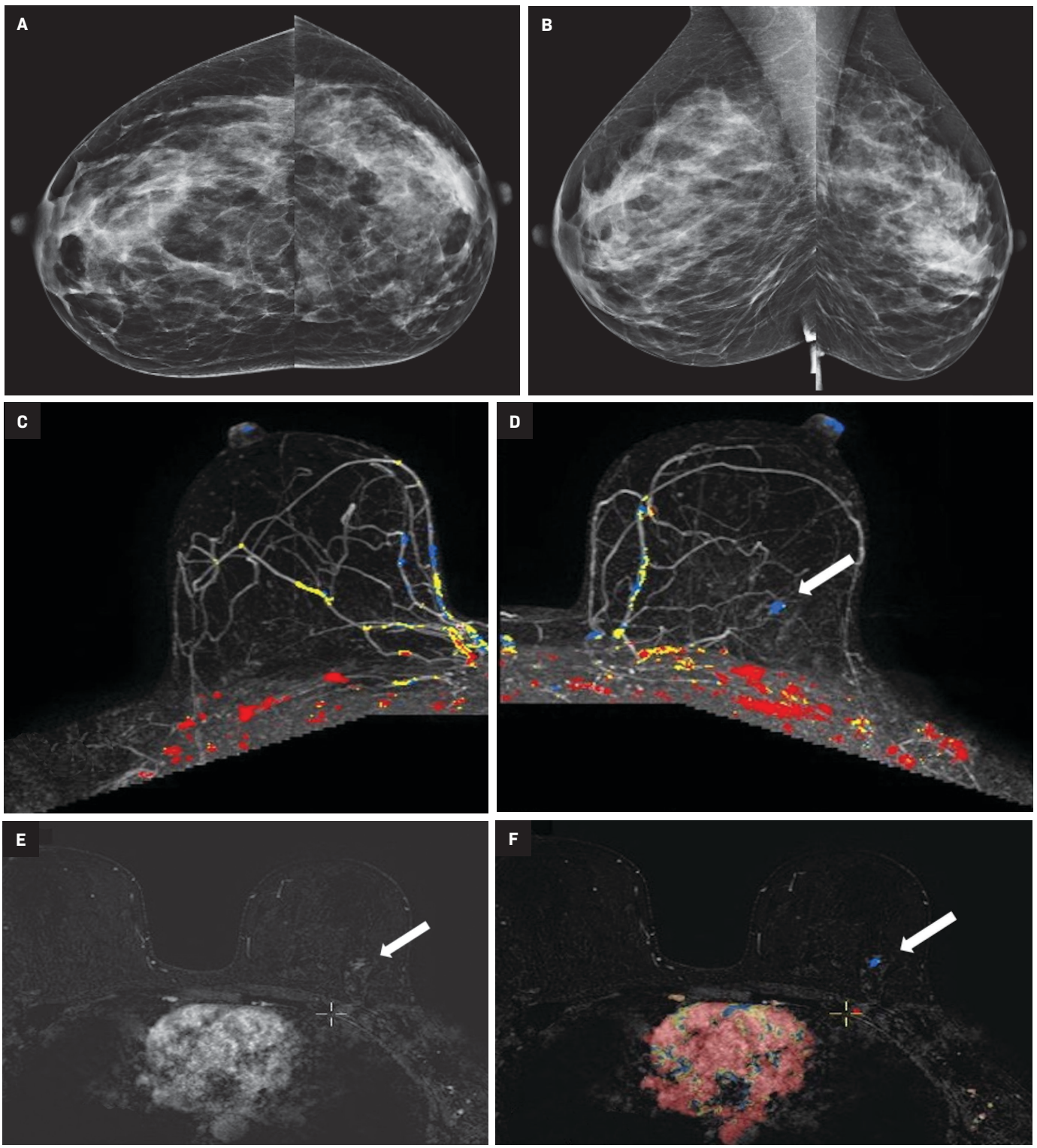

risk for breast cancer as ≥20%. The BRCAPRO model calculates the patient's lifetime risk for breast cancer as <20%. Figure 3 depicts the risk assessment values for each model and the factors included in each model.

Based on the results of the Tyrer-Cuzick and CanRisk models, the patient is considered high risk. Per NCCN guidelines, they should consider screening mammography and screening MRI 10 years prior to the age of diagnosis of the youngest first-degree relative, but not before age 30. Because the patient's sister was diagnosed with breast cancer at age 44, screening mammography and screening MRI could have been considered as early as age 34.

The patient pursued screening mammography and MRI (Figure 4). The mammogram was normal, with dense breast tissue. Screening MRI demonstrated focal clumped non-mass enhancement in the left outer breast. MRI-guided biopsy was performed and revealed DCIS with a microinvasive component.

Conclusion

Numerous risk assessment models are available to calculate a woman's lifetime risk of developing and/or carrying a gene mutation that may predispose her to developing breast cancer. Knowledge of risk may help to inform individual screening practices. Risk assessment models have different strengths and weaknesses that may increase or limit use in certain populations. Further understanding and evaluation of risk assessment models are needed to increase their utilization. Increased breast cancer risk assessment among diverse populations can identify women who may be at high risk for breast cancer. Guideline-based breast cancer screening in these populations serves as an opportunity to address known breast cancer mortality disparities.

References

1) Siegel RL, Miller KD, Wagle NS, Jemal A. Cancer statistics, 2023. *CA Cancer J Clin*. 2023;73(1):17-48.

2) Giaquinto AN, Sung H, Miller KD, et al. Breast cancer statistics, 2022. *CA Cancer J Clin*. 2022;72(6):524-541.

3) DeSantis CE, Ma J, Gaudet MM, et al. Breast cancer statistics, 2019. *CA Cancer J Clin*. 2019;69(6):438-451.

4) Ban KA, Godellas CV. Epidemiology of breast cancer. *Surg Oncol Clin N Am*. 2014;23(3):409-422.

5) Monticciolo DL, Malak SF, Friedewald SM, et al. Breast cancer screening recommendations inclusive of all women at average risk: update from the ACR and Society of Breast Imaging. *J Am Coll Radiol*. 2021;18(9):1280-1288.

6) Referenced with permission from the NCCN Clinical Practice Guidelines in Oncology (NCCN Guidelines®) for Breast Cancer V.4.2023. © National Comprehensive Cancer Network I. All rights reserved. Accessed April 14, 2023. To view the most recent and complete version of the guideline, go online to NCCN.org.

7) Referenced with permission from the NCCN Clinical Practice Guidelines in Oncology (NCCN Guidelines®) for Breast Cancer Risk Reduction V.1.2022. © National Comprehensive Cancer Network I. All rights reserved. Accessed [April 14, 2023]. To view the most recent and complete version of the guideline, go online to NCCN.org.

8) Gail MH, Brinton LA, Byar DP, et al. Projecting individualized probabilities of developing breast cancer for white females who are being examined annually. *J Natl Cancer Inst*. 1989;81(24):1879-1886.

9) Baker LH. Breast cancer detection demonstration project: five-year summary report. *CA Cancer J Clin*. 1982;32(4):194.

10) Anderson S, Ahnn S, Duff K. NSABP Breast Cancer Prevention Trial risk assessment program, version 2. *NSABP Biostatistical Center Technical Report*. 1992;12

11) Institute NC. The Breast Cancer Risk Assessment Tool. Accessed April 14, 2023, https://bcrisktool.cancer.gov/

12) Rockhill B, Spiegelman D, Byrne C, Hunter DJ, Colditz GA. Validation of the Gail et al. model of breast cancer risk prediction and implications for chemoprevention. *J Natl Cancer Inst*. 2001;93(5):358-366.

13) Gail MH. Choosing breast cancer risk models: importance of independent validation. Oxford University Press; 2020. p. 433-435.

14) Wang X, Huang Y, Li L, Dai H, Song F, Chen K. Assessment of performance of the Gail model for predicting breast cancer risk: a systematic review and meta-analysis with trial sequential analysis. *Breast Cancer Res*. 2018;20(1):1-19.

15) Matsuno RK, Costantino JP, Ziegler RG, et al. Projecting individualized absolute invasive breast cancer risk in Asian and Pacific Islander American women. *J Natl Cancer* Inst. 2011;103(12):951-961.

16) Banegas MP, John EM, Slattery ML, et al. Projecting individualized absolute invasive breast cancer risk in US Hispanic women. *J Natl Cancer Inst*. 2017;109(2):djw215.

17) Gail MH, Costantino JP, Pee D, et al. Projecting individualized absolute invasive breast cancer risk in African American women. *J Natl Cancer Inst*. 2007;99(23):1782-1792.

18) Tyrer J, Duffy SW, Cuzick J. A breast cancer prediction model incorporating familial and personal risk factors. *Stat Med*. 2004;23(7):1111-1130.

19) Anderson H, Bladström A, Olsson H, Möller TR. Familial breast and ovarian cancer: a Swedish population-based register study. *Am J Epidemiol*. 2000;152(12):1154-1163.

20) Cuzick J. IBIS Breast Cancer Risk Evaluation Tool.

21) IBIS Risk Assessment Tool.

22) Kurian AW, Hughes E, Simmons T, et al. Performance of the IBIS/Tyrer-Cuzick model of breast cancer risk by race and ethnicity in the Women's Health Initiative. *Cancer*. 2021;127(20):3742-3750.

23) Brentnall AR, Harkness EF, Astley SM, et al. Mammographic density adds accuracy to both the Tyrer-Cuzick and Gail breast cancer risk models in a prospective UK screening cohort. *Breast Cancer Res*. 2015;17:1-10.

24) Pal Choudhury P, Brook MN, Hurson AN, et al. Comparative validation of the BOADICEA and Tyrer-Cuzick breast cancer risk models incorporating classical risk factors and polygenic risk in a population-based prospective cohort of women of European ancestry. *Breast Cancer Res*. 2021;23:1-5.

25) Boughey JC, Hartmann LC, Anderson SS, et al. Evaluation of the Tyrer-Cuzick (International Breast Cancer Intervention Study) model for breast cancer risk prediction in women with atypical hyperplasia. *J Clin Oncol*. 2010;28(22):3591.

26) Lo LL, Milne RL, Liao Y, Cuzick J, Terry MB, Phillips K-A. Validation of the IBIS breast cancer risk evaluator for women with lobular carcinoma in-situ. *Br J Cancer*. 2018;119(1):36-39.

27) Tice JA, Cummings SR, Smith-Bindman R, Ichikawa L, Barlow WE, Kerlikowske K. Using clinical factors and mammographic breast density to estimate breast cancer risk: development and validation of a new predictive model. *Ann Intern Med*. 2008;148(5):337-347.

28) Tice JA, Miglioretti DL, Li C-S, Vachon CM, Gard CC, Kerlikowske K. Breast density and benign breast disease: risk assessment to identify women at high risk of breast cancer. *J Clin Oncol*. 2015;33(28):3137.

29) Consortium BCS. Breast Cancer Surveillance Consortium Risk Calculator V2. Updated July 17, 2015. Accessed April 14, 2023. https://tools.bcsc-scc.org/BC5yearRisk/calculator.htm

30) Vachon CM, Pankratz VS, Scott CG, et al. The contributions of breast density and common genetic variation to breast cancer risk. *J Natl Cancer Inst*. 2015;107(5):dju397.

31) Berry DA, Parmigiani G, Sanchez J, Schildkraut J, Winer E. Probability of carrying a mutation of breast-ovarian cancer gene BRCA1 based on family history. *J Natl Cancer Inst*. 1997;89(3):227-237.

32) Parmigiani G, Berry DA, Aguilar O. Determining carrier probabilities for breast cancer–susceptibility genes BRCA1 and BRCA2. *Am J Med Genet*. 1998;62(1):145-158.

33) BayesMendel R package.

34) Terry MB, Liao Y, Whittemore AS, et al. 10-year performance of four models of breast cancer risk: a validation study. *Lancet Oncol*. 2019;20(4):504-517.

35) Antoniou AC, Hardy R, Walker L, et al. Predicting the likelihood of carrying a BRCA1 or BRCA2 mutation: validation of BOADICEA, BRCAPRO, IBIS, Myriad and the Manchester scoring system using data from UK genetics clinics. *J Med Genet*. 2008;45(7):425-431.

36) Fernández LO, Márquez-Aragonés M, Romero-Laorden N, et al. Limited value of currently used germline brca mutations predictive tools in prostate cancer. *Ann Oncol*. 2017;28:v286.

37) Lee A, Mavaddat N, Wilcox AN, et al. BOADICEA: a comprehensive breast cancer risk prediction model incorporating genetic and nongenetic risk factors. *Genet Med*. 2019;21(8):1708-1718.

38) Carver T, Hartley S, Lee A, et al. CanRisk Tool—A web interface for the prediction of breast and ovarian cancer risk and the likelihood of carrying genetic pathogenic variants. *Cancer Epidemiol Biomarkers Prev*. 2021;30(3):469-473.

39) Archer S, Babb de Villiers C, Scheibl F, et al. Evaluating clinician acceptability of the prototype CanRisk tool for predicting risk of breast and ovarian cancer: A multi-methods study. *PLoS One*. 2020;15(3):e0229999.

40) Antoniou AC, Pharoah PD, McMullan G, et al. A comprehensive model for familial breast cancer incorporating BRCA1, BRCA2 and other genes. *Br J Cancer*. 2002;86(1):76-83.

41) Antoniou AC, Cunningham A, Peto J, et al. The BOADICEA model of genetic susceptibility to breast and ovarian cancers: updates and extensions. *Br J Cancer*. 2008;98(8):1457-1466.

42) Lee AJ, Cunningham AP, Kuchenbaecker K, Mavaddat N, Easton DF, Antoniou AC. BOADICEA breast cancer risk prediction model: updates to cancer incidences, tumour pathology and web interface. *Br J Cancer*. 2014;110(2):535-545.

43) Lee AJ, Cunningham AP, Tischkowitz M, et al. Incorporating truncating variants in PALB2, CHEK2, and ATM into the BOADICEA breast cancer risk model. *Genet Med*. 2016;18(12):1190-1198.

44) Lee A, Mavaddat N, Cunningham A, et al. Enhancing the BOADICEA cancer risk prediction model to incorporate new data on RAD51C, RAD51D, BARD1 updates to tumour pathology and cancer incidence. *J Med Genet*. 2022;59(12):1206-1218.

45) Carver T. What information do the breast and ovarian cancer models use to determine risks? Updated December 5, 2022. Accessed April 13, 2023, https://canrisk.atlassian.net/wiki/spaces/FAQS/pages/3211464/What+information+do+the+breast+and+ovarian+cancer+models+use+to+determine+risks

46) Lakeman IM, Rodríguez-Girondo M, Lee A, et al. Validation of the BOADICEA model and a 313-variant polygenic risk score for breast cancer risk prediction in a Dutch prospective cohort. *Genet Med*. 2020;22(11):1803-1811.

47) Lee A, Yang X, Tyrer J, et al. Comprehensive epithelial tubo-ovarian cancer risk prediction model incorporating genetic and epidemiological risk factors. *J Med Genet*. 2022;59(7):632-643.

48) Yang X, Eriksson M, Czene K, et al. Prospective validation of the BOADICEA multifactorial breast cancer risk prediction model in a large prospective cohort study. *J Med Genet*. 2022;59(12):1196-1205.

49) Carver T. Can I use the CanRisk Tool to estimate risks for populations outside Europe? Updated July 22, 2021. Accessed April 13, 2023, 2023. https://canrisk.atlassian.net/wiki/spaces/FAQS/pages/28180481/Can+I+use+the+CanRisk+Tool+to+estimate+risks+for+populations+outside+Europe.

Minimizing the Pain of Local Anesthetic Injection

Matthew Henry, MD, MS; Youngchae Lee, MD; Daniel L. Kirkpatrick, MD

Minimizing pain is an important component of any procedure. When poorly controlled, procedural pain can be an important source of patient dissatisfaction.[1] While intravenous sedation decreases patient pain and anxiety, administering a local anesthetic is critical to generate as little pain as possible. While they are excellent at decreasing pain, local anesthetics can cause pain when infused. Patients are often cautioned about the "stick and burn" that accompanies injection. However, when the injection is performed properly, pain can be limited to the initial needlestick and followed by an otherwise pain-free procedure.[2,3] With the number of cases performed in an average interventional radiology (IR) practice daily, there are many opportunities to refine local anesthetic technique and improve patient satisfaction.

Mechanism of Pain

Nociceptors are free nerve endings that originate from peripheral nerves and are sensitive to noxious mechanical, temperature, or chemical insults.[2,4,5] There are two types of nociceptive axons, A-delta fibers and C-fibers.[2,4,5] A-delta fibers are myelinated fibers responsible for communicating sharp, transient pain. C-fibers are unmyelinated and communicate dull pain. When exposed to inflammatory signaling molecules, the depolarization threshold of peripheral nociceptors is lowered. Pain signals are carried to the dorsal horn of the spinal cord and ascend centrally through the spinothalamic and spinoreticulothalamic tracts. The spinothalamic tract communicates sharp pain, and the spinoreticulothalamic tract communicates dull, poorly localized pain.

Pain from local anesthetic injection comes from two sources.[2] The first is mechanical trauma from needle insertion, which is carried by A-delta fibers. The second is from infiltration, which distends the affected tissues and exposes nociceptors to the acidic solution. This component is carried by C-fibers.

Lidocaine

Lidocaine is near ubiquitous in surgical and interventional suites, owing to its excellent safety profile.[6] This paper will focus on the use of lidocaine, although the principles translate to other local anesthetics.

When injected, lidocaine diffuses through the cell membrane and blocks the voltage-gated sodium channels in peripheral nociceptors.[1,2] Onset of analgesia is usually under one minute and can last 2-5 hours.[6,7,8] In adults, the maximum dose of lidocaine is 4 mg/kg (total dose no greater than 350 mg) and 7 mg/kg (total dose no greater than 500 mg) when combined with epinephrine.[6,7] In children, the maximum dose of lidocaine is 2 mg/kg (total dose no greater than 150 mg) and 4.5 mg/kg (total dose no greater than 150 mg) when combined with epinephrine.[6]

Procedural Preparation

Buffering with Sodium Bicarbonate

The physiologic pH of the body is slightly alkaline, ranging between 7.35 and 7.45. In contrast, lidocaine has a pH of 6.09 in the 1% formulation and 6.00 in the 2% formulation.[9] With the addition of 1:100,000

Affiliations: Department of Interventional Radiology, Medical College of Wisconsin, Milwaukee, Wisconsin (Dr Henry); Department of Pharmacology, Yonsei University College of Medicine, Seoul, Korea (Dr Lee); Department of Interventional Radiology, University of Michigan School of Medicine, Ann Arbor, Michigan (Dr Kirkpatrick). The authors declare no conflicts of interest, financial or otherwise.
Keywords: Lidocaine, Local Anesthesia, Pain, Interventional Radiology

Figure 1. Needle insertion for local anesthesia. On the left, proper technique is shown with the needle being inserted perpendicular to the skin surface. On the right, suboptimal technique is demonstrated. Insertion at a shallower angle results in transgression of more nerve fibers, leading to more pain with insertion.

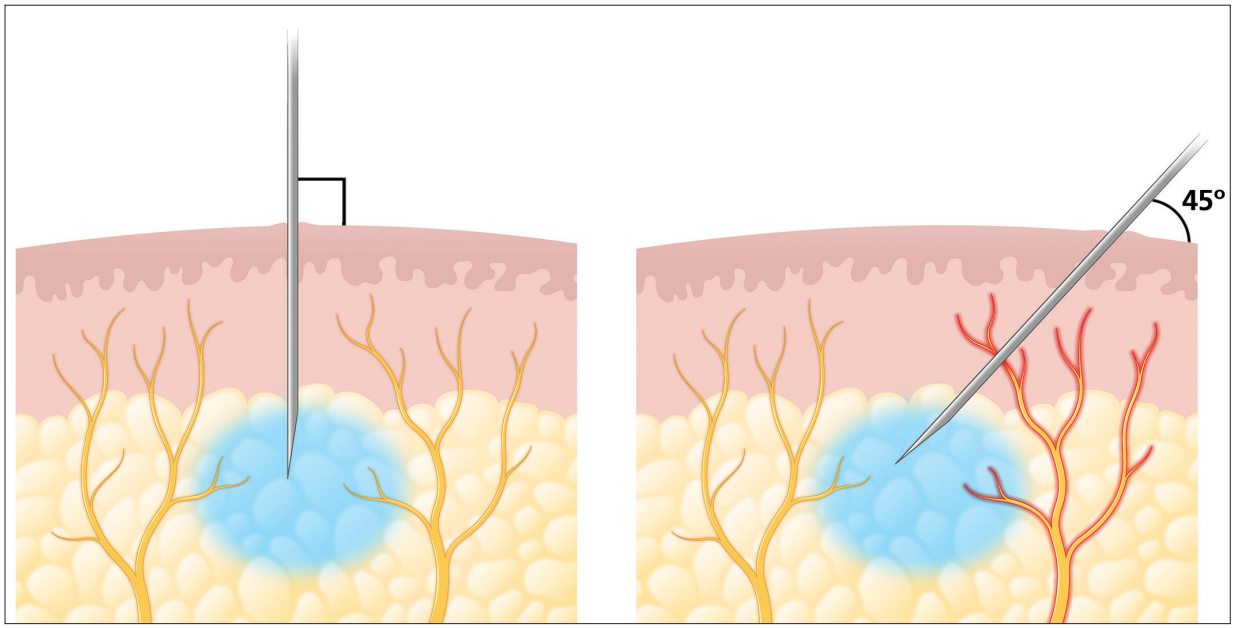

epinephrine, which will be discussed elsewhere, the pH drops to 4.2, which is about 1000 times more acidic than physiologic pH.[9] The acidic nature of lidocaine is theorized to be one source of pain with local anesthesia.[9] This can be addressed by buffering lidocaine with sodium bicarbonate to achieve a neutral pH. At a physiologic pH, more molecules of lidocaine diffuse through nociceptive cell membranes resulting in a faster onset of action.[10] Several double-blind, randomized controlled studies (RCT) have confirmed a statistically significant decrease in pain when buffered lidocaine is used.[11,12]

The most widely reported buffering technique is the addition of 1 mL of 8.4% sodium bicarbonate to 10 mL of 1% lidocaine with 1:100,000 epinephrine.[9] The resulting 1:10 mixture has a pH of 7.4. This cocktail is stable at room temperature for at least one week and has no risk of precipitation.[9] The concentration of epinephrine can be expected to fall by 25% per week, although this can be obviated by creating the mixture at the beginning of the day or prior to every case.[2]

Addition of Epinephrine

Lidocaine most commonly comes in 1% and 2% formulations, which can be modified with the addition of epinephrine. Classically, lidocaine with epinephrine is used to reduce procedural bleeding. Vasoconstriction from the added epinephrine is short lived but has the benefit of blanching the skin, which can help identify areas that have already been anesthetized. In addition, vasoconstriction reduces blood flow to the treatment zone, increasing local drug concentration.[2] Epinephrine also results in faster onset of pain relief and increases the duration of relief up to 10 hours.[13]

Warming to Body Temperature

The solubility of lidocaine increases with rising temperature.[14] Like buffering with bicarbonate, more lidocaine diffusing across nociceptive cell membranes results in a faster onset of action.[15,16] Lidocaine can be warmed to 70° C without affecting its efficacy.[15] A 2017 RCT showed a statistically significant decrease in pain with warming.[17] Pain relief with warming is independent of the pain relief from buffering to a neutral pH.[16] In addition, buffering and warming have a synergistic effect, and provide the greatest relief when combined.[18,19] Finally, warming lidocaine has no detrimental effect on the duration of analgesia.[16]

Use of Finer Needles

Higher-gauge needles require less force to pierce the skin, contact fewer nociceptors, and slow the speed of injection. Several studies have investigated the use of higher gauge needles (23 to 32 gauge) and found a linear decrease in pain with increasing needle gauge.[20-23] As a result, 27–32-gauge needles are recommended.

Maintaining needle sharpness is also important for pain control. A blunt needle requires more force to pierce the skin, increases friction as the needle passes through tissue, and generates more pain.[21] Needle sharpness can be maintained by minimizing the number of needle insertions, exchanging blunted

Figure 2. Proper technique for anesthetizing the parietal pleura (R, rib in cross section; P, parietal pleura). Note that local anesthetic should be infiltrated along the entire needle course, including the densely innervated parietal pleura. Similar technique is used to anesthetize the peritoneum for a paracentesis.

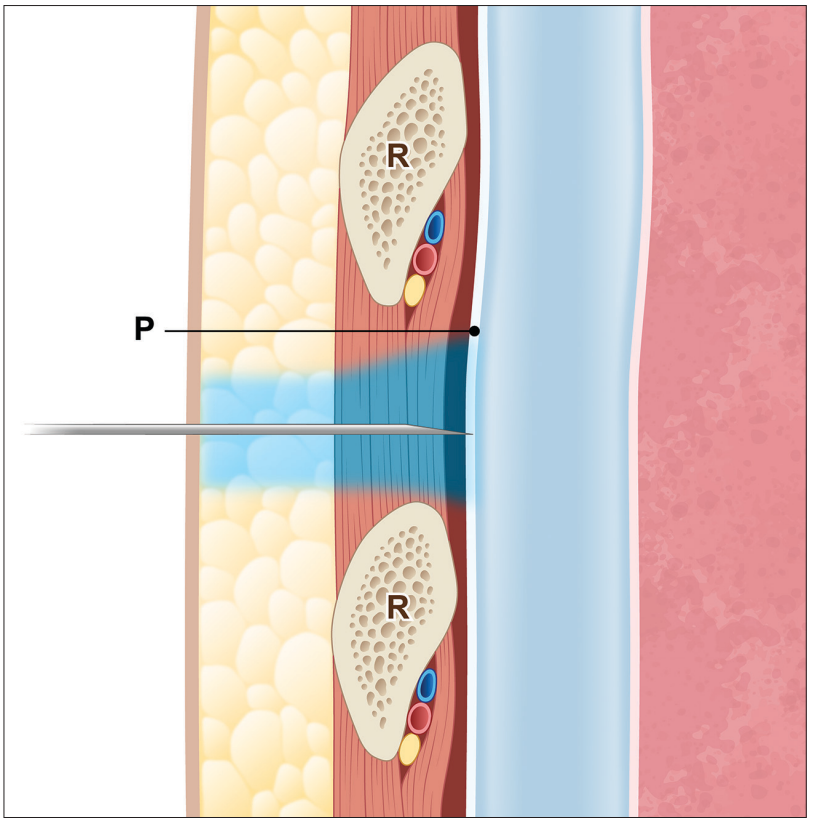

Figure 3. Proper technique for anesthetizing bone. The periosteum (P) is densely innervated and can generate pain if not included in the local anesthetic field.

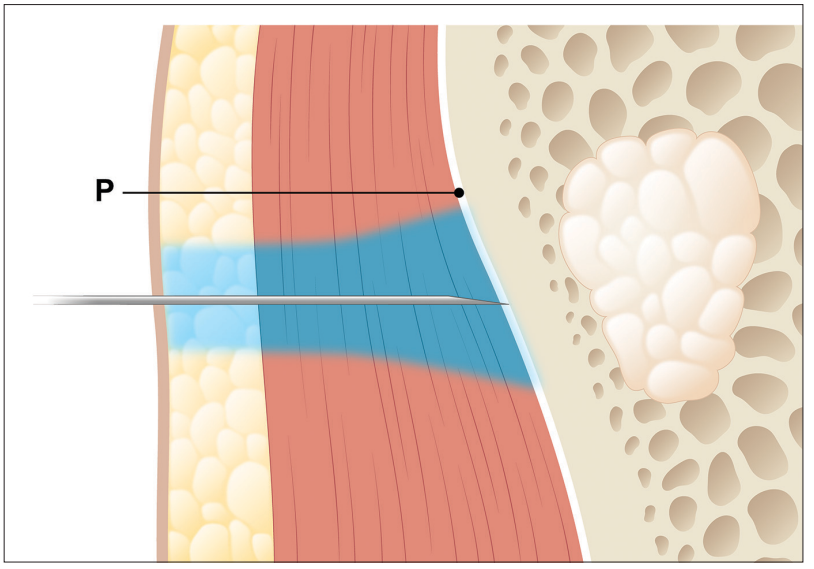

needles for new ones, and using separate needles for drawing up and injecting lidocaine.[21,24]

Patient Preparation

Skin Preparation

Applying a eutectic mixture of local anesthetics (EMLA) cream can help reduce the pain of the needle transgressing the skin. The most common EMLA cream is a topical oil and water emulsion of 2.5% prilocaine and 2.5% lidocaine. Several studies have shown a statistically significant decrease in pain when the skin is pretreated with a topical anesthetic.[2,25] The primary limitations of EMLA cream are the time to maximum effect and the depth of penetration. EMLA requires at least 60 minutes to anesthetize to a depth of 3 mm and up to 120 minutes to a depth > 5 mm.[25,26]

An alternative to EMLA cream is cooling the skin,[27] usually with an ice pack. This technique originated in dentistry, as topical anesthetics cannot be used on mucosal surfaces. Cooling is less efficacious than topical anesthetics but has a faster onset of action and is more cost-effective.[27]

Management of Expectations and Distraction

Anxiety plays a prominent role in pain perception, and many patients experience anxiety prior to procedures.[28,29] Speaking with patients and establishing a level of trust can set the tone for the remainder of the encounter. Distraction can also help decrease pain. Engaging the patient in conversation; asking them to perform a task and/or slowly exhale during injection; nurse coaching; and hypnosis can all decrease pain.[30] Finally, asking the patient to look away from the injection has been shown to decrease pain perception.[31]

Figure 4. Proper technique for anesthetizing the patient for a nephrostomy tube (blue) exchange but can be generalized to any tube exchange. The entirety of the drain tract should be anesthetized to minimize pain during the exchange.

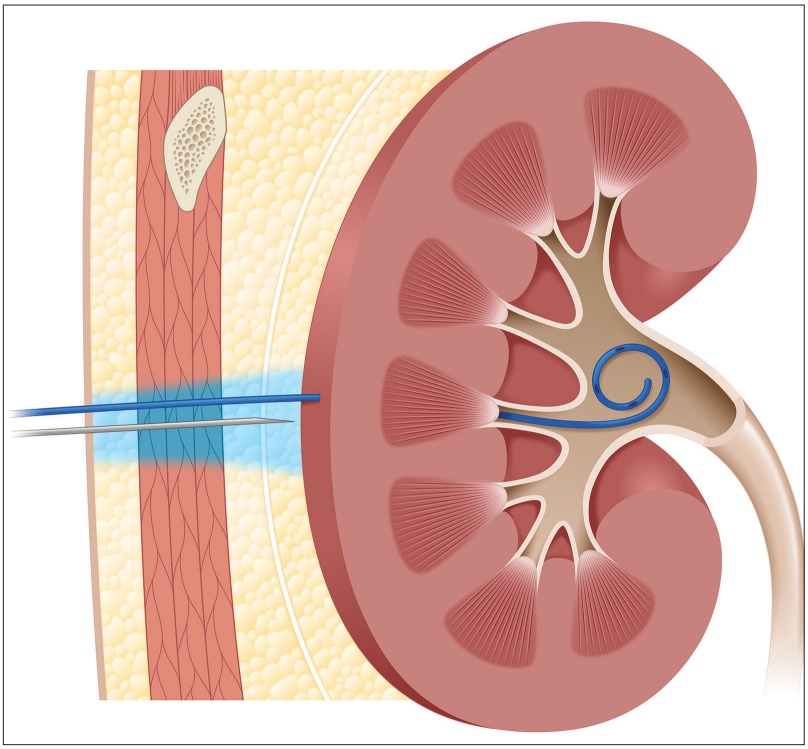

Injection Technique

Gate Theory

When a nociceptor is activated, the pain signal is transmitted to first-order neurons at the synapse. When pain is the only signal transmitted, the strength of the signal is maximized. However, when nearby non-pain-signaling axons are also activated, transmission of the pain signal at the synapse is decreased.[32] In simple terms, there is a limit to the amount of pain that can be communicated at the synapse, and this can be diluted by additional stimuli. In practice, application of light touch, pressure, or vibration near the site of injection can decrease pain.[33,34] An additional technique is to spray a small amount of lidocaine on the skin immediately prior to needle insertion. This simple technique has shown a statistically significant decrease in pain.[35]

Needle Insertion

When the needle enters the skin, it directly stimulates nociceptors, which transmit sharp pain through A-delta fibers. The needle should be quickly inserted into the skin perpendicular to the skin surface (Figure 1). Theoretically, this minimizes direct contact with nociceptors. This technique has been shown to decrease pain when compared to inserting the needle at a 45-degree angle.[36] Once inserted, care should be taken to keep the needle as still as possible, which will also decrease pain.[37] The number of needle sticks should also be minimized.

Site and Rate of Injection

Once the needle is inserted, lidocaine should be injected subcutaneously rather than intradermally. Subcutaneous injection generates less pain than intradermal injection while achieving the same analgesic effect.[2] A deeper injection also treats the nerve roots supplying the dermis, making intradermal injection unnecessary.[2] When a wider region must be anesthetized, lidocaine should be injected while advancing the needle to anesthetize nociceptors prior to needle traversal.

The rate of injection is also critical in decreasing pain.[2,3] Several studies have demonstrated less pain with slower versus faster injections.[38,39] Determining how slowly to inject, however, is difficult. The two studies cited judged a slow injection as one ranging between 2 and 4mL/min and a fast injection ranging between 7.5 and 12 mL/min. In the authors' experience, an injection rate of 2-4 mL/min is usually sufficient.

Physician Attention and Care

Finally, as lidocaine is infused, the physician should closely watch the patient for signs of pain, paying special attention to the face. Subtle signs such as wincing, pursing of the lips, and clenching the jaw can give immediate feedback that pain is being generated. With time, practice, and close attention to the patient, physicians can refine their technique and approach mastery of injection.

Anesthetic Use in Interventional Radiology

Local anesthesia is used in almost every procedure in IR, and these preparation and techniques are sufficient in many cases. However, they may be modified in certain situations to attain the best results. The most important of these circumstances are any interventions that transgress the pleura, peritoneum, or periosteum, and those that traverse a solid organ.

The parietal pleura and peritoneum are well-innervated and transgression with a needle will result in sharp, well-localized pain. Special care should be taken to anesthetize these layers, otherwise the patient will still feel sharp pain as the

needle passes through (Figure 2). On ultrasound, the pleural or peritoneal linings appear as a thin, echogenic layer. When lidocaine is infused liberally in and around the lining, the echogenic line will disappear. The anesthetized area can then be transgressed by the relevant device without discomfort.

The periosteum is another well-innervated structure that can result in sharp, well-localized pain if not properly anesthetized (Figure 3). Infusing lidocaine into the subcutaneous tissues is not sufficient, and the patient will still experience pain when the needle pierces the periosteum. Special care should be taken when performing biopsies or any other bony intervention to infuse lidocaine within and over the periosteum.

The liver, spleen, and kidneys are frequently involved in vascular and extravascular interventions. A 2019 randomized controlled study showed that subcostal approaches to hepatic interventions are less painful than intercostal approaches.[40] When placing or exchanging a catheter involving the liver or kidneys, the entirety of the tract should be anesthetized, not just the subcutaneous tissues (Figure 4).

Conclusion

Inadequate pain control is an important source of patient dissatisfaction. However, using proper technique to administer local anesthesia can measurably reduce pain. Each patient represents an opportunity to improve and refine these techniques. With time and close attention to each patient, physicians may approach the goal of a nearly pain-free procedure.

References

1) Culp WC Jr, Culp WC. Practical application of local anesthetics. *J Vasc Interv Radiol.* 2011;22(2):111-118. doi: 10.1016/j.jvir.2010.10.005

2) Strazar AR, Leynes PG, Lalonde DH. Minimizing the pain of local anesthesia injection. *Plast Reconstr Surg.* 2013;132(3):675-684. doi: 10.1097/PRS.0b013e31829ad1e2

3) Farhangkhoee H, Lalonde J, Lalonde DH. Teaching medical students and residents how to inject local anesthesia almost painlessly. *Can J Plast Surg.* 2012;20(3):169-172. doi: 10.1177/229255031202000315

4) Koch SC, Acton D, Goulding M. Spinal Circuits for Touch, Pain, and Itch. *Annu Rev Physiol.* 2018;80:189-217. doi: 10.1146/annurev-physiol-022516-034303

5) Dubin AE, Patapoutian A. Nociceptors: the sensors of the pain pathway. *J Clin Invest.* 2010;120(11):3760-3772. doi: 10.1172/JCI42843

6) Cherobin ACFP, Tavares GT. Safety of local anesthetics. *An Bras Dermatol.* 2020;95(1):82-90. doi: 10.1016/j.abd.2019.09.025

7) Romagnoli S, Fanelli F, Barbani F, et al. CIRSE Standards of Practice on Analgesia and Sedation for Interventional Radiology in Adults. *Cardiovasc Intervent Radiol.* 2020;43(9):1251-1260. doi: 10.1007/s00270-020-02536-z

8) Thomson CJ, Lalonde DH. Randomized double-blind comparison of duration of anesthesia among three commonly used agents in digital nerve block. *Plast Reconstr Surg.* 2006;118(2):429-432. doi: 10.1097/01.prs.0000227632.43606.12.

9) Frank SG, Lalonde DH. How acidic is the lidocaine we are injecting, and how much bicarbonate should we add? *Can J Plast Surg.* 2012;20(2):71-73. doi: 10.1177/229255031202000207

10) Steele EA, Ng JD, Poissant TM, Campbell NM. Comparison of injection pain of articaine and lidocaine in eyelid surgery. *Ophthalmic Plast Reconstr Surg.* 2009;25(1):13-15. doi: 10.1097/IOP.0b013e3181912016

11) Cepeda MS, Tzortzopoulou A, Thackrey M, Hudcova J, Arora Ghandi P, Schumann R. Adjusting the pH of lidocaine for reducing pain on injection. *Cochrane Database Syst Rev.* 2010;(12):CD006581. doi: 10.1002/14651858.CD006581.pub2

12) Burns CA, Ferris G, Feng C, Cooper JZ, Brown MD. Decreasing the pain of local anesthesia: A prospective, double-blind comparison of buffered, premixed 1% lidocaine with epinephrine versus 1% lidocaine freshly mixed with epinephrine. *J Am Acad Dermatol.* 2006;54:128–131. doi: 10.1016/j.jaad.2005.06.043

13) Malamed SF, Tavana S, Falkel M. Faster onset and more comfortable injection with alkalinized 2% lidocaine with epinephrine 1:100,000. *Compend Contin Educ Dent.* 2013;34(1):10-20

14) Powell MF. Stability of lidocaine in aqueous solution: effect of temperature, pH, buffer, and metal ions on amide hydrolysis. *Pharm Res.* 1987;4:42–45. doi: 10.1023/a:1016477810629

15) Johansen RB, Schafer NC, Brown PI. Effect of extreme temperatures on drugs for prehospital ACLS. *Am J Emerg Med.* 1993;11:450–452. doi: 10.1016/0735-6757(93)90080-u

16) Hogan ME, vanderVaart S, Perampaladas K, Machado M, Einarson TR, Taddio A. Systematic review and meta-analysis of the effect of warming local anesthetics on injection pain. *Ann Emerg Med.* 2011;58:86–98.e1. doi: 10.1016/j.annemergmed.2010.12.001

17) Lundbom JS, Tangen LF, Wågø KJ, et al. The influence of Lidocaine temperature on pain during subcutaneous injection. *J Plast Surg Hand Surg.* 2017;51(2):118-121. doi: 10.1080/2000656X.2016.1194281

18) Mader TJ, Playe SJ, Garb JL. Reducing the pain of local anesthetic infiltration: Warming and buffering have a synergistic effect. *Ann Emerg Med.* 1994;23:550–554. doi: 10.1016/s0196-0644(94)70076-1

19) Yang CH, Hsu HC, Shen SC, Juan WH, Hong HS, Chen CH. Warm and neutral tumescent anesthetic solutions are essential factors for a less painful injection. *Dermatol Surg.* 2006;32:1119–1122. doi: 10.1111/j.1524-4725.2006.32254.x

20) Arendt-Nielsen L, Egekvist H, Bjerring P. Pain following controlled cutaneous insertion of needles with different diameters. *Somatosens Mot Res.* 2006;23:37–43. doi: 10.1080/08990220600700925

21) Gill HS, Prausnitz MR. Does needle size matter? *J Diabetes Sci Technol.* 2007;1:725-729. doi: 10.1177/193229680700100517

22) Watts AC, McEachan J. The use of a fine-gauge needle to reduce pain in open carpal tunnel decompression: a randomized controlled trial. *J Hand Surg [Br].* 2005;30:615–617. doi: 10.1016/j.jhsb.2005.06.021

23) Wågø KJ, Skarsvåg TI, Lundbom JS et al. The importance of needle gauge for pain during injection of lidocaine. *J Plast Surg Hand Surg.* 2016;50:115–118. doi: 10.3109/2000656X.2015.1111223

24) Ağaç E, Güneş UY. Effect on pain of changing the needle prior to administering medicine intramuscularly: A randomized controlled trial. *J Adv Nurs.* 2011;67:563–568. doi: 10.1111/j.1365-2648.2010.05513.x

25) Gajraj NM, Pennant JH, Watcha MF. Eutectic mixture of local anesthetics (EMLA) cream. Anesth Analg. 1994;78:574–583

26) Cárceles MD, Alonso JM, García-Muñoz M, Nájera MD, Castaño I, Vila N. Amethocaine-lidocaine cream, a new topical formulation for preventing venopuncture-induced pain in children. *Reg Anesth Pain Med.* 2002;27:289–295.

27) Kuwahara RT, Skinner RB. Emla versus ice as a topical anesthetic. *Dermatol Surg.* 2001;27:495–496. doi: 10.1046/j.1524-4725.2001.00343.x

28) van Wijk AJ, Hoogstraten J. Anxiety and pain during dental injections. *J Dent.* 2009;37:700–704. doi: 10.1016/j.jdent.2009.05.023

29) Okawa K, Ichinohe T, Kaneko Y. Anxiety may enhance pain during dental treatment. *Bull Tokyo Dent Coll.* 2005;46:51–58. doi: 10.2209/tdcpublication.46.51

30) Uman LS, Chambers CT, McGrath PJ, Kisely S. A systematic review of randomized controlled trials examining psychological interventions for needle-related procedural pain and distress in children and adolescents: An abbreviated Cochrane review. *J Pediatr Psychol.* 2008;33:842–854. doi: 10.1093/jpepsy/jsn031

31) Höfle M, Hauck M, Engel AK, Senkowski D. Viewing a needle pricking a hand that you perceive as yours enhances unpleasantness of pain. *Pain.* 2012;153:1074–1081. doi: 10.1016/j.pain.2012.02.010

32) Mendell LM. Constructing and deconstructing the gate theory of pain. *Pain.* 2014;155(2):210-216. doi: 10.1016/j.pain.2013.12.010

33) Nanitsos E, Vartuli R, Forte A, Dennison PJ, Peck CC. The effect of vibration on pain during local anaesthesia injections. *Aust Dent J.* 2009;54:94-100. doi: 10.1111/j.1834-7819.2009.01100.x

34) Baxter AL, Cohen LL, McElvery HL, Lawson ML, von Baeyer CL. An integration of vibration and cold relieves venipuncture pain in a pediatric emergency department. *Pediatr Emerg Care.* 2011;27(12):1151-1156. doi: 10.1097/PEC.0b013e318237ace4

35) Patel BK, Wendlandt BN, Wolfe KS, et al. Comparison of Two Lidocaine Administration Techniques on Perceived Pain from Bedside Procedures - A Randomized Clinical Trial. *Chest.* 2018;154(4):773-780. doi: 10.1016/j.chest.2018.04.018

36) Martires KJ, Malbasa CL, Bordeaux JS. A randomized controlled crossover trial: Lidocaine injected at a 90-degree angle causes less pain than lidocaine injected at a 45-degree angle. *J Am Acad Dermatol.* 2011;65:1231–1233. doi: 10.1016/j.jaad.2011.04.011

37) Michael AA, Moorjani GR, Peisajovich A, Park KS, Sibbitt WL Jr, Bankhurst AD. Syringe size: Does it matter in physician-performed procedures? *J Clin Rheumatol.* 2009;15:56–60. doi: 10.1097/RHU.0b013e31819c1fc4

38) Scarfone RJ, Jasani M, Gracely EJ. Pain of local anesthetics: rate of administration and buffering. *Ann Emerg Med.* 1998;31(1):36-40. doi: 10.1016/s0196-0644(98)70278-1

39) Serour F, Mandelberg A, Mori J. Slow injection of local anaesthetic will decrease pain during dorsal penile nerve block. *Acta Anaesthesiol Scand.* 1998;42(8):926-928. doi: 10.1111/j.1399-6576.1998.tb05351.x

40) Pezeshki Rad M, Abbasi B, Morovatdar N, Sadeghi M, Hashemi K. Pain in percutaneous liver core-needle biopsy: a randomized trial comparing the intercostal and subcostal approaches. *Abdom Radiol (NY).* 2019;44(1):286-291. doi: 10.1007/s00261-018-1704-z

An Overview of Extracorporeal Membrane Oxygenation

Felipe Sanchez Tijmes, MD; Andrea Fuentealba, MD; Mario Arias Graf, MD; Stefano Zamarin Brocco; Gauri Rani Karur MBBS, MD; Elsie Nguyen, MD; Yasbanoo Moayedi, MD, MHSc; Kate Hanneman, MD, MPH

Extracorporeal membrane oxygenation (ECMO) is an advanced life support technique employed for severe respiratory, cardiac, or combined cardiopulmonary failure refractory to conventional treatments.[1] The main objective of ECMO is to oxygenate systemic venous blood and remove carbon dioxide while the failing lung or heart are allowed to recover, or to serve as a bridge to longer-term life support therapies or transplantation.[2]

While traditionally viewed as a rescue therapy, ECMO has seen a notable surge in recent decades. Data from the international registry of the Extracorporeal Life Support Organization (ELSO) show that 16,803 ECMO procedures were conducted across 557 healthcare institutions worldwide in 2022.[3]

Complications related to ECMO are identified in nearly half of patients.[4] The most common include hemorrhage, thromboembolic disease, renal failure, sepsis, and vascular injury.[4]

Noninvasive imaging plays a pivotal role in the assessment of ECMO patients, serving as a critical tool to detect complications or malpositioning of ECMO cannulas.[5] Consequently, an understanding of normal and abnormal imaging appearances is imperative. Furthermore, an awareness of the hemodynamic disturbances that may arise with ECMO, necessitating specific considerations when planning contrast-enhanced studies, is essential for radiologists and imaging technologists.[6] This article reviews the fundamentals of ECMO, explores the various cannulation techniques, and provides practical insights for the technical planning of contrast-enhanced CT studies in patients under ECMO support.

Fundamental Concepts

A standard ECMO circuit consists of several key components: an inflow cannula that drains deoxygenated venous blood from the body, a mechanical pump facilitating circulation of blood within the system, a membrane oxygenator that removes carbon dioxide and replenishes oxygen, a heat exchanger to warm blood as it passes through the oxygenator, and an outflow, or reinfusion, cannula that returns the oxygenated blood to circulation (Figure 1).[7]

There are two primary ECMO configurations, differentiated by the location and function of the return cannula: Veno-venous (VV) and Veno-arterial (VA) circuits. VV-ECMO is designed to provide respiratory support without cardiac support, as the oxygenated blood is reinfused to the systemic venous circulation. Therefore, this configuration relies on optimal cardiac function and is used only when cardiac output is adequate.

Conversely, VA-ECMO provides cardiac and respiratory support, bypassing the heart and lungs in a fashion similar to conventional cardiopulmonary bypass. In VA-ECMO, the return cannula is placed in the systemic arterial circulation, so the external pump aids in circulating the blood throughout the body.[7,8]

Affiliations: Joint Department of Medical Imaging, University Health Network, University of Toronto; Toronto General Hospital, Toronto, Ontario, Canada (Drs Sanchez Tijmes, Karur, Nguyen, Hanneman); Department of Medical Imaging, Clinica Santa Maria, Universidad de los Andes, Santiago, Chile (Drs Sanchez Tijmes, Arias Graf); Department of Radiology, University of Colorado - Anschutz Medical Campus, Aurora, Colorado (Dr Fuentealba); Department of Radiology, Clinica las Condes, Universidad Finis Terrae, Santiago, Chile (Dr Zamarin Brocco); Division of Cardiology, Peter Munk Cardiac Centre, Toronto General Hospital, University Health Network, University of Toronto, and Toronto General Hospital, Toronto, Ontario, Canada (Dr Moayedi).
Disclosures: None. Presented as an educational exhibit at the 2021 Radiological Society of North America Annual Meeting. Chicago, Illinois.
Dr Hanneman is also a member of the *Applied Radiology* Editorial Advisory Board. She was recused from the double-blinded peer review process for this manuscript.
Keywords: ECMO, Chest CT, Chest X-ray, Veno-venous ECMO, Veno-arterial ECMO.

Figure 1. Fundamentals of the ECMO circuit. Deoxygenated venous blood is drained from the body through a drainage cannula and circulated through the ECMO machine by a mechanical pump. The blood is oxygenated, and carbon dioxide is removed by a membrane oxygenator connected to an oxygen-air blender, conventionally referred to as a sweep gas. Oxygenated blood is then reinfused by an outflow cannula to the systemic arterial (VA-ECMO) or venous (VV-ECMO) vascular system.

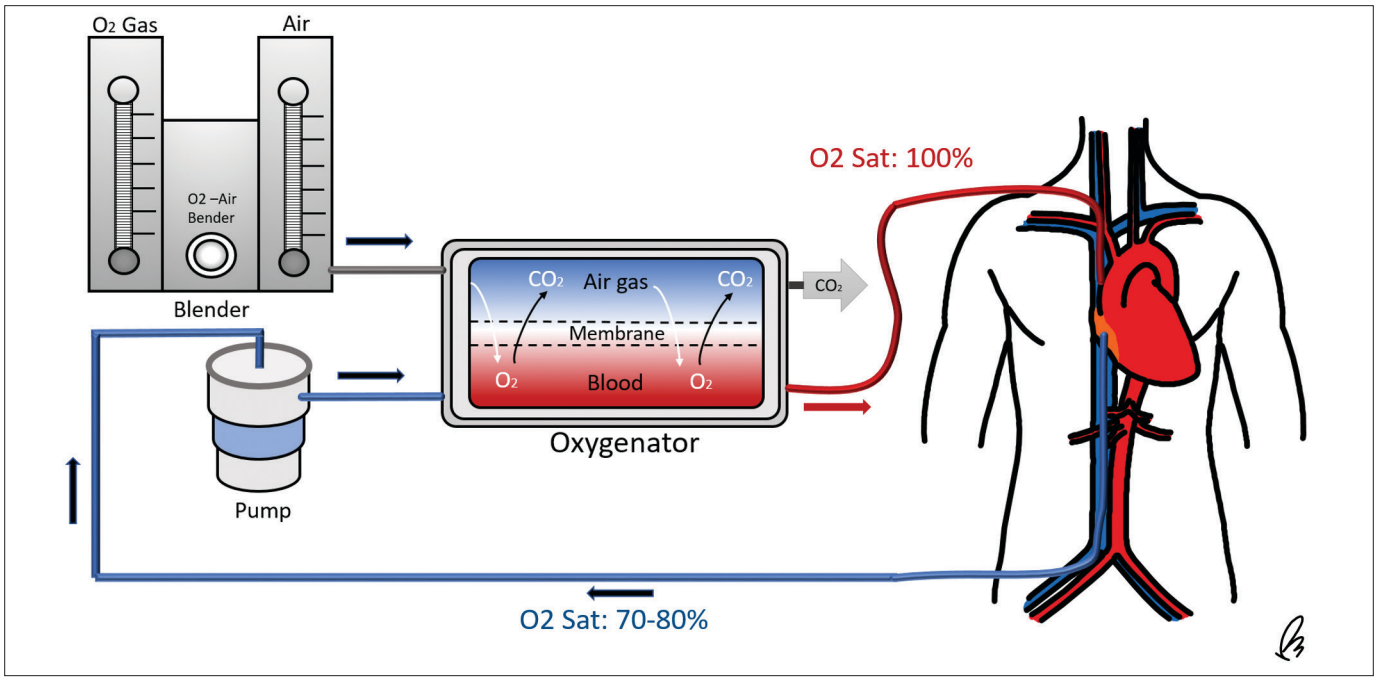

Figure 2: Cannulation strategies for VV-ECMO. (A) Inferior vena cava-right atrium (IVC-RA). The drainage cannula should be placed within the IVC through a femoral vein, and the reinfusion cannula in the superior cavoatrial junction or RA through the right internal jugular vein (IJV) (B) Femoral vein-femoral vein. Both cannulas enter through different femoral veins. The drainage cannula is located within the IVC in a lower position than in the IVC-RA approach. The reinfusion cannula should be located higher than the drainage cannula, at the level of the RA or cavoatrial junctions. (C) Single cannulation. A double lumen bicaval cannula with three ports is inserted through the right IJV. The proximal and distal ports drain deoxygenated blood and should be located in the superior and inferior vena cava, respectively. The mid port reinfuses oxygenated blood and should rest in the RA, aiming towards the tricuspid valve.

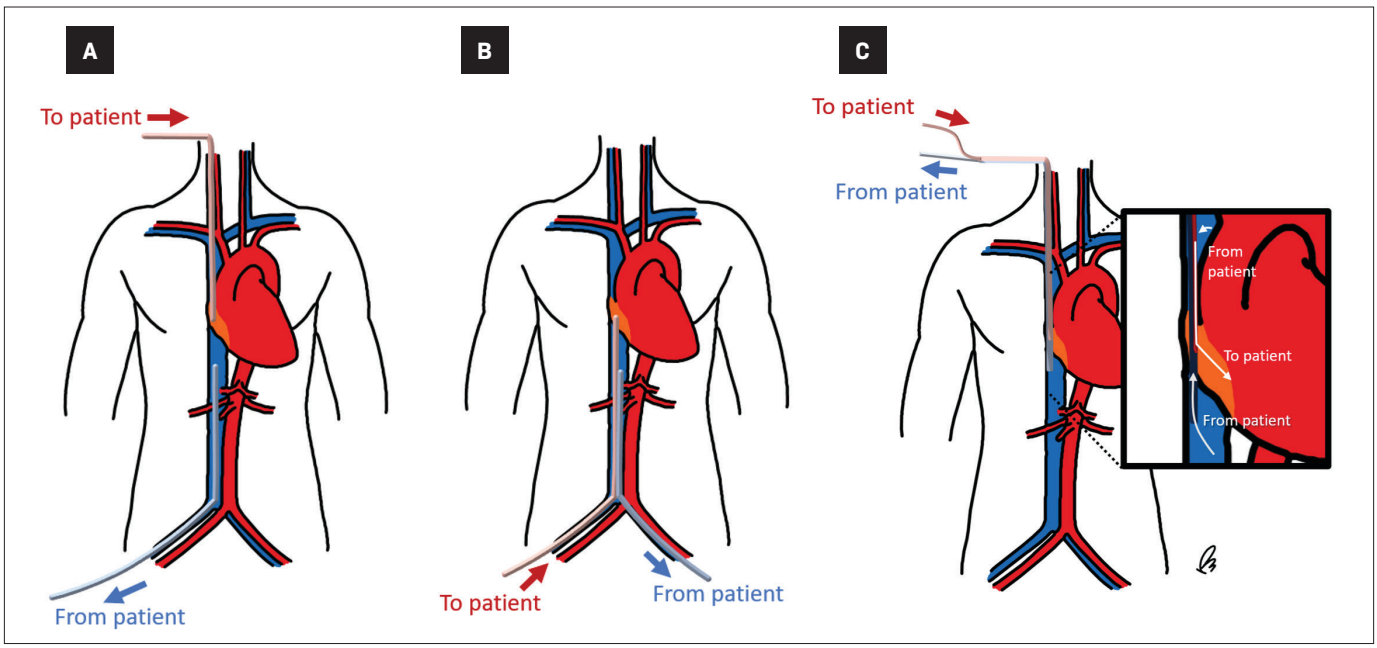

Figure 3. IVC-RA approach in an adult with severe ARDS due to COVID-19. Frontal chest X-ray (A) and chest CT coronal reformat (B) show the reinfusion cannula located at the level of superior cavoatrial junction (red arrows) and the drainage cannula within the inferior cavoatrial junction (blue arrows). Drainage cannula side-ports are also noted (yellow arrowheads). Single cannulation VV-ECMO in an adult with influenza pneumonia, frontal chest X-ray (C) and chest CT coronal reformat (D) depict a dual lumen bicaval cannula. The drainage ports are located within the superior SVC and inferior cavoatrial junction (blue arrows), and the reinfusion port rests within the superior cavoatrial junction (red arrowheads). Extensive bilateral airspace and interstitial opacities are seen in both patients.

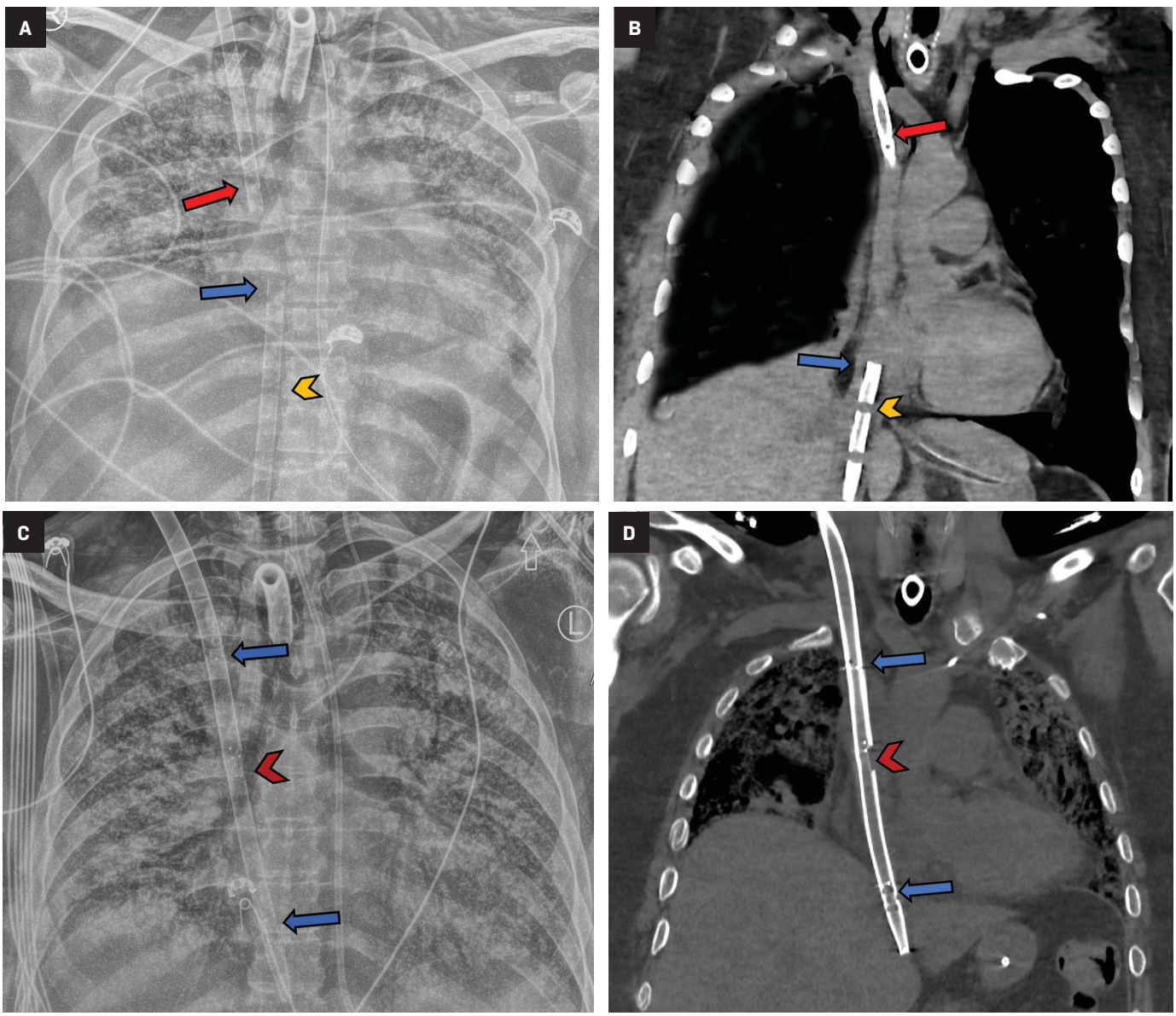

There are various cannulation alternatives for VV- and VA-ECMO; these are indicated based on availability and patient conditions and lead to different imaging appearances.[9]

Role of Imaging

Noninvasive imaging plays a pivotal role in the assessment of cannula positioning and timely detection of complications.[10] Transthoracic or transesophageal echocardiography and fluoroscopy are usually used for guidance during initial cannulation.[9,11] Chest and abdominal radiography is useful following initial placement to confirm adequate cannula positioning and reveal any unintended migration. Additionally, the radiographs may depict early signs of complications such as hemothorax or pneumothorax.

Ultrasound is a portable and readily available modality that may be employed to monitor complications such as insertion site hematomas, deep vein thrombosis, or distal limb hypoperfusion.

Computed tomography may be required to evaluate suspected complications that cannot be fully

Figure 4. Cannulation strategies for veno-arterial ECMO. In central VA-ECMO (A), the drainage and reinfusion cannulas are positioned directly into the RA and ascending aorta, respectively. Central VA-ECMO is typically initiated in the operating room for postcardiotomy patients who are unable to be weaned off cardiopulmonary bypass. In peripheral VA-ECMO: The venous cannula may be placed within the SVC, RA, or IVC and may be inserted through a femoral vein or, less frequently, the IJV. The arterial cannula is most commonly inserted through a femoral vein contralateral to the drainage cannula, terminating in the external or common iliac arteries, or within the distal abdominal aorta (B). Less frequently, the arterial cannula may be inserted through the axillary, common carotid, innominate, or subclavian arteries towards the ascending aorta (C).

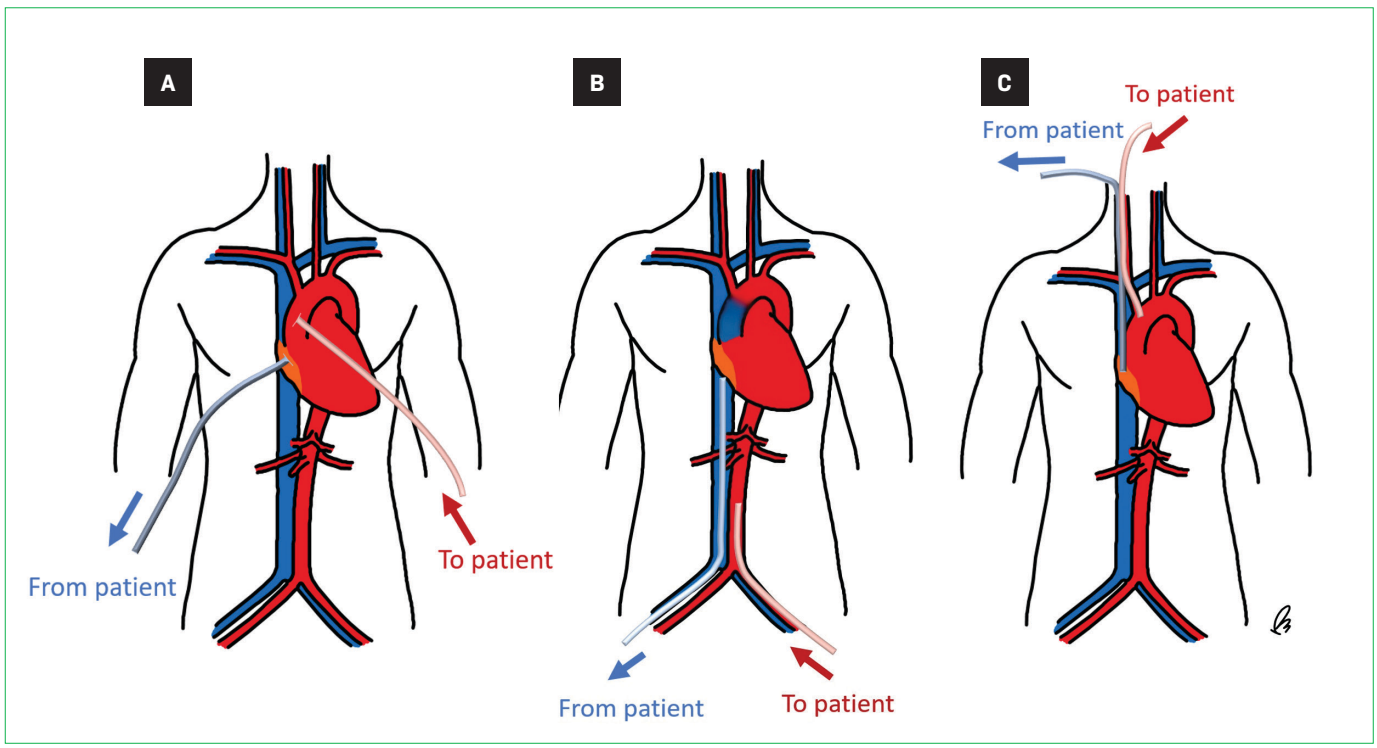

Figure 5. Central VA-ECMO in an adult with severe myocarditis and ARDS. Frontal chest X-ray (A) and chest CT coronal reformat (B) show transthoracic ECMO cannulas. The drainage cannula enters through the inferior SVC and terminates near the inferior cavoatrial junction (blue arrows). The arterial cannula enters through the ascending aorta towards the proximal aortic arch (red arrows). There are bilateral interstitial and airspace inflammatory opacities in both lungs.

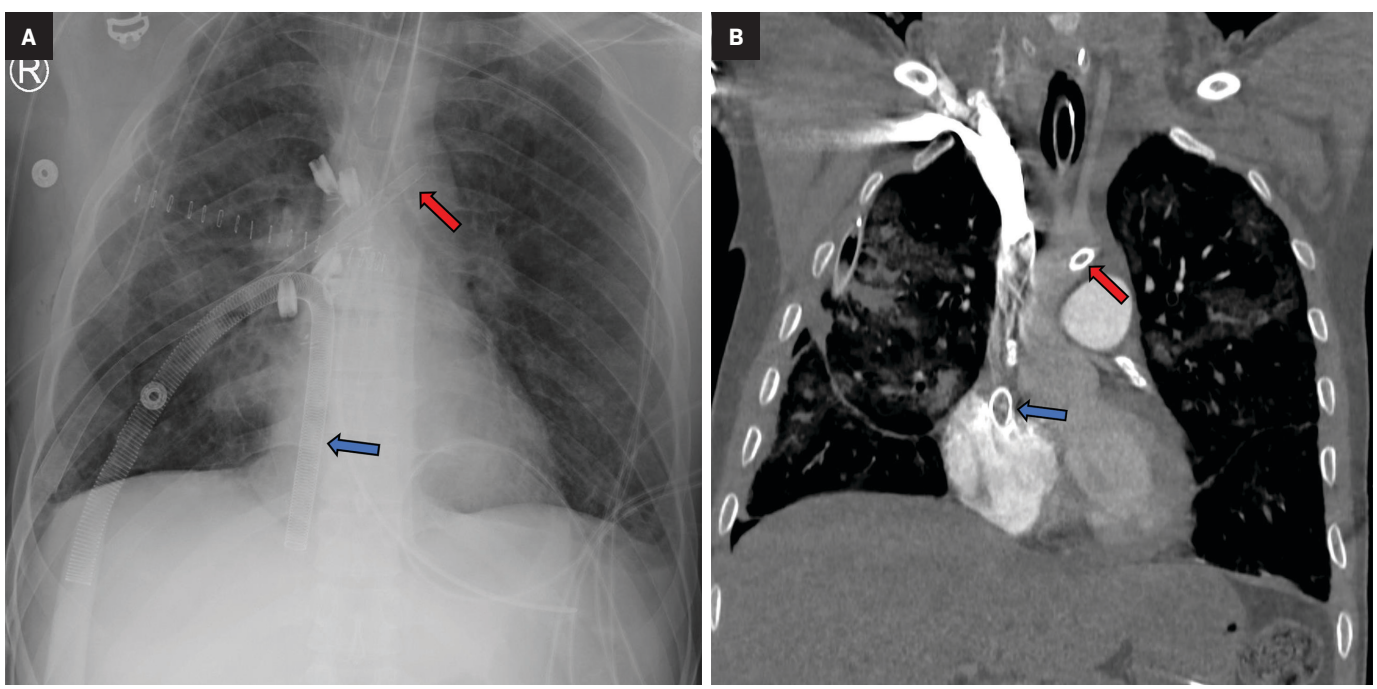

Figure 6. Peripheral VA-ECMO in an adult with dilated cardiomyopathy and cardiogenic shock. Abdominal CT scout view (A) and coronal reformats (B, C) show the drainage cannula within the hepatic IVC (blue arrows) and the arterial cannula within the left external iliac artery (red arrows). The left ventricle is severely dilated and shows multiple peripheral thrombi (arrowheads).

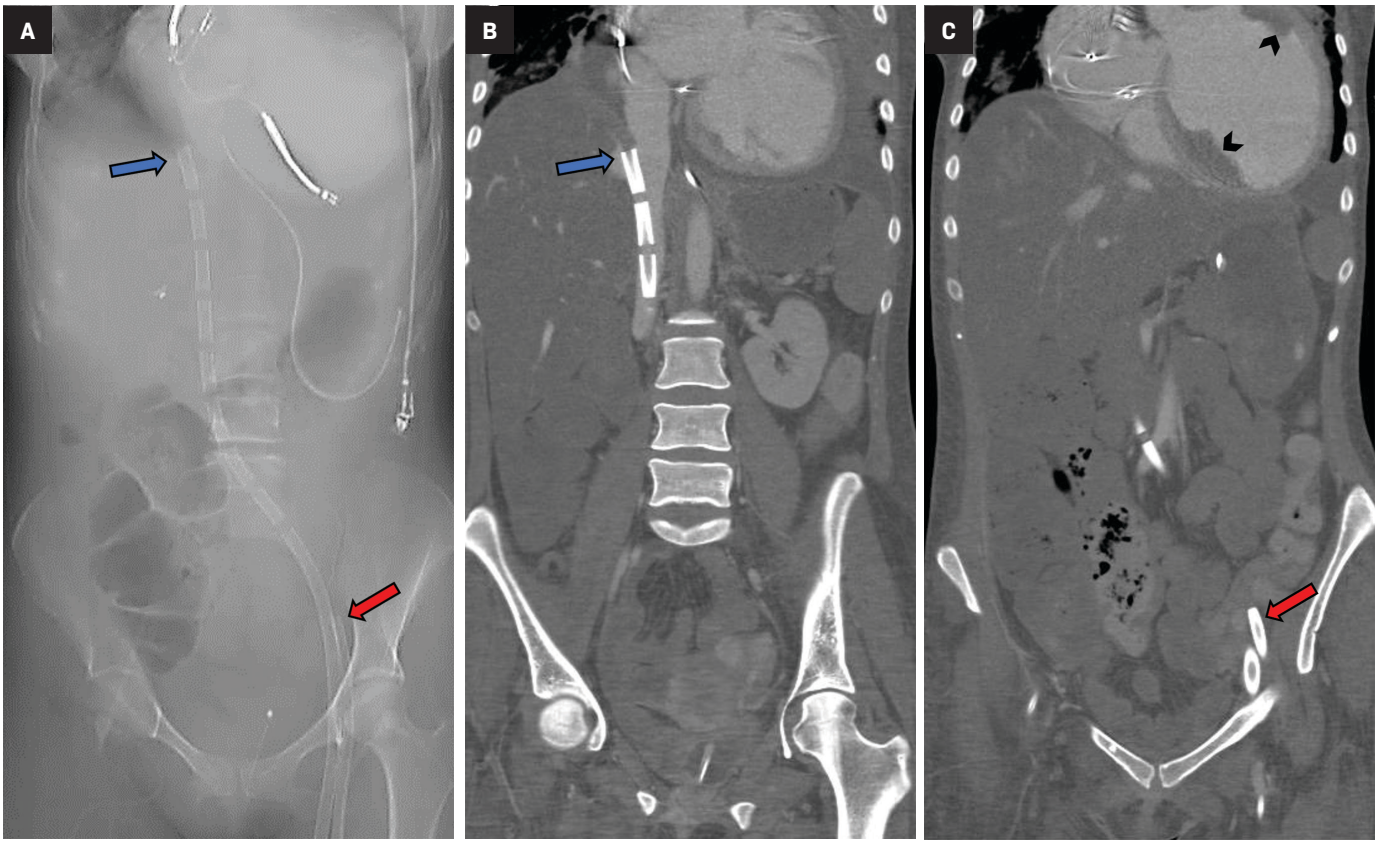

evaluated by radiography or ultrasound. The modality's high spatial resolution allows for accurate assessment of cannula positioning. Additionally, administration of intravenous contrast allows for comprehensive evaluation of complications, including bleeding, vascular injury, and thromboembolic disease.

Veno-Venous ECMO: Subtypes and Normal Appearances

VV-ECMO may be considered in patients with severe, acute, and reversible respiratory failure that is refractory to standard medical management [12] or those who require a bridge to lung transplantation.[13] A complete list of indications may be found in the latest ELSO guidelines.[12] At present, the only absolute contraindication for initiating VV-ECMO is an expected inability of the patient to recover without a feasible plan for decannulation.[12]

VV-ECMO can be performed either with two single-lumen cannulas or with a single dual-lumen cannula (Figure 2).[14] When two single cannulas are used, they may be placed in the following locations:

- **Inferior Vena Cava - Right atrium** The drainage cannula should be positioned within the IVC through a femoral vein with the side ports at the level of the hepatic veins, and the reinfusion cannula should be positioned in the superior cavoatrial junction or right atrium through the right IJV.[9,12,14] Direction of the flow may be switched, but the latter configuration is preferred.[14,15] Correct positioning of the cannulas is critical to prevent recirculation of reinfused oxygenated blood into the ECMO circuit before entering the systemic circulation; however, there is no standard distance that should be maintained between the ports.[12,16]
- **Femoral vein-Femoral vein**. In this approach, both cannulas enter through different femoral veins. The drainage cannula is located within the IVC, usually lower than with the IVC-RA approach. The reinfusion cannula should be located higher than the drainage cannula, at the level of the right atrium or cavoatrial junctions. This approach poses a higher risk of oxygenated blood recirculation, as both cannulas may be positioned closer together, but the complexity of insertion is lower, and it avoids the risk of neck vessel cannulation injury.[8,17]

Single cannulation is achieved by inserting a double-lumen bicaval cannula with three ports through the right IJV. The proximal and distal

Figure 7. Hemodynamics of peripheral VA-ECMO and dual circulation. During femoral arterial cannulation, the reinfused oxygenated blood takes a non-physiological route towards the upper body, counter to the direction of blood propelled by the patient's heart. This can lead to a phenomenon termed "dual circulation," in which the lower body receives adequate oxygenation while the upper body experiences hypoxemia (A). Contrast-enhanced chest CT sagittal reformat (B) shows a watershed area at the distal ascending aorta, as the reinfused retrograde oxygenated blood competes with the antegrade deoxygenated blood coming from the bypassed lungs (arrow).

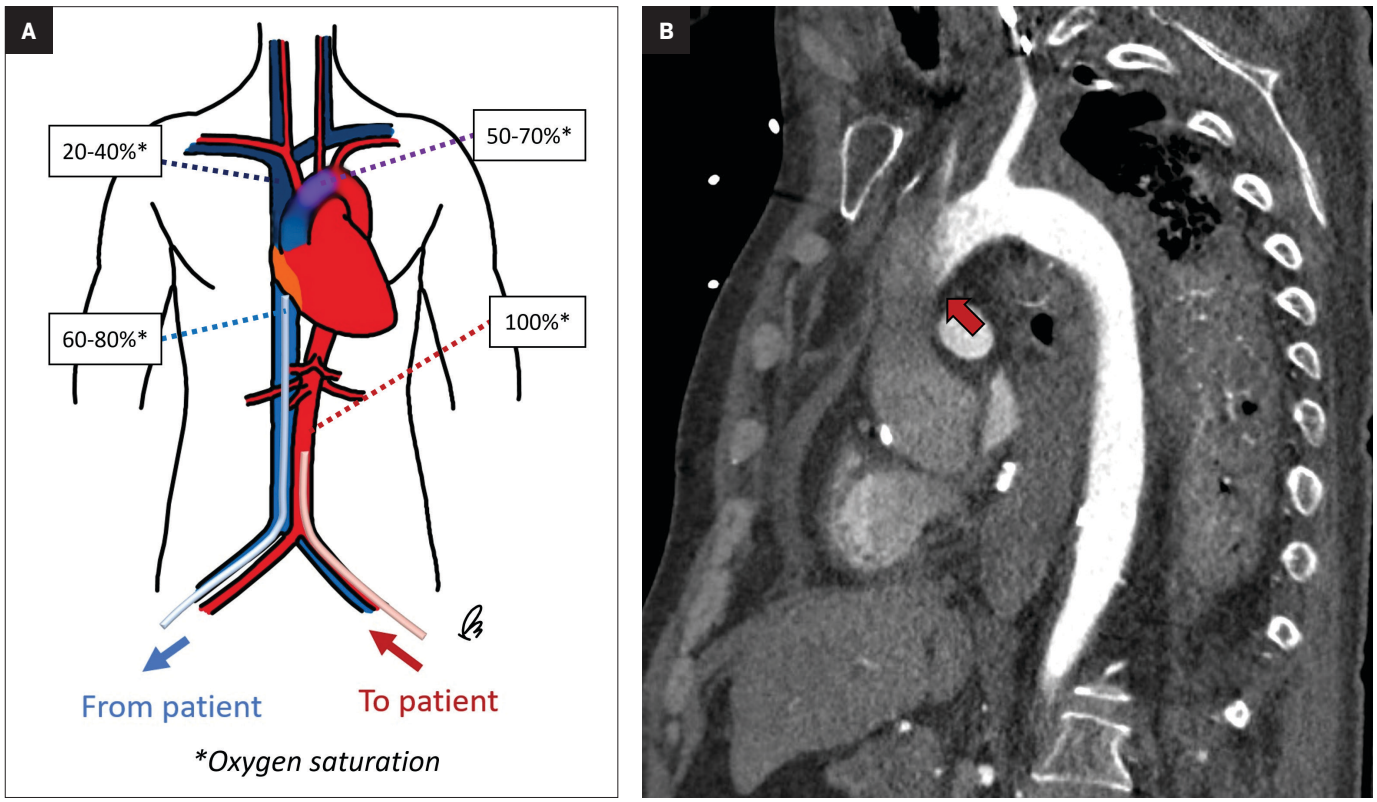

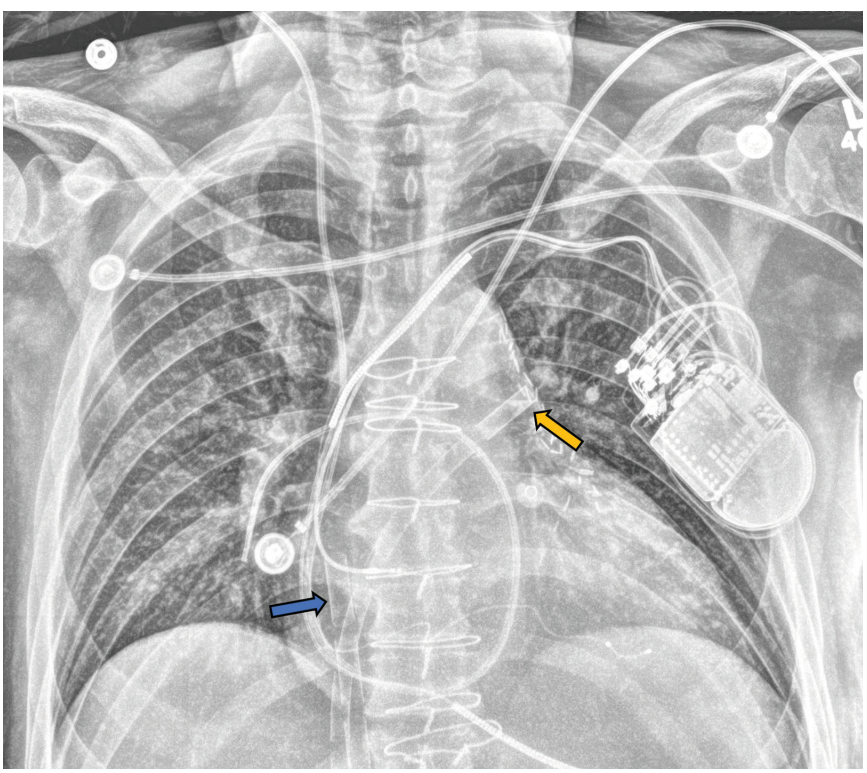

Figure 8. VA-ECMO in an adult with decompensated heart failure. Frontal chest X-ray shows an inflow cannula that has slightly migrated towards the RA (blue arrow). A transeptal venting cannula courses from the IVC towards the RA (yellow arrow).

Table 1: Strategies for optimizing contrast-enhanced CT during ECMO.

TYPE OF ECMO		AORTA CTA	HEAD & NECK CTA	PULMONARY ARTERY CTA	CARDIAC CHAMBERS	PORTAL-VENOUS PHASE
VA-ECMO	Central / Upper body Peripheral	Contrast should be administrated through the oxygenator inlet without modifying ECMO flow.		Contrast should be administrated through a central venous line while reducing ECMO flow as much as possible, in order to avoid pulmonary circulation bypass.	Contrast administered through the oxygenator inlet. Aim for a delayed equilibrium phase as not all the cardiac chambers may opacify at the first pass of contrast bolus.	Administer contrast through the oxygenator inlet without modifying ECMO flow.
	Femoral Peripheral	In patients with low cardiac output, contrast should be injected through the oxygenator inlet without modifying ECMO flow (retrograde filling). In patients with preserved cardiac function, use of a central venous line is recommended while reducing ECMO flow.	Contrast should be administrated through a central venous line while reducing ECMO flow.			
VV-ECMO	IVC-RA	Contrast should be administered through the oxygenator inlet with a usual ECMO flow. If a central venous line is required for injection, it is advisable to reduce ECMO flow to decrease recirculation of intravenous contrast				
	F-F					

VA-ECMO: Veno-arterial ECMO; VV-ECMO: Veno-venous ECMO; IVC-RA: Inferior vena cava-Right atrium; F-F: femoral vein-femoral vein. Based on references 40-43.

ports drain deoxygenated blood and should be located in the superior and inferior vena cava, respectively. The mid port reinfuses oxygenated blood from the ECMO circuit and should rest in the RA, aiming towards the tricuspid valve.[9,18] While dual-lumen VV-ECMO presents greater technical challenges compared to double cannulation methods, it offers advantages such as reduced recirculation rates and reduced bleeding risk due to the need for just a single vessel puncture. This is largely because most of the deoxygenated blood is drained from the proximal part of the cannula at the SVC (Figure 3).[19,20]

Veno-Arterial ECMO: Subtypes and Normal Appearances

VA-ECMO has evolved as a salvage strategy for patients with cardiogenic shock or cardiac arrest unresponsive to conventional treatments.[21,22] However, lack of clear evidence has resulted in a low-level recommendation and no clear society-endorsed guidelines.[23,24] In individuals experiencing severe yet potentially reversible cardiac injury like myocarditis, post-cardiotomy shock, or myocardial ischemia, VA-ECMO can serve as a bridge to recovery. Alternatively, for those with acute exacerbations of chronic cardiac failure or extensive myocardial infarction, VA-ECMO might be employed as a bridge to candidacy for a longer-term left ventricular assist device or heart transplantation.[25,26]

As in VV-ECMO, different circuit configurations account for distinct imaging appearances. The two main approaches are central and peripheral cannulation (Figure 4).[27] Central VA-ECMO is typically initiated in the operating room for post-cardiotomy patients who cannot be weaned off cardiopulmonary bypass. The drainage and reinfusion cannulas are generally positioned directly into the RA and ascending aorta, respectively (Figure 5).[28] With this configuration, the reinfused, oxygenated blood circulates in an antegrade, physiological direction. Owing to its invasive character, central VA-ECMO is primarily used during surgery when a patient is experiencing cardiogenic shock while the chest is still open.[29]

Peripheral VA-ECMO is established by cannulating a peripheral vein and artery. A key advantage of peripheral VA-ECMO is more rapid initiation; this method can be implemented outside of the operating room and even during ongoing chest compressions.[30] The venous cannula may be strategically placed within the SVC, RA, or IVC with insertion through a femoral vein or, less frequently, the IJV. [31] The arterial cannula is most commonly inserted through a femoral artery, terminating in the external or common iliac arteries or within the distal abdominal aorta (Figure 6).[31] Though this approach is faster and technically less complex, the reinfused oxygenated blood takes a nonphysiological route towards the upper body, con-

Figure 9. Contrast CT studies in ECMO patients. (A) Thoracic aorta CT angiography of an adult connected to peripheral VA-ECMO. Contrast was administered through a peripheral venous line while decreasing ECMO flow. Coronal reformat shows adequate opacification of the thoracic aorta (red arrow) and poor opacification of the abdominal aorta (blue arrow) as there is decreased antegrade flow secondary to cardiac failure. (B) Coronal reformat of a CT pulmonary angiogram in an adult VV-ECMO patient with respiratory failure resulting from influenza pneumonia. There is sufficient opacification of the pulmonary arterial vasculature. Contrast was administered through a left peripheral venous line. ECMO flow was decreased during acquisition to avoid recirculation, and no contrast was seen entering the inflow cannula (blue arrow). (C) Coronal reformat of a portal venous phase CT in a VV-ECMO patient. A peripheral contrast injection was performed while maintaining ECMO flow, followed by a delayed CT acquisition (90 seconds after injection). There is adequate parenchymal and cardiac chamber opacification.

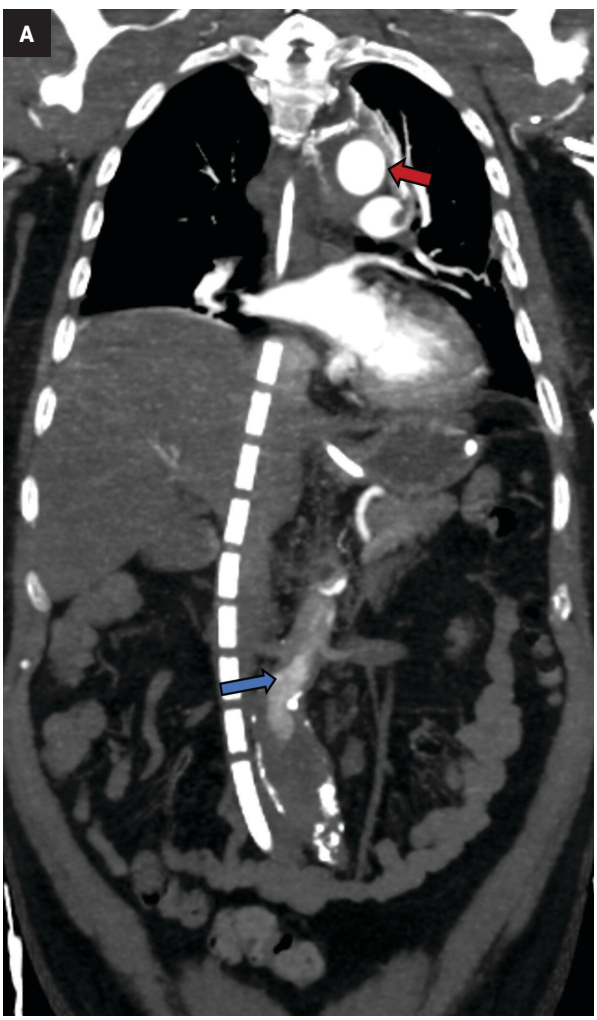

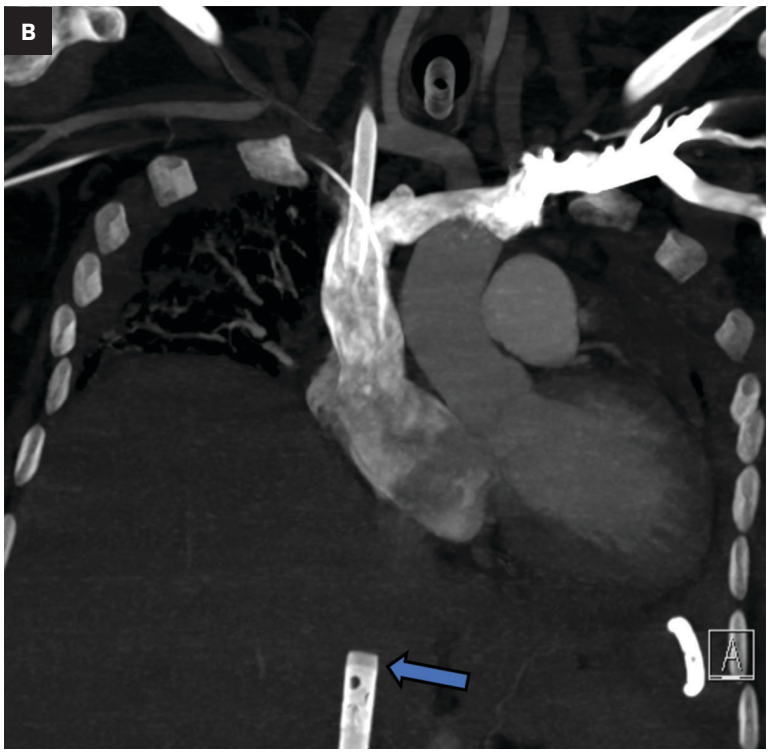

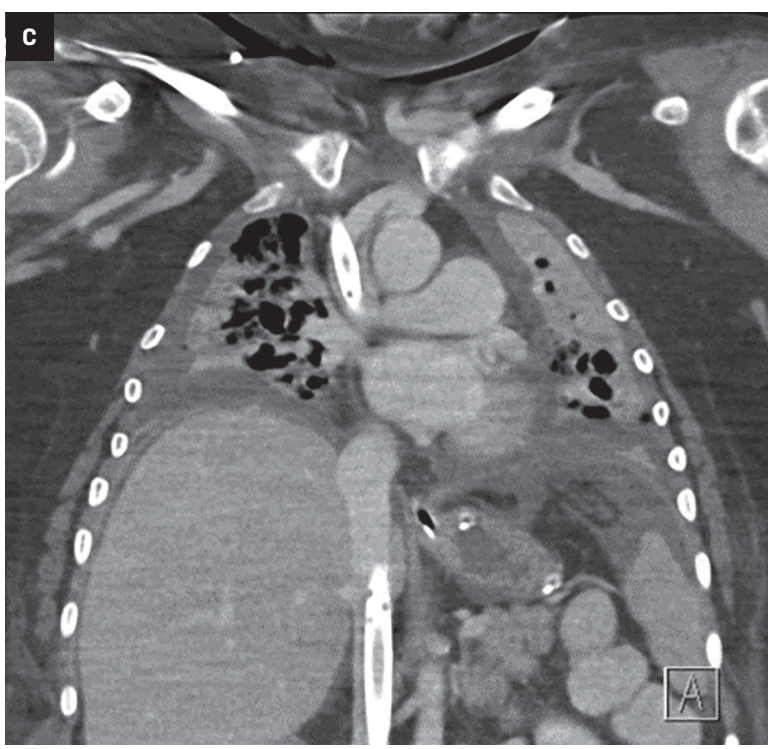

trary to the natural direction of the antegrade cardiac output.[32] This can lead to a phenomenon termed "dual circulation," also known as "Harlequin syndrome" or "North-South syndrome." In this scenario, the lower body receives adequate oxygenation while the upper body experiences hypoxemia. The reinfused oxygenated blood supplies the lower body and then is drained by the IVC cannula. In contrast, the upper body is supplied mostly with desaturated blood from the left ventricle, which then drains to the SVC and circulates through the failing lungs without passing through the ECMO machine (Figure 7).[33]

Less frequently, the arterial cannula

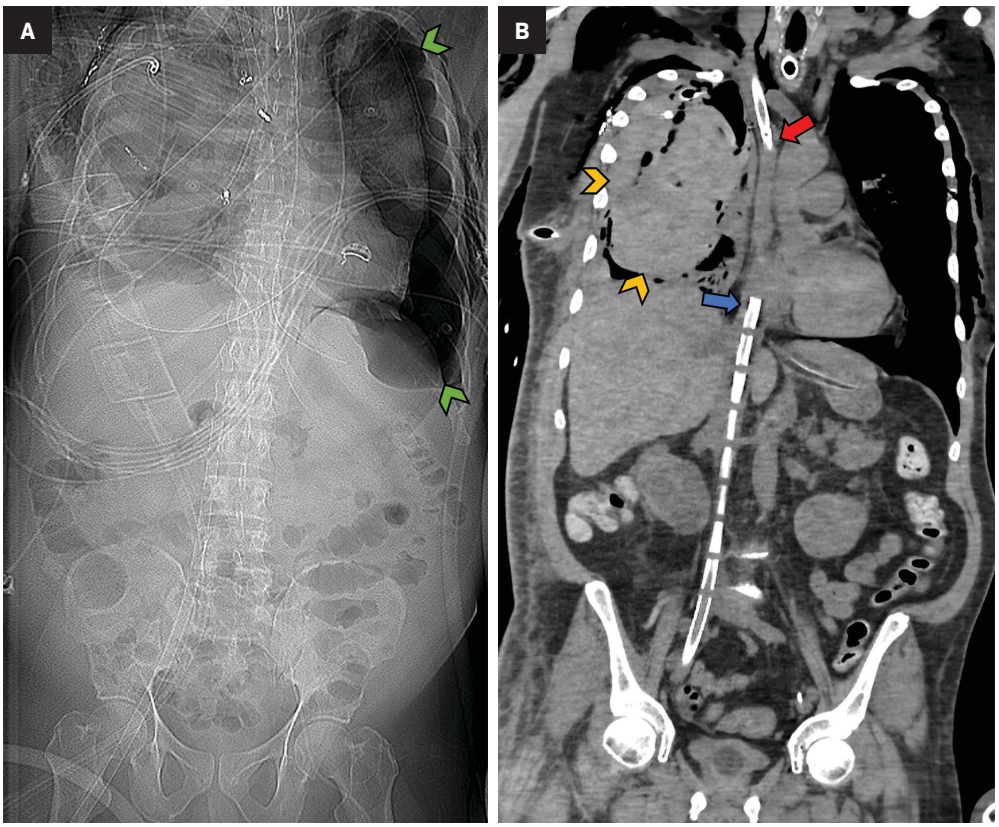

Figure 10. An adult connected to VV-ECMO owing to severe COVID-19 presented an abrupt decrease in hemoglobin. Chest, abdomen, and pelvis CT scout views (A) and coronal reformats (B) show a large, right-pleural hematoma (yellow arrowheads). There is also a large left pneumothorax (green arrowheads). The inflow (blue arrow) and outflow (red arrow) cannulas are located within the SVC and inferior cavoatrial junction.

may be inserted through the axillary, common carotid, innominate, or subclavian arteries toward the ascending aorta.[34] This approach provides a more physiological anterograde flow of deoxygenated blood, facilitates ambulation, diminishes the risk of limb ischemia, and may increase cerebral oxygen saturation levels. However, it is associated with an increased risk of bleeding and requires surgical placement.[35]

When VA-ECMO is used in the setting of severe left ventricular dysfunction, left-heart, end-diastolic pressures can increase significantly and cause pulmonary congestion and edema. Left-heart unloading or venting can be achieved by various interventions, including placement of a transeptal cannula connected to the venous ECMO circuit within the left atrium,[36] which should not be misinterpreted as an abnormally positioned cannula (Figure 8). Additional temporary devices such as a heart pump or an intra-aortic balloon pump may be used in conjunction with VA-ECMO to help further unload the left ventricle.[37-39]

Contrast-enhanced Computed Tomography

Several factors must be considered to ensure the success of contrast-enhanced CT studies for patients undergoing ECMO circulation (Table 1, Figure 9). The contrast distribution patterns can differ from those with normal physiology and are determined by the unique hemodynamic changes induced by the ECMO circuit.[40]

Patients with VV-ECMO typically have normal cardiac output and similar hemodynamics to patients without extracorporeal support. For such patients, intravenous contrast should be administrated through the oxygenator inlet within the ECMO machine. While a fraction of the contrast might recirculate through the ECMO circuit before entering the systemic arterial circulation, the amount is generally not significant and ECMO flow can be maintained during the examination. Recirculation of IV contrast is higher when a venous line is used for injection. In these instances, it is advisable to reduce ECMO flow during injection.[41]

Different strategies are required for VA-ECMO contingent upon the imaging target, arterial cannulation strategy, and the patient's cardiac output.[42] When systemic arterial enhancement is required, the oxygenator pathway is recommended for patients with either central or upper body peripheral cannulation. For those undergoing femoral cannulation, the contrast delivery method hinges on the interplay between cardiac output and ECMO flow rates. In patients with low cardiac output, oxygenator injection with retrograde filling of the aorta is favored while maintaining the ECMO flow. Conversely, injection through a venous line is preferred for patients with higher cardiac outputs while ECMO flow should be decreased, if safe to do so,

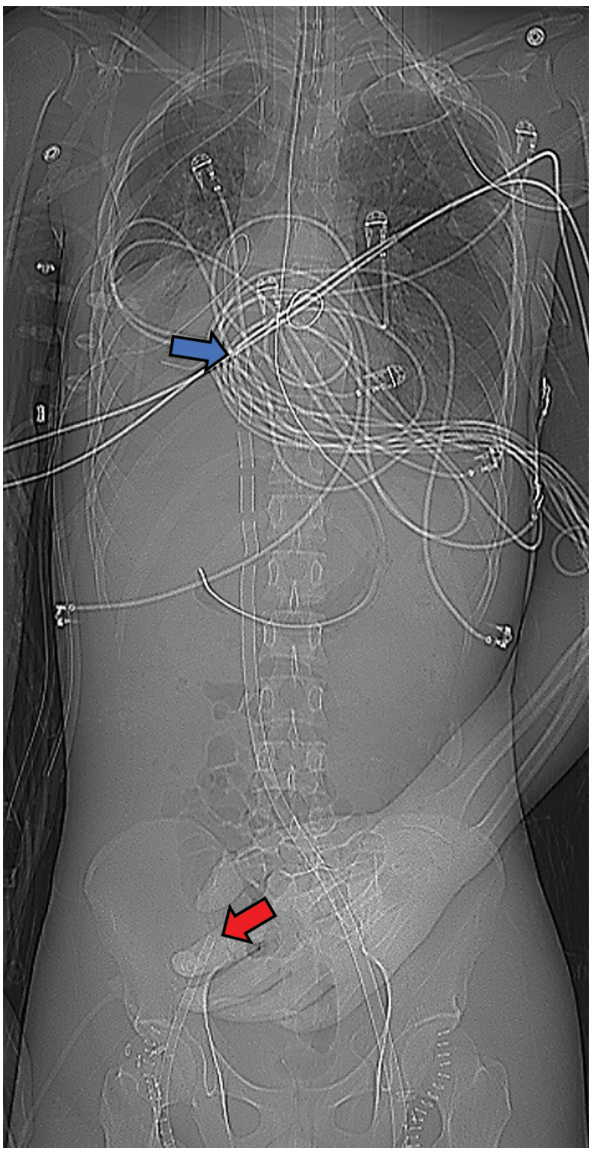

Figure 11. An adult with altered mental status after decannulation of VA-ECMO. Pre-cannulation CT scout image (A) shows the inflow (blue arrow) and outflow (red arrow) cannulas at the level of the inferior cavoatrial junction and left common iliac artery. Axial (B) noncontrast brain CT obtained post-decannulation show a large acute left frontal intraparenchymal hematoma with mild adjacent edema (yellow arrow).

during the acquisition phase.[41-43]

Pulmonary artery evaluation is challenging for all VA-ECMO configurations, as blood bypasses the pulmonary arteries. Contrast should be administered through a venous line while reducing the pump flow rate as much as possible.[42]

If parenchymal enhancement is required (ie, a portal-venous phase), contrast should be injected through the oxygenator, and ECMO flow can be maintained (applicable for all cannulation strategies).[41]

To ensure patient safety, it is recommended that contrast-enhanced CT studies be performed with a perfusionist present, particularly when adjustments to ECMO flow are required.

A Range of Potential Complications

The overall benefit, incidence of adverse events, and mortality associated with ECMO remain topics of ongoing debate. Various meta-analyses and registries report overall in-hospital survival rates for patients with ECMO in the range of 38-43%.[4,44-47]

Patients with ECMO are at increased risk of bleeding, given their need for anticoagulation and higher prevalence of coagulopathies compared to the general population.[48] Nearly half of patients experience hemorrhage, with the cannulation and surgical areas as the most common sites of bleeding, followed by hemothoraces and hemopericardium.[44,48] Chest radiography is useful for identifying hemothoraces and hemopericardium as new pleural collections or enlargement of the cardiopericardial silhouette, respectively, which can be confirmed by CT (Figure 10).

Neurological complications, while less frequent, are associated with significant morbidity and mortality. Intracranial hemorrhage and ischemic

Figure 12. Vascular complications in an adult VA-ECMO patient, status post-aortic valve replacement. CT scout image (A) shows the inflow (blue arrow) and outflow (red arrow) cannulas at the level of the inferior cavoatrial junction and left external iliac arteries. Contrast-enhanced axial chest CT (B) shows a large central pulmonary embolism (yellow arrowheads). Axial abdominal CT (C) shows acute dissection of the abdominal aorta (green arrowhead), probably resulting from vascular injury during arterial cannulation.

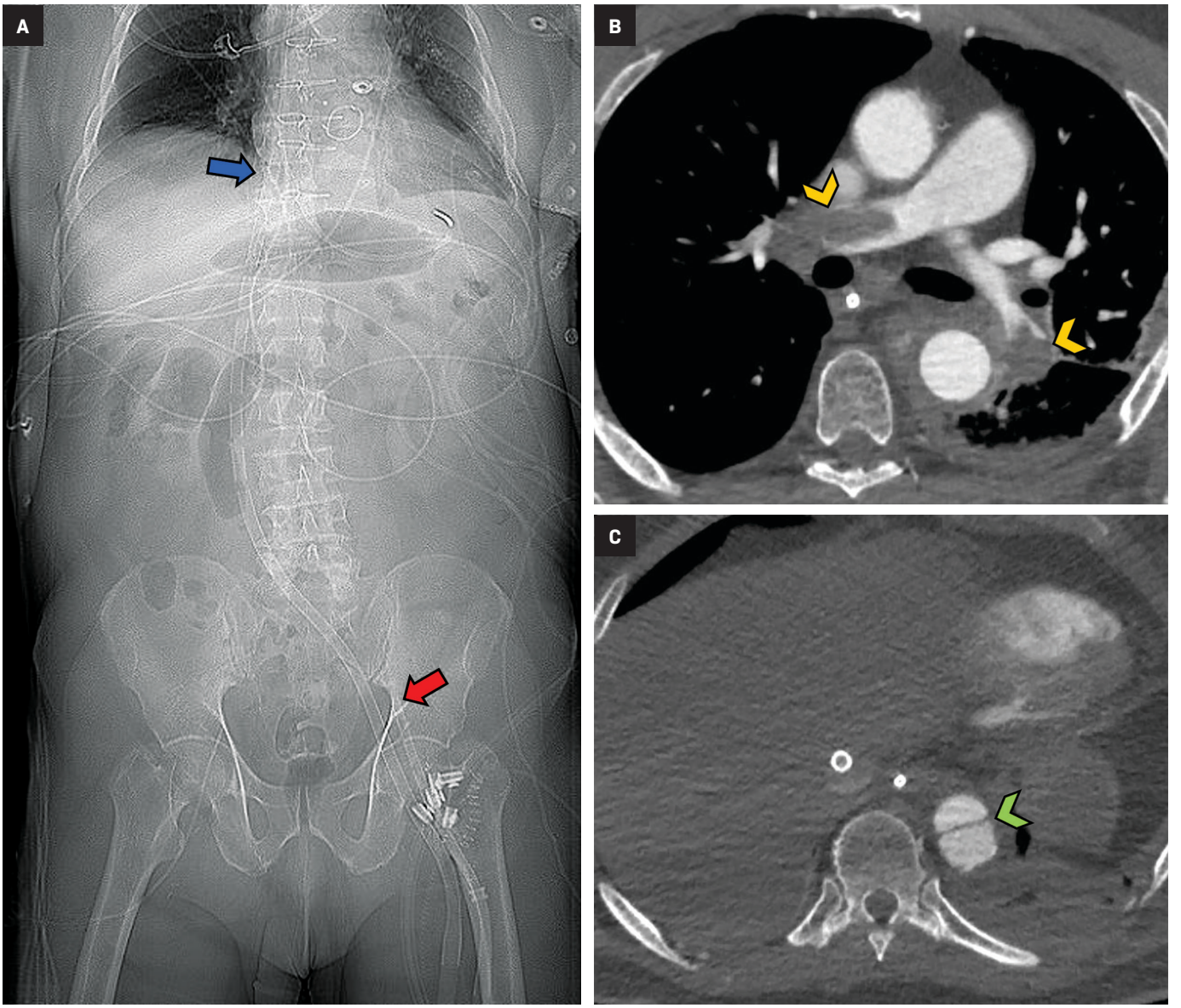

stroke may be observed in approximately 3% and 1.4% of patients, respectively, although they carry a mortality rate as high as 80% (Figure 11).[49]

Thromboembolic disease is frequent in patients connected to extracorporeal life support. The incidence of deep vein thrombosis is estimated at 53% and is more prevalent in VV-ECMO than in VA-ECMO.[50] Hemocompatibility within the ECMO circuit may trigger an inflammatory response and initiate the clotting cascade. Moreover, the mechanical stress may affect the arrangement of coagulation factors, posing a significant challenge for anticoagulation (Figure 12).[51]

Vascular complications, including access vessel obstruction with resultant limb ischemia, traumatic arterial dissection, and transection can occur in up to 30% of patients, are more frequent with VA-ECMO,[52] and are associated with increased mortality.[53] Other complications include renal failure, superimposed infection, sepsis, disseminated intravascular coagulation, and ECMO circuit component clots.[44]

Conclusion

As ECMO utilization increases in the treatment of severe cardiopulmonary failure, familiarity with the different types of ECMO circuits, expected locations of cannulas, optimal CT imaging protocols and possible

complications is essential for radiologists to ensure accurate imaging interpretation and diagnosis.

References

1) von Bahr V, Hultman J, Eksborg S, Frenckner B, Kalzén H. Long-Term Survival in Adults Treated With Extracorporeal Membrane Oxygenation for Respiratory Failure and Sepsis. *Crit Care Med.* Feb 2017;45(2):164-170. doi: 10.1097/ccm.0000000000002078.

2) Gajkowski EF, Herrera G, Hatton L, Velia Antonini M, Vercaemst L, Cooley E. ELSO Guidelines for Adult and Pediatric Extracorporeal Membrane Oxygenation Circuits. *Asaio j.* Feb 1 2022;68(2):133-152. doi: 10.1097/mat.0000000000001630.

3) Extracorporeal Life Support Organization (ELSO) ECLS International Summary of Statistics. website. https://www.elso.org/registry/internationalsummaryandreports/internationalsummary.aspx. Published 2023. Updated April 18, 2023. Accessed September 26, 2023.

4) Zangrillo A, Landoni G, Biondi-Zoccai G, et al. A meta-analysis of complications and mortality of extracorporeal membrane oxygenation. *Crit Care Resusc.* Sep 2013;15(3):172-178.

5) Gaddikeri R, Febbo J, Shah P. Imaging Adult ECMO. *Current Problems in Diagnostic Radiology.* 2021/11/01/ 2021;50(6):884-898. doi: https://doi.org/10.1067/j.cpradiol.2020.10.018.

6) Shen J, Tse JR, Chan F, Fleischmann D. CT Angiography of Venoarterial Extracorporeal Membrane Oxygenation. *Radiographics : a review publication of the Radiological Society of North America, Inc.* 2022/01/01 2021;42(1):23-37. doi: 10.1148/rg.210079.

7) Squiers JJ, Lima B, DiMaio JM. Contemporary extracorporeal membrane oxygenation therapy in adults: Fundamental principles and systematic review of the evidence. *The Journal of Thoracic and Cardiovascular Surgery.* 2016;152(1):20-32. doi: 10.1016/j.jtcvs.2016.02.067.

8) Wrisinger WC, Thompson SL. Basics of Extracorporeal Membrane Oxygenation. *Surg Clin North Am.* Feb 2022;102(1):23-35. doi: 10.1016/j.suc.2021.09.001.

9) Pavlushkov E, Berman M, Valchanov K. Cannulation techniques for extracorporeal life support. *Ann Transl Med.* Feb 2017;5(4):70. doi: 10.21037/atm.2016.11.47.

10) Lee S, Chaturvedi A. Imaging adults on extracorporeal membrane oxygenation (ECMO). *Insights into imaging.* Dec 2014;5(6):731-742. doi: 10.1007/s13244-014-0357-x.

11) Calcaterra D, Heather B, Kohl LP, Erickson HL, Prekker ME. Bedside veno-venous ECMO cannulation: A pertinent strategy during the COVID-19 pandemic. *J Card Surg.* Jun 2020;35(6):1180-1185. doi: 10.1111/jocs.14641.

12) Tonna JE, Abrams D, Brodie D, et al. Management of Adult Patients Supported with Venovenous Extracorporeal Membrane Oxygenation (VV ECMO): Guideline from the Extracorporeal Life Support Organization (ELSO). *Asaio j.* Jun 1 2021;67(6):601-610. doi: 10.1097/mat.0000000000001432.

13) Kim K, Leem AY, Kim SY, et al. Complications related to extracorporeal membrane oxygenation support as a bridge to lung transplantation and their clinical significance. *Heart Lung.* Nov-Dec 2022;56:148-153. doi: 10.1016/j.hrtlng.2022.07.008.

14) Frenckner B, Broman M, Broomé M. Position of draining venous cannula in extracorporeal membrane oxygenation for respiratory and respiratory/circulatory support in adult patients. *Crit Care.* Jun 15 2018;22(1):163. doi: 10.1186/s13054-018-2083-0.

15) Ling SK-h. Comparison of atrio-femoral and femoro-atrial venovenous extracorporeal membrane oxygenation in adult. *Perfusion.* 2022;37(1):14-18. doi: 10.1177/0267659120969020.

16) Conrad SA, Wang D. Evaluation of Recirculation During Venovenous Extracorporeal Membrane Oxygenation Using Computational Fluid Dynamics Incorporating Fluid-Structure Interaction. *Asaio j.* Aug 1 2021;67(8):943-953. doi: 10.1097/mat.0000000000001314.

17) Burrell AJC, Ihle JF, Pellegrino VA, Sheldrake J, Nixon PT. Cannulation technique: femoro-femoral. *Journal of thoracic disease.* Mar 2018;10(Suppl 5):S616-s623. doi: 10.21037/jtd.2018.03.83.

18) Shaheen A, Tanaka D, Cavarocchi NC, Hirose H. Veno-Venous Extracorporeal Membrane Oxygenation (VV ECMO): Indications, Preprocedural Considerations, and Technique. *J Card Surg.* Apr 2016;31(4):248-252. doi: 10.1111/jocs.12690.

19) Parker LP, Svensson Marcial A, Brismar TB, Broman LM, Prahl Wittberg L. Hemodynamic and recirculation performance of dual lumen cannulas for venovenous extracorporeal membrane oxygenation. *Scientific Reports.* 2023/05/08 2023;13(1):7472. doi: 10.1038/s41598-023-34655-1.

20) Abrams D, Bacchetta M, Brodie D. Recirculation in venovenous extracorporeal membrane oxygenation. *Asaio j.* Mar-Apr 2015;61(2):115-121. doi: 10.1097/mat.0000000000000179.

21) Lorusso R, Centofanti P, Gelsomino S, et al. Venoarterial Extracorporeal Membrane Oxygenation for Acute Fulminant Myocarditis in Adult Patients: A 5-Year Multi-Institutional Experience. *The Annals of thoracic surgery.* Mar 2016;101(3):919-926. doi: 10.1016/j.athoracsur.2015.08.014.

22) Kagawa E, Inoue I, Kawagoe T, et al. Assessment of outcomes and differences between in- and out-of-hospital cardiac arrest patients treated with cardiopulmonary resuscitation using extracorporeal life support. *Resuscitation.* Aug 2010;81(8):968-973. doi: 10.1016/j.resuscitation.2010.03.037.

23) Richardson AC, Tonna JE, Nanjayya V, et al. Extracorporeal Cardiopulmonary Resuscitation in Adults. Interim Guideline Consensus Statement From the Extracorporeal Life Support Organization. *ASAIO Journal.* 2021;67(3):221-228. doi: 10.1097/mat.0000000000001344.

24) Panchal AR, Bartos JA, Cabañas JG, et al. Part 3: Adult Basic and Advanced Life Support: 2020 American Heart Association Guidelines for Cardiopulmonary Resuscitation and Emergency Cardiovascular Care. *Circulation.* 2020;142(16_suppl_2):S366-S468. doi: doi:10.1161/CIR.0000000000000916.

25) Pavasini R, Cirillo C, Campo G, et al. Extracorporeal Circulatory Support in Acute Coronary Syndromes: A Systematic Review and Meta-Analysis. *Crit Care Med.* Nov 2017;45(11):e1173-e1183. doi: 10.1097/ccm.0000000000002692.

26) de Waha S, Fuernau G, Eitel I, Desch S, Thiele H. Long-term prognosis after extracorporeal life support in refractory cardiogenic shock - results from a real-world cohort. *EuroIntervention.* Jun 20 2016;12(3):414. doi: 10.4244/eijv12i3a71.

27) Rao P, Khalpey Z, Smith R, Burkhoff D, Kociol RD. Venoarterial Extracorporeal Membrane Oxygenation for Cardiogenic Shock and Cardiac Arrest. *Circulation: Heart Failure.* 2018;11(9):e004905. doi: doi:10.1161/CIRCHEARTFAILURE.118.004905.

28) Biancari F, Perrotti A, Dalén M, et al. Meta-Analysis of the Outcome After Postcardiotomy Venoarterial Extracorporeal Membrane Oxygenation in Adult Patients. *J Cardiothorac Vasc Anesth.* Jun 2018;32(3):1175-1182. doi: 10.1053/j.jvca.2017.08.048.

29) Rubino A, Costanzo D, Stanszus D, et al. Central Veno-Arterial Extracorporeal Membrane Oxygenation (C-VA-ECMO) After Cardiothoracic Surgery: A Single-Center Experience. *Journal of Cardiothoracic and Vascular Anesthesia.* 2018;32(3):1169-1174. doi: 10.1053/j.jvca.2017.12.003.

30) Camp PC, Jr. Short-Term Mechanical Circulatory Support. *Operative Techniques in Thoracic and Cardiovascular Surgery.* 2013;18(3):239-251. doi: 10.1053/j.optechstcvs.2013.11.004.

31) Jayaraman AL, Cormican D, Shah P, Ramakrishna H. Cannulation strategies in adult veno-arterial and veno-venous extracorporeal membrane oxygenation: Techniques, limitations, and special considerations. *Ann Card Anaesth.* Jan 2017;20(Supplement):S11-s18. doi: 10.4103/0971-9784.197791.

32) Sorokin V, MacLaren G, Vidanapathirana PC, Delnoij T, Lorusso R. Choosing the appropriate configuration and cannulation strategies for extracorporeal membrane oxygenation: the potential dynamic process of organ support and importance of hybrid modes. *Eur J Heart Fail.* May 2017;19 Suppl 2:75-83. doi: 10.1002/ejhf.849.

33) Contento C, Battisti A, Agrò B, et al. A novel veno-arteriovenous extracorporeal membrane oxygenation with double pump for the treatment of Harlequin syndrome. *Perfusion.* 2020;35(1_suppl):65-72. doi: 10.1177/0267659120908409.

34) Biscotti M, Bacchetta M. The “Sport Model”: Extracorporeal Membrane Oxygenation Using the Subclavian Artery. *The Annals of thoracic surgery.* 2014;98(4):1487-1489. doi: 10.1016/j.athoracsur.2014.02.069.

35) Chicotka S, Rosenzweig EB, Brodie D, Bacchetta M. The "Central Sport Model": Extracorporeal Membrane Oxygenation Using the Innominate Artery for Smaller Patients as Bridge to Lung Transplantation. *Asaio j.* Jul/Aug 2017;63(4):e39-e44. doi: 10.1097/mat.0000000000000427.

36) Bernhardt AM, Hillebrand M, Yildirim Y, et al. Percutaneous left atrial unloading to prevent pulmonary oedema and to facilitate ventricular recovery under extracorporeal membrane oxygenation therapy. *Interact Cardiovasc Thorac Surg.* Jan 1 2018;26(1):4-7. doi: 10.1093/icvts/ivx266.

37) Takeda K, Garan AR, Topkara VK, et al. Novel minimally invasive surgical approach using an external ventricular assist device and extracorporeal membrane oxygenation in refractory cardiogenic shock. *Eur J Cardiothorac Surg.* Mar 1 2017;51(3):591-596. doi: 10.1093/ejcts/ezw349.

38) Rao P, Mosier J, Malo J, et al. Peripheral VA-ECMO with direct biventricular decompression for refractory cardiogenic shock. *Perfusion.* Sep 2018;33(6):493-495. doi: 10.1177/0267659118761558.

39) Cappannoli L, Galli M, Zito A, et al. Venoarterial extracorporeal membrane oxygenation (VA-ECMO) with vs. without left ventricular unloading by Impella: a systematic review and meta-analysis. *European Heart Journal - Quality of Care and Clinical Outcomes.* 2022;9(4):358-366. doi: 10.1093/ehjqcco/qcac076.

40) Liu K-L, Wang Y-F, Chang Y-C, et al. Multislice CT Scans in Patients on Extracorporeal Membrane Oxygenation: Emphasis on Hemodynamic Changes and Imaging Pitfalls. *Korean J Radiol.* 6/ 2014;15(3):322-329. https://doi.org/10.3348/kjr.2014.15.3.322.

41) Gullberg Lidegran M, Gordon Murkes L, Andersson Lindholm J, Frenckner B. Optimizing Contrast-Enhanced Thoracoabdominal CT in Patients During Extracorporeal Membrane Oxygenation. *Academic Radiology.* 2021;28(1):58-67. doi: 10.1016/j.acra.2020.01.029.

42) Shen J, Tse JR, Chan F, Fleischmann D. CT Angiography of Venoarterial Extracorporeal Membrane Oxygenation. *Radiographics : a review publication of the Radiological Society of North America, Inc.* 2022;42(1):23-37. doi: 10.1148/rg.210079.

43) Lambert L, Grus T, Balik M, Fichtl J, Kavan J, Belohlavek J. Hemodynamic changes in patients with extracorporeal membrane oxygenation (ECMO) demonstrated by contrast-enhanced CT examinations - implications for image acquisition technique. *Perfusion.* 2017;32(3):220-225. doi: 10.1177/0267659116677308.

44) Rajsic S, Treml B, Jadzic D, et al. Extracorporeal membrane oxygenation for cardiogenic shock: a meta-analysis of mortality and complications. *Ann Intensive Care.* Oct 5 2022;12(1):93. doi: 10.1186/s13613-022-01067-9.

45) Xie A, Phan K, Tsai YC, Yan TD, Forrest P. Venoarterial extracorporeal membrane oxygenation for cardiogenic shock and cardiac arrest: a meta-analysis. *J Cardiothorac Vasc Anesth.* 2015;29(3):637-645. doi: 10.1053/j.jvca.2014.09.005.

46) Wilson-Smith AR, Bogdanova Y, Roydhouse S, et al. Outcomes of venoarterial extracorporeal membrane oxygenation for refractory cardiogenic shock: systematic review and meta-analysis. *Ann Cardiothorac Surg.* Jan 2019;8(1):1-8. doi: 10.21037/acs.2018.11.09.

47) Supady A, Taccone FS, Lepper PM, et al. Survival after extracorporeal membrane oxygenation in severe COVID-19 ARDS: results from an international multicenter registry. *Critical Care.* 2021/03/01 2021;25(1):90. doi: 10.1186/s13054-021-03486-9.

48) Aubron C, DePuydt J, Belon F, et al. Predictive factors of bleeding events in adults undergoing extracorporeal membrane oxygenation. *Ann Intensive Care.* Dec 2016;6(1):97. doi: 10.1186/s13613-016-0196-7.

49) Lorusso R, Gelsomino S, Parise O, et al. Neurologic Injury in Adults Supported With Veno-Venous Extracorporeal Membrane Oxygenation for Respiratory Failure: Findings From the Extracorporeal Life Support Organization Database. *Crit Care Med.* Aug 2017;45(8):1389-1397. doi: 10.1097/ccm.0000000000002502.

50) Iannattone PA, Yang SS, Koolian M, Wong EG, Lipes J. Incidence of Venous Thromboembolism in Adults Receiving Extracorporeal Membrane Oxygenation: A Systematic Review. *Asaio j.* Dec 1 2022;68(12):1523-1528. doi: 10.1097/mat.0000000000001694.

51) Abruzzo A, Gorantla V, Thomas SE. Venous thromboembolic events in the setting of extracorporeal membrane oxygenation support in adults: A systematic review. *Thrombosis Research.* 2022/04/01/ 2022;212:58-71. doi: https://doi.org/10.1016/j.thromres.2022.02.015.

52) Jia D, Yang IX, Ling RR, et al. Vascular Complications of Extracorporeal Membrane Oxygenation: A Systematic Review and Meta-Regression Analysis. *Crit Care Med.* Dec 2020;48(12):e1269-e1277. doi: 10.1097/ccm.0000000000004688.

53) Tanaka D, Hirose H, Cavarocchi N, Entwistle JW. The Impact of Vascular Complications on Survival of Patients on Venoarterial Extracorporeal Membrane Oxygenation. *The Annals of thoracic surgery.* May 2016;101(5):1729-1734. doi: 10.1016/j.athoracsur.2015.10.095.

AppliedRadiology®

The Journal of Practical Medical Imaging and Management

UPDATE YOUR SUBSCRIPTION

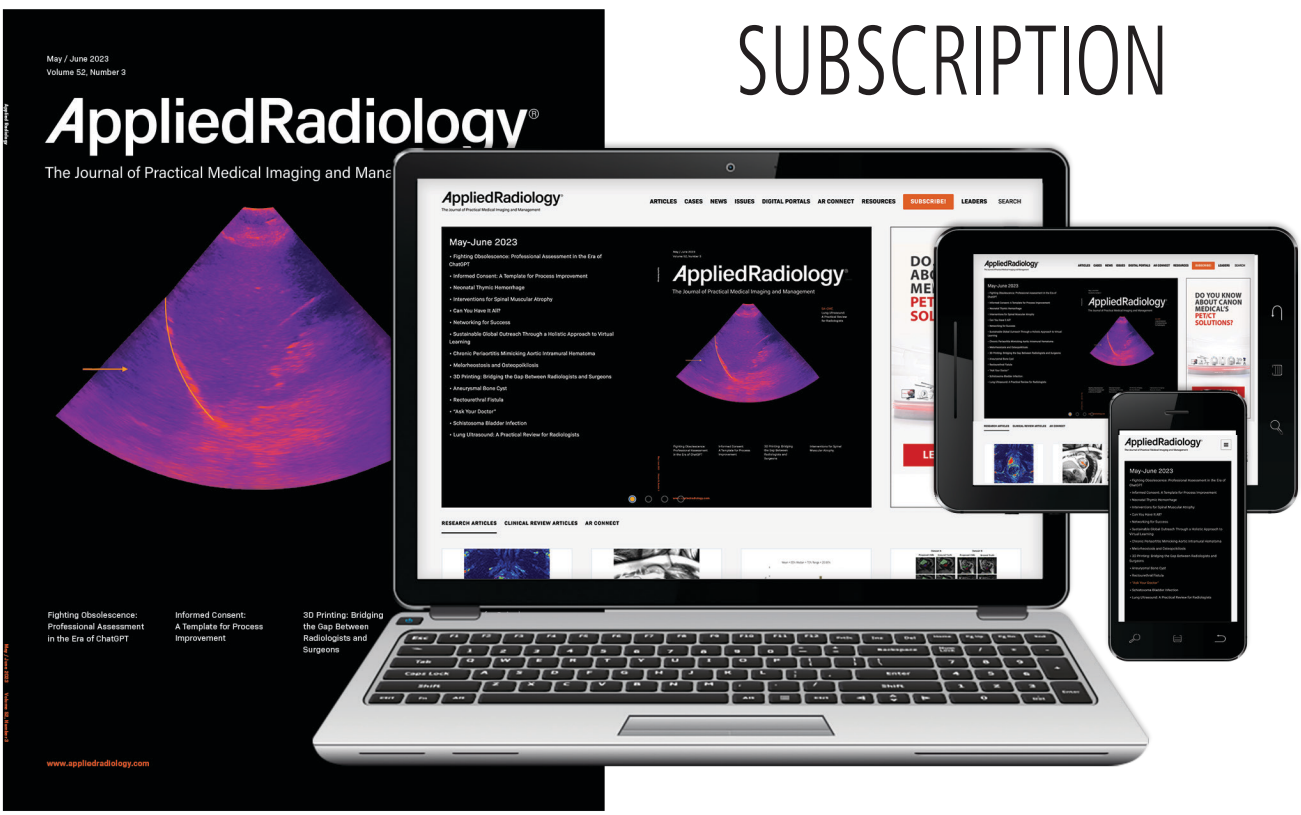

Since 1972, *Applied Radiology* has brought physician-authored clinical review articles to the radiology community.

Applied Radiology content includes clinical review articles, radiological cases, and specialty columns such as Eye on AI and the ever-popular Wet Read by C. Douglas Phillips, MD, FACR.

Now you can have it all your way (FREE) without missing a single issue.

Please take a moment to update your subscription preferences.

appliedradiology.com/#subscribe

The Compounded Value of AI Beyond Radiology

Lizette Heine, PhD

In healthcare, doctors help people; artificial intelligence (AI) helps doctors help people. It may sound trite, but it is important to adopt this philosophy as a guiding principle in product development. The US Food and Drug Administration (FDA) has approved close to 700 AI-enabled medical devices,[1] and an even larger number of algorithms are being developed and deployed in research institutions. Each of these products and algorithms can handle a specific task, often with superhuman performance. However, it is easy to lose track of what is most important: the impact of these products on patient care.

Historically, AI products have faced several challenges to clinical implementation and, therefore, to realization of their full potential within the broader healthcare system. For one, an important bias that plagues AI algorithms relates to the heterogeneity of medical scans; depending on whether the software or algorithm being used was trained on them, different acquisition protocols or scan quality can cause unreliable results.[2]

Affiliation: Dr Heine is the director of clinical science at DeepHealth, Rotterdam, The Netherlands.

Overfitting might also happen, causing the software to underperform on new sets of data. This can occur when certain types of data are under-represented in the training set. An example of this is a skin-cancer evaluation application trained on only one skin color.

Luckily, these issues are beginning to be addressed. The significance of racial bias in radiology[3] is reflected in current guidelines,[4] and some institutions are tackling the issues by providing open source data and labels. Large databases are available to innovators tackling cancer [5] and COVID,[6] and more are expected in the coming years. For instance, the Oregon-Massachusetts Mammography Database project aims to catalogue 220,000 annotated mammograms with ground truth labels.[7]

Rigorous clinical evaluation of real-world use by independent third parties is the best way to thoroughly assess AI-enabled products and the possible biases affecting their performance. Studying accuracy, sensitivity, specificity, and user interaction with the AI solution is the first step in quantifying patient impact. Such assessments will also inform further software development, and thus improve the software and its value to patients.

The clinical usefulness and value of AI products along the entire patient pathway deserves more attention. Nowadays, evaluations of such tools and technologies are often limited to assessing their impacts on radiologist efficiency, accuracy,[8] consistency of diagnostic evaluations,[9] and/or cost.[10] While these assessments are necessary, useful, and valuable, AI products could have compounding effects on other specialties. An important next step in AI development would be to reuse AI results within multiple steps of the healthcare pathway. For example, results from a screening AI could also be used for diagnosis, interventional therapy, measuring treatment response, or even clinical trials. The potential additional benefits of such compounding effects could positively impact AI utilization in healthcare as a whole.

Take prostate MRI. Current recommendations call for MR imaging prior to biopsy to decrease the number of biopsies and missed cancers.[11] AI can assist radiologists,, especially trainees, in evaluating the prostate and in creating structured reports and segmentations.[12]

The software output can then be imported into fusion-capable biopsy systems. This would free up

urologists' time, as they no longer would have to manually segment the lesions based on textual or paper-drawn reporting. The same segmentations can also assist other physicians, for instance, by informing treatment-dose calculations to reduce damage to surrounding tissue, or in performing MRI-guided radiotherapy.

A clear understanding of the larger healthcare system around each AI product's use-case will reveal what features can provide a more complete understanding of AI's real value. Evaluating this is not an easy task, as the benefits will be different for each stakeholder. More research methods are needed to focus on compounded benefits, particularly for products whose costs are primarily borne by one department, while the benefits accrue across other service lines.

Artificial intelligence will bolster the performance of radiologists and that of the wider healthcare system. More real-world studies of diagnostic AI will demonstrate clinical utility for the radiology department and beyond. When we think more holistically about the positive effects on the overall healthcare system, we can truly assess the level of value a given product adds to patient care.

References

1) FDA. Artificial Intelligence and Machine Learning (AI/ML)-Enabled Medical Devices. https://www.fda.gov/medical-devices/software-medical-device-samd/artificial-intelligence-and-machine-learning-aiml-enabled-medical-devices (2023). Accessed December 11, 2023.

2) D Drukker K, Chen W, Gichoya J, et al. Toward fairness in artificial intelligence for medical image analysis: identification and mitigation of potential biases in the roadmap from data collection to model deployment. *J Med Imaging* (Bellingham). 2023;10(6):061104. doi:10.1117/1.JMI.10.6.061104

3) Gichoya J W, et al. AI recognition of patient race in medical imaging: a modelling study. *Lancet Digit. Health. 2022;* 4: e406–e414.

4) FDA. Diversity Plans to Improve Enrollment of Participants From Underrepresented Racial and Ethnic Populations in Clinical Trials; Draft Guidance for Industry; Availability. https://www.fda.gov/regulatory-information/search-fda-guidance-documents/diversity-plans-improve-enrollment-participants-underrepresented-racial-and-ethnic-populations (2022).

5) The Cancer Imaging Archive (TCIA). https://imaging.cancer.gov/informatics/cancer_imaging_archive.htm. Accessed October 27, 2023.

6) MIDRC. https://www.midrc.org. Accessed October 27, 2023.

7) The Oregon-Massachusetts Mammography Database. https://mpsych.org/omama/.

8) Martins Jarnalo C O, Linsen P V M, Blazís S P, van der Valk P H M, Dieckens D B M. Clinical evaluation of a deep-learning-based computer-aided detection system for the detection of pulmonary nodules in a large teaching hospital. *Clin. Radiol.* 2021; 76: 838–845.

9) Lotter W, et al. Robust breast cancer detection in mammography and digital breast tomosynthesis using an annotation-efficient deep learning approach. *Nat. Med.* 2021; 27, 244–249.

10) van Leeuwen K G, et al. Cost-effectiveness of artificial intelligence aided vessel occlusion detection in acute stroke: an early health technology assessment. *Insights Imaging.* 2021; 12: 1-9.

11) Wei J T, et al. Early detection of prostate cancer: AUA/SUO Guideline Part I: Prostate Cancer Screening. *J. Urol.* 2023; 210: 46–53.

12) Faiella E, Vertulli D, Esperto F, et al. Quantib prostate compared to an expert radiologist for the diagnosis of prostate cancer on mpMRI: a sngle-center preliminary study. *Tomography*. 2022;8(4):2010-2019. Published 2022 Aug 13. doi:10.3390/tomography8040168

Tele-Ultrasound: Meeting Global Imaging Challenges

Diana L. Dowdy, DNP, CNM, RDMS; Robert D. Harris, MD, MPH

According to The World Health Organization (WHO), diagnostic ultrasonography (US) is one of the most important technologies in developing countries. Access to US is now considered a minimal global standard. The WHO reports that medical imaging is needed for diagnosis in 20-30 percent of clinical cases, and that US and/or conventional radiology would be sufficient for up to 90 percent of those cases.[1] Unfortunately, two-thirds of the world's population, especially people living in low- and middle-income countries (LMICs), have no access to medical imaging. For example, in Malaysia, there are approximately 30 radiologists per million people compared to the desired goal of 50 per million in 2030.[2]

The availability of US services in underserved areas is limited by many factors. A lack of trained sonographers/sonologists and appropriate equipment, along with inadequate infrastructure, are two major ones.[3] To help solve these challenges, telemedicine, including teleradiology and tele-ultrasound (TUS), can be employed to provide responses to clinical situations in the absence of on-site specialists.[4] Indeed, multiple studies have shown that TUS improves access to, and reduces the costs of, healthcare in remote geographic regions with limited infrastructure.[3,5]

Tele-ultrasound can take place in two ways: asynchronously or in real time. In asynchronous TUS, static images or clips are captured and stored for later review by radiologists (a process also known as "store and forward"). The benefits of asynchronous TUS include training local practitioners to obtain clips of a body region or target organ using basic scanning protocols. One method consists of volume sweep imaging a target to create a tomographic series or 3D capture of the region.[6] In an emergency, first responders can obtain and send a sweep to a remotely located radiologist for interpretation, if not for immediate evaluation, then for later validation/refutation of a preliminary diagnosis.

Real-time TUS, on the other hand, allows the expert observer to be virtually present during scanning, enabling direct feedback and enhancing the expert's ability to guide the operator and improve image quality. Real-time TUS quality is improving almost by the day. A smartphone or similar device can be connected to the probe to observe the person scanning while generating a split-screen image for both participants. One side shows the practitioner performing the scan, while the other shows the image (Figure 1). The receiving expert can remotely move a cursor over the sender's image, demonstrating correct location or orientation. The sending provider can also move a cursor in response (Figure 2). Both participants can also view each other, allowing for virtual "hands-on" instruction (Figure 3). These capabilities have been revolutionary for US education and mentoring.

Indeed, with the growing availability of commercial off-the-shelf software, high-definition images using Windows or Android configurations can now be transferred around the world in seconds over Wi-Fi and 5G networks that provide 100 times faster data transmission rates (up to 10 gigabytes per second), and capacities more than 100 times that of 4G technology.

Tele-Ultrasound Effectiveness

Over the past 10 years, numerous studies have examined the utility of TUS in settings where other technologies are unavailable, cost-prohibitive, or unable to be properly maintained.

Table 1 offers a summary of systematic reviews of TUS publications from 1950 to 2020.[1]

Affiliations: Ms Dowdy is a certified nurse-midwife and registered diagnostic sonographer at Women4Women in Huntsville, Alabama, and Women's POCUS director at InnovatED Ultrasound in Nashville, Tennessee. Dr Harris is a professor of radiological sciences, at Drexel University College of Medicine-Allegheny Health Network, in Pittsburgh, Pennsylvania.

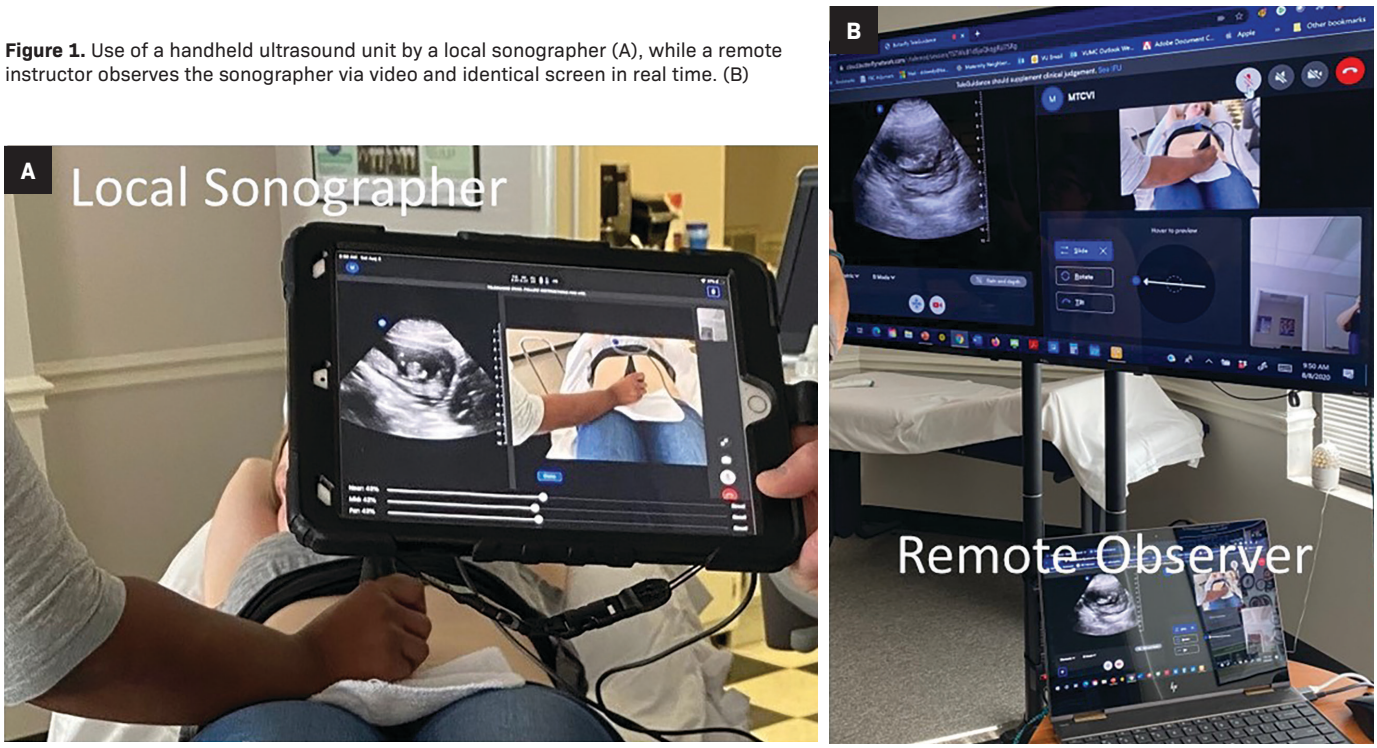

Figure 1. Use of a handheld ultrasound unit by a local sonographer (A), while a remote instructor observes the sonographer via video and identical screen in real time. (B)

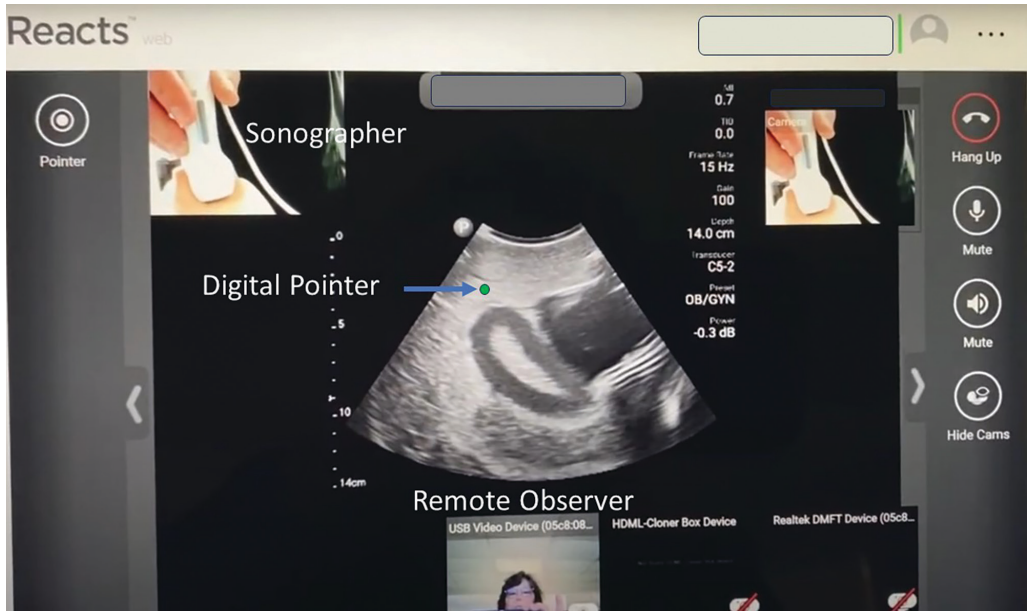

Figure 2. Use of the Reacts™ platform demonstrating the sonographer's hand position (upper left), the remote observer's view of the image (center) with a digital pointer, and an image of the remote observer (bottom). The digital pointer can be manipulated by both the sonographer and observer.

Asynchronous training with TUS suffers from difficulty in recruiting and retaining reliable learners, however it does provide for learner flexibility. Many pilot projects in LMICs have been initiated by organizations such as RAD-AID™. Asynchronous training is followed by hands-on training/mentorship. Outcomes data will be essential to validate the effectiveness of TUS as it expands throughout these regions.

Novel Approaches to Come

Telemedicine is quickly becoming adaptable to many different situations and scenarios. FaceTime™ video conferencing via iPhone, for example, is demonstrating utility not just with telemedicine in general but also in ultrasound consultation specifically.

One drone-based product involves flying US units to inaccessible locations for catastrophic emergencies, and to vulnerable populations for whom transport is impractical or undesirable. This can be particularly useful in war

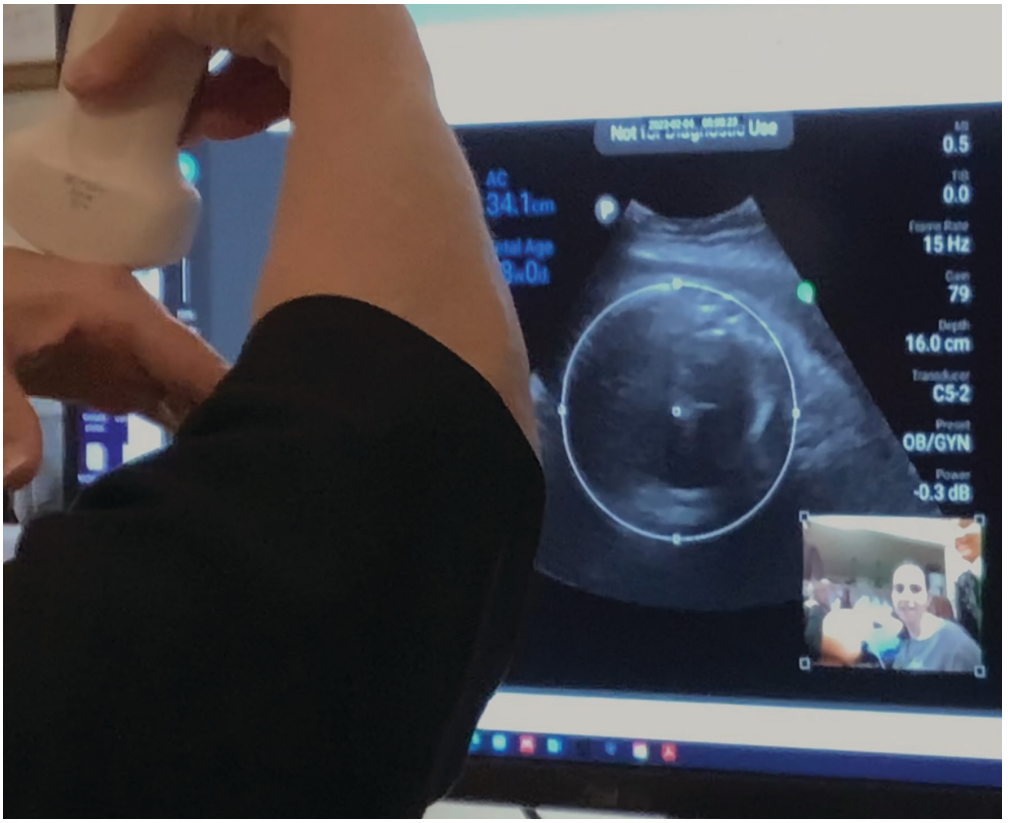

Figure 3. A remote educator demonstrating hand postition change to a local sonographer (lower right) via the educator's desktop. The educator can view the sonographer's scan technique (lower right) as well as the image capture (center).

Table 1. Strengths and Challenges of Tele-Ultrasound

STRENGTHS	CHALLENGES
-Universal utility for remote areas with radiology personnel deficit	-Not a replacement for in-person scanning -Obstacles for local training and certification -Limited expert consultants -Limited ability to observe subtle techniques (orientation/scan technique)
-Equipment/telecom costs offset by improved access and healthcare savings -Available low-cost machines, web interfaces, platforms and data storage -Improved data transfer rates for large files	-Infrastructure-dependent -Equipment and supply costs -Diverse machine types -Insufficient, or poorly maintained local equipment
-Wireless networks more reliable; some HIPAA compliant	-Unreliable or absent WIFI/satellite access -Limited data use on local cell services
Data Security	
-Conversion to DICOM available on most/all newer machines, allowing transmission to PACs	-Archiving data security concerns -Some countries prohibit patient data out of the country -Potential for hacking

zones, wilderness rescues, and other areas and circumstances with little access to imaging.

In obstetric US, a novel, self-operated home system that attaches to a smartphone (known as INSTINCT®) is being used for fetal assessment, including a basic biophysical profile. In one study, it has demonstrated high accuracy in assessing fetal heart rate, amniotic fluid index, and fetal tone.[7]

Artificial Intelligence and Tele-Ultrasound

Amid the limited resources and lack of expert sonographers in many LMICs, artificial intelligence (AI) offers the

opportunity for even the inexperienced to acquire diagnostic-quality images. In the US and Europe, some agencies have been granted regulatory approval to process images using AI guidance. In this process, after entering anthropometric information, a transducer is placed on the patient. The operator is instructed on probe placement and movement, and the picture is automatically captured as soon as the device detects a high-quality image, essentially performing volume sweep imaging. AI-assisted TUS is still investigational; to ensure accuracy, a large database of condition-specific and normal images will be required to build the algorithms needed to train the technology. Nevertheless, AI-assisted guidance for all US procedures may eventually become commonplace. Deep-learning algorithms for precision US interpretation are also in early development; these tools are being studied for their ability to evaluate condition and injury severity for real-time clinical decision making.[8]

Conclusion

Tele-ultrasound has been shown to improve access to, and reduce the costs of healthcare in, remote areas with limited infrastructure. Rapidly evolving technology will promote increased implementation of TUS, especially in settings with few trained professionals. Affordable pocket/hand-held devices are increasingly available globally, providing excellent platforms for the application of TUS. As global connectivity expands, particularly with improved cellular and internet access, TUS is quickly becoming more feasible worldwide.

Although TUS applications are unlikely to fully replace hands-on scanning or human professional judgment in clinical decision making, they will continue to advance in the years ahead. Radiologists must remain up to date on technical innovations and consider leveraging TUS as a tool to expand high levels of care to those in need around the world.

References

1) Recker F, Höhne E, Damjanovic D, & Schäfer VS. US in Telemedicine: A Brief Overview. *Applied Sciences.* 2022; 12(3):958. https://doi.org/10.3390/app12030958

2) 2. Henderson M. Radiology facing a global shortage. *RSNA News.* May 10, 2022.. https://www.rsna.org/news/2022/may/global-radiologist-shortage.

3) 3.Ewing B & Holmes D. Evaluation of current and former teleradiology systems in Africa: A review. *Annals of Global Health.* (2022), 8(1); 43.

4) Arbeille P, Zuj K, Saccomandi A, Ruiz J, Andre E, de la Porte C et al. Teleoperated echograph and probe transducer for remote US investigation on isolated patients. *Telemedicine and e-Health*. 2016; 22(7); 599-607

5) 5. Britton N., Miller M, Safadi S, Siegel A, Levine A, & McCurdy et al. Tele-US in resource-limited settings: A systematic review. *Frontiers in Public Health*. 2019 7(244); 1-13.

6) 6. Carbone MF. A tele-ultrasonographic platform to collect specialist second opinion in less specialized hospitals. *Updates in Surgery.* (2018) 70; 409-413.

7) 7. Hadar E, Wolff L, Tenenbaum-Gavish K, Eisner M, Shmueli A, Barbash-Hazan S et al. Mobile self-operated home US system for remote fetal assessment during pregnancy. *Telemedicine and e-Health.* 2022; 28(1); 93-101.

8) 8. Liua S, Wanga, Yangb X Leia B, Liua L, Lia S, et al. Deep learning in medical ultrasound analysis: a review. *Engineering.* 2019; S(2); 261-275. https://doi.org/10.1016/j.eng.2018.11.020

Residency is More Than Just Image Interpretation

Yasha Parikh Gupta, MD

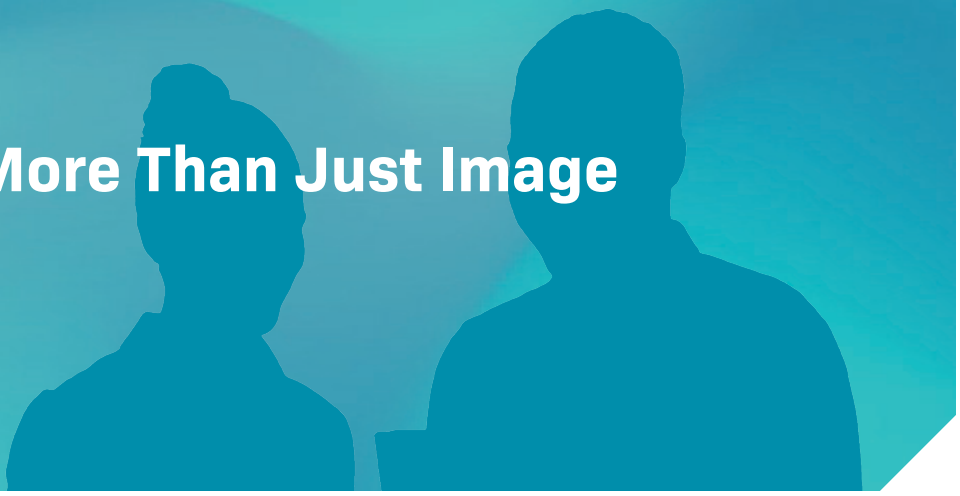

Radiology residency is a time when you, as a physician, will learn the essential skills of image interpretation. Between year 1 and year 4, you can expect to see exponential growth in your knowledge of imaging and mastery of the nuances required to carry out the responsibilities of your chosen profession.

And yet there are other, supplemental skills that you should be sure to learn during this time, not just to make you a more competent radiologist, but also to develop yourself as a well-rounded physician who can succeed in both patient care and your specialty within the profession.

Make Yourself Clear

One of the most important skills is communication. As radiologists, we primarily communicate through our reports. Throughout our journey as physicians (perhaps even as patients) we have all experienced a variety of reporting styles. We have encountered concise radiologists who get right to the point. We have also encountered verbose radiologists who take pride in extensively detailing every incidental finding in every image.

There is no right or wrong when it comes to style; while learning which one works for you is important, making sure to highlight the most actionable findings clearly to all readers should be your top priority. Obtaining feedback from those around you is a good way to figure out what works and what doesn't. Read as many reports as possible to learn what you like and do not like.

Lead the Way

Another valuable skill is leadership. Leadership skills can only be acquired through practice, and residency is a great time to start working on and solidifying them. Serving as a chief resident, for example, affords experience in learning how to balance the needs of various parties and how to behave as a role model to your co-residents. To be sure, serving as a chief resident will require a large time commitment, but it can also be an especially transformative experience.

There likely are also many opportunities to practice leadership skills within your own department and as part of organizations such as the American College of Radiology and the Radiological Society of North America. Many of these positions require minimal time on your part, but they can help you hone your communication skills and provide great networking opportunities that can serve you for the rest of your career.

Teach Yourself a Lesson

Teaching is also a skill well worth practicing during residency. Many programs are affiliated with medical schools; you may find yourself reading studies with a student at your side. You may

Dr Gupta is a radiologist at Keck Medicine at USC, Los Angeles, California. She is also a member of the Editorial Advisory Board of *Applied Radiology.*

also be presented with opportunities to teach at the medical school itself. Your day-to-day activities as a radiologist, moreover, will require the ability to teach to some degree, whether it's educating the physicians who come to your reading room to review study findings, or it's offering a phone or video consult.

Get Technical

Finally, technical skills such as ultrasound scanning and interventional procedures are very important to learn during residency. These skills can be extremely useful when you are asked to take a second look by a technologist. Experienced technologists are often great teachers, and you may never again get the kind of time to dedicate to learning scanning and procedural techniques that you have during training. You may think you're "never going to need that skill," but you also never truly know where your career may lead you. You may someday need to know how to perform a breast biopsy—despite swearing off mammography for life!

Residency is more than just a time to learn how to be a radiologist. It is a time to learn how to run an imaging service, and while the main part of your job is to read images, becoming a valued team player is just as important.

Residency can feel very long, but it is actually quite a brief portion of your career. Devote as much time as you can to learning about communicating, leading, teaching, and honing the technical skills that will serve you well once you begin practicing independently.

AI's Diversity Problem in Radiology: Addressing Algorithm Bias

Kerri Reeves

Kerri Reeves is a contributing editor based in Ambler, PA.

As the volume and breadth of healthcare data continue to expand, so too are the opportunities to apply artificial intelligence-based solutions (AI) to a growing number of medical tasks, including many in radiology.

However, care must be taken, many experts say, to ensure that the promise of AI reaches all patients, regardless of race, gender, and other demographics, by making it a priority to train the underlying algorithms of AI solutions on as many diverse patient populations as possible.

The AI Toolkit is Growing

More than 520 AI-based medical algorithms cleared by the US Food and Drug Administration (FDA) are helping to make diagnoses, treatment recommendations, and health outcomes predictions.[1] They are also streamlining administrative functions related to billing, patient records, and pre-authorizations.

In radiology, nearly 400 dedicated AI-based algorithms are being applied to spot potentially cancerous lesions, to advance image processing tasks, to generate 3-D models, and to assist in generating reports. [1]

Yet, while the potential of AI to continue improving upon medical imaging is promising, concerns are being raised about bias—specifically with respect to bias in the datasets used to train AI solutions in healthcare.

"We need datasets that represent the beautiful diversity of our patients, whether that's gender, ethnicity, age, or any other type of diversity," says K. Elizabeth Hawk, MS, MD, PhD, assistant professor at the Stanford School of Medicine, interim chief of health sciences, and associate clinical professor of nuclear medicine at the University of California San Diego. "Otherwise, [algorithms] may underperform for the under-represented patient populations."

Dr Hawk and Sonia Gupta, MD, chief medical officer of Enterprise Imaging at Optum and a radiologist specializing in oncology, shared their thoughts on the need for more diverse AI-training datasets in an interview with *Applied Radiology* editor-in-chief Erin Simon Schwartz, MD, at RSNA 2023 in Chicago. Their conversation followed a panel discussion at the meeting.[2]

To avoid bias, patient harm, and discrimination in the provision of care, the data used to train AI algorithms must include the full range of patient gender, ethnicity, race, age, and geography, as well as any with genetic predispositions to certain diseases and/or issues with access to healthcare services, says Dr Gupta.

For example, she argues, an algorithm designed for cancer detection should incorporate data from patients with reliable access to regular screening, as well as from those who do not have those advantages. These populations commonly include ethnic and racial minorities, women, and children, among others, who may be excluded from the datasets used to train computer programs.

Dr Gupta cites age diversity as a particular concern as it relates to identifying and meeting the healthcare needs of children.

"[We need] more algorithms that are developed exclusively for pediatrics because we [often] go backwards in that we start with adults and then hope that we can retrofit it to children, but it's not

the same," Dr Gupta says. "Children are not little adults … . [They have] completely different physiology and disease processes."

"It's important to bring pediatric radiologists to that design table," adds Dr Hawk. "A lot of these AI development teams have been focused on adult algorithms … and when they start looking to develop more pediatric algorithms, it's important to bring radiologist voices to the design process."

"When we don't have diversity of data … it actually deepens healthcare disparities across the globe, not only for our patients, but also for our provider teams," she says.

With respect to geographic diversity, Dr Hawk argues that US healthcare would greatly benefit by doing more to integrate rural populations in the training of AI algorithms. The same is true for improving gender diversity; she notes that algorithm re-approvals through the FDA provide an opportunity to "tune-up" existing algorithms.

"That's a good time to look at the blind spots like gender diversity and make sure that the new datasets include a wider gender diversity, depending on the algorithm [and its needs]," Dr Hawk says.

AI Bias in Healthcare Coming Under Scrutiny

The impact of bias on healthcare AI has captured the attention of legislators. In November, The Senate Health, Education, Labor, and Pensions Committee held a hearing on policy considerations for AI in healthcare, and The House Energy and Commerce Subcommittee held one on considerations for Congress as AI evolves. Participants shared concerns about inequitable use of AI that could exacerbate health disparities.[3]

US Sen. Ben Ray Luján of New Mexico noted that AI data gathered mostly from male patients performed poorly when physicians applied it to female patients. Sen. Luján also pointed to an algorithm designed to diagnose skin cancer trained on lighter-skinned patients that would fail on darker-skinned people.[3]

A study addressing patient health management and published in the journal *Science* also showed that algorithms used in healthcare are racially biased.[4] This study found "large racial biases" in the prediction of healthcare costs over illness resulting from unequal access to care. In addition, market forces and pre-existing societal prejudices of the data itself also play a role in the under-representation of certain populations, according to a recent article in the *Harvard Business Review*.[5]

Overcoming bias in the development of healthcare algorithms is challenging. Many algorithms are proprietary, and humans often cannot know specifically what pieces of information are used by a given AI-based program to make recommendations, how those data are weighted by the program, or even what data are included or excluded.[6]

Developers and users alike largely cannot reason through AI's "decisions." As disparities arise, there is a risk of patterns being repeated, resulting in the further amplification of existing inequities.

For example, one study that examined algorithmic underdiagnosis in the classification of pathologies across three large chest X-ray datasets and a multi-source dataset found that classifiers produced using state-of-the-art computer vision techniques consistently and selectively underdiagnosed

certain underserved patient populations. The study also found that the underdiagnosis rate was higher for intersectional underserved subpopulations such as, for example, Hispanic female patients.[7]

The researchers concluded that the deployment of AI systems with such biases for medical imaging-based diagnosis risks worsening existing care biases and leading to unequal access to medical treatment.[7]

Improving Data Diversity

While developers are limited by the availability of diverse datasets and technological aspects of algorithm training, there are ways to reduce AI bias in medicine. Focusing on diversity within algorithm development teams, including members' age, race, gender, and geography, can help to ensure data representation across populations, Dr Hawk says.

"Really look at the [development] team … and ask, 'will this represent the diversity of my practice or where I want my practice to go?'" Dr Hawk says. "If [the company] has a homogeneous team with homogeneous minds problem-solving … around how to create an algorithm, then they're going to design something that looks and feels like a solution for *their* problems." She adds that this can adversely impact the providers who use the technology and their patients whose disparities are deepened by its use.

Increased diversity of a development team also can result in a comprehensive evaluation of technology performance for every user, Dr Hawk says. She cites the example of an employee for whom English is a second language benefiting from a natural language processing algorithm.

"If you have diversity in your team, they will [ensure] that diversity was created in the design process of the algorithm," she says.

Improving diversity, equity, and inclusion in radiology, as a whole, is long overdue, says Dr Gupta, who notes the under-representation of minorities and women in the specialty. Statistics show that only 23% of radiologists are women; only 1.7% are Black; and 3.7% are Hispanic or Latino, compared to 6.2% and 5.3% of medical school graduates overall, and 13% and 18% of the population, respectively.[8]

"[Our] specialty is a leader in healthcare in developing AI, and if our trainees, residents, and fellows don't reflect the diversity of the general population, then we're not going to reflect more diversity as we develop AI and get these algorithms into the market," Dr Gupta says. "Going to the source—the radiologists who are becoming leaders in the AI space within healthcare—is really important."

Involving a more diverse body of stakeholders in training, reviewing, and supervising development of the algorithms, and validating the data, will help address bias issues within healthcare AI.

Leaders must "guide the needle into a better direction that lessens healthcare inequity, improves diversity across our field, [and] really places an element of empathy, kindness and patient-centered care into the work that we're doing," Dr Hawk says.

References

1) Fornell D. FDA has now cleared more than 500 healthcare AI algorithms. Health Exec. Feb 6, 2023. Accessed via https://healthexec.com/topics/artificial-intelligence/fda-has-now-cleared-more-500-healthcare-ai-algorithms.

2) AI: The Importance of Diversity in Data. 2020. Applied Radiology, accessed via https://appliedradiology.com/articles/ai-the-importance-of-diversity-in-data.

3) Health Subcommittee Hearing: "Understanding How AI is Changing Health Care." Nov. 29, 2023. House Committee on Energy & Commerce, accessed via https://energycommerce.house.gov/events/health-subcommittee-hearing-understanding-how-ai-is-changing-health-care.

4) Obermeyer Z, Powers B, Vogeli C, Mullainathan S. Dissecting racial bias in an algorithm used to manage the health of populations. *Science.* 2019; 366(6464): 447-453. Doi: 10.1126/science.aax23.

5) Friis S, Riley J. Eliminating algorithmic bias is just the beginning of equitable AI. Harvard Business Review. Sept 29, 2003. Accessed via https://hbr.org/2023/09/eliminating-algorithmic-bias-is-just-the-beginning-of-equitable-ai#:~:text=Algorithmic%20bias%20often%20occurs%20because,baked%20into%20the%20data%20itself.

6) Sharfstein J. How health care algorithms and AI can help and harm. Johns Hopkins Bloomberg School of Public Health. May 2, 2023. Accessed via https://publichealth.jhu.edu/2023/how-health-care-algorithms-and-ai-can-help-and-harm.

7) Seyyed-Kalantari L, Zhang H, McDermott M, et al. Underdiagnosis bias of artificial intelligence algorithms applied to chest radiographs in under-served patient populations. *Nat Med.* 2021; 27, 2176-2182. https://doi.org/10.1038/s41591-021-01595-0

8) Omofoye T, Bradshaw M. The emerging diverse radiology workplace: case studies on the importance of inclusion in radiology training programs, *Acad Rad,* 2023; 30:(5) 983-990. ISSN 1076-6332, doi: https://doi.org/10.1016/j.acra.2022.05.012

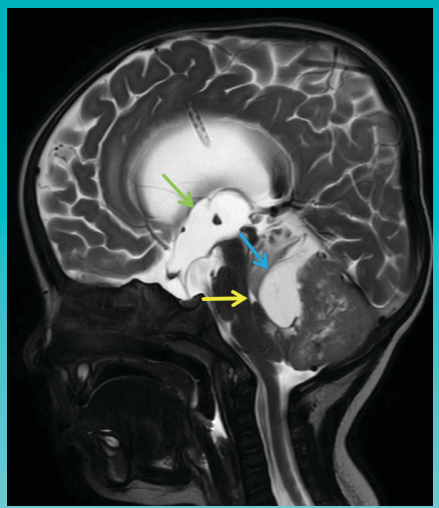

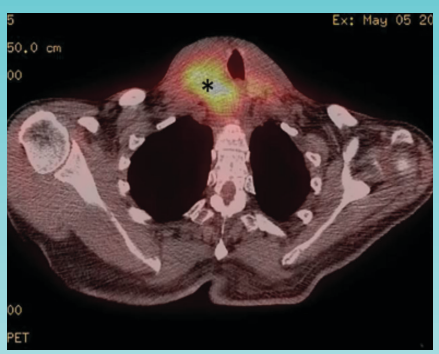

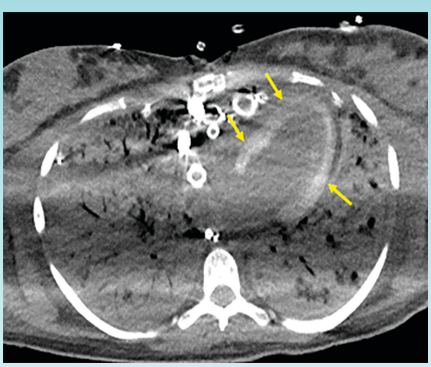

AppliedRadiology®

The Journal of Practical Medical Imaging and Management

Call for Cases

If you have an interesting case we want to know about it!

Sharing your case is a fantastic opportunity to gain recognition for your work and receive feedback from peers all over the world!

Author Guidelines* can be found at

https://appliedradiology.com/author-guidelines

- Abdominal
- Thoracic
- Genitourinary
- GI
- Emergency
- Interventional
- Vascular
- Peds
- Breast
- Neuro
- MSK
- Oncologic
- Cardiac
- Molecular Imaging
- Nuclear Medicine

* Cases undergo peer review before being accepted for publication.

PRINT / ONLINE

RADIOLOGICAL CASE

Sepsis-induced Rapid Left Ventricular Calcification

Sherif Moawad, MD; Ahmad Kattan, MD; Terrence Lewis, MD

Case Summary

An adult presented to the emergency department with fever and sepsis 7 days postpartum. Pregnancy course and delivery were uncomplicated. Blood cultures were positive for group A streptococcus, and aggressive antibiotics and supportive management were initiated. Shortly afterward, the patient arrested and was placed on extracorporeal membrane oxygenation (ECMO) after attempts to restore cardiac rhythm failed. Acute renal failure, disseminated intravascular coagulation (DIC), and generalized ecchymosis with skin blisters occurred on the second day. A noncontrast computed tomography (CT) scan of the chest on day 5 revealed acute respiratory distress syndrome (ARDS) and early calcification of the left ventricular papillary muscles and myocardium with sparing of the endocardium. This finding was confirmed by echocardiography. The calcifications appeared more dense on follow-up CT images; however, the cardiac ejection fraction (EF) was within normal limits (60%).

Imaging Findings

Noncontrast chest CT demonstrated ARDS and early diffuse calcifications involving the left ventricle myocardium and the papillary muscles (Figure 1). However, serum calcium and phosphorus were not elevated and no dystrophic calcifications were noted elsewhere. These findings were confirmed by trans-esophageal echocardiography, which showed dense left ventricle myocardium (Figure 2). These calcifications did not significantly affect the left ventricular EF, which was 60% (n = ≥55%). Follow-up CT chest one month later

Diagnosis

Discussion

EMAIL ANNOUNCEMENT

AppliedRadiology® 50

The Journal of Practical Medical Imaging and Management

Featured Case

Sepsis-induced Rapid Left Ventricular Calcification

Case Summary

An adult presented to the emergency department with fever and sepsis 7 days postpartum. Pregnancy course and delivery were uncomplicated.

View this Case

SOCIAL MEDIA

AppliedRadiology @Applied_Rad · May 29

What's your dx? Patient presented to the emergency department with fever and sepsis 7 days postpartum Full case and answer bit.ly/3PPOS8F #radiology #RadRes #FOAMed #FOAMrad #RadTwitter

3 35 110

What is AI up to?

C. Douglas Phillips, MD

Not sure how many of you were able to get to RSNA 2023. I'm not going to say it was back to full speed, but it was pretty close.

The varying intensity of the meeting is still a little odd to me. On Tuesday you got through the bridge from the East building only by bending forward and moving into the press of humanity. It is a little like leaning into a gale-force wind. To say nothing of being greeted a hundred times by people you know, which mandates a five- to ten-minute discussion as humanity streams by you on all sides. A trip across that bridge is a minimum 20-minute process. I love it.

I will eventually miss RSNA quite a lot. Not going to RSNA is something I will undoubtedly have to start getting used to as I move along to the "next phase" of my career (fewer meetings, more talk about retirement). But what happened at RSNA 2023? What was new? What made people happy (or depressed)?

AI.

Jeez, I'm pretty sure that ChatGPT (or perhaps a clone of it) and its latest iteration will soon be chewing my food for me. If it lets me eat. It may not have the need for me.

I was very fortunate this year to moderate the annual Image Interpretation Session. Smart folks looked at some nearly impossible cases I gathered with the assistance of my colleagues. And they hammered them. These are some very intelligent people. But you know, at some point I wonder if they all just presented the cases to their AI system and said, "Hey, AI, what is this case?"

Not this year, but at some point, it is a possibility. You know what's coming? We will have patients taking their online images and their history and physical exam findings and inputting it all into their free AI program. And we will get insistent letters saying things like, "Why didn't you think about sparganosis?" "Don't you want to order a serum molybdenum level on me? Please see attached AI comments."

And you know what else? I don't think our non-radiology colleagues are immune to this at all. You can click boxes and say where it hurts, and these programs can do your work-up. When AI programs get ordering and admitting privileges we are in trouble. Surgical robots are already out there; with time they will also know what to do on their own. "Hi, I'm Bill, your anesthesia robot. And this is Suzy, your surgery robot. Don't worry, you won't feel a thing."

I love what I do, don't get me wrong. However, I am on many levels happy to be at the point in my career where I am, as opposed to just starting out.

I wonder if AI needs a cup of coffee in the morning to get started? A mid-day chocolate? Does it like a cold martini at the end of a particularly bad day? Can it write a humorous send-up of humans?

Yeah, unlikely.

Keep doing that good work. Mahalo.

Dr Phillips is a Professor of Radiology, Director of Head and Neck Imaging, at Weill Cornell Medical College, NewYork-Presbyterian Hospital, New York, NY. He is a member of the *Applied Radiology* Editorial Advisory Board.

Complications of Anorexia Nervosa

Rami M. El-Baba, DO; Charles Messerly, DO; Ahmad Tahawi; Kevin R. Carter, DO

Case Summary

A young adult presented to the emergency department following a fall from bed. On examination, the patient was noted to be severely cachectic with a body mass index (BMI) of 12.9 and a visible deformity of the distal left femur. Patients with a BMI <15 are characterized by the DSM-5 as having extreme anorexia nervosa (AN).[1]

The patient complained of distal left thigh pain and bilateral foot pain. They reported recently experiencing bilateral foot edema, for which they poked their feet with sewing needles in an attempt to relieve the pressure. Per the patient's parent, they had an extensive history of hospitalizations for AN-related medical complications. During workup, the patient underwent lower extremity and pelvic radiography, noncontrast CT of the head, chest, abdomen, and pelvis; and MRI of the feet to assess for osteomyelitis.

Affiliations: Department of Radiology, Loyola University Medical Center-Maywood, Ilinois (Dr El-Baba); Department of Radiology, Mclaren Oakland, Pontiac, Michigan (Drs Messerly, Carter); Department of Radiology, Beaumont-Farmington Hills, Farmington Hills, Michigan (Dr Tawahi).

Imaging Findings

Knee radiography demonstrated an oblique, impacted fracture of the distal femoral metaphysis superimposed on diffuse bony demineralization. Pelvis radiography revealed an acute, comminuted fracture of the right greater trochanter, as well as remote fractures of the bilateral superior pubic rami (Figure 1). Additionally, Rigler sign, air outlining both sides of the colon wall was also seen (Figure 1). Sagittal CT of the spine revealed multiple vertebral body compression fractures (Figure 1).

Axial noncontrast brain CT demonstrated diffuse prominence of the ventricles and sulci, out of proportion to the patient's age (Figure 2). Axial abdominal CT revealed retroperitoneal gas dissecting along the inferior vena cava and into the inferior mediastinum as well as significant bowel-wall pneumatosis of the ascending and transverse colon, and free air within the peritoneal cavity (Figure 3).

Magnetic resonance imaging of the feet revealed premature conversion of red marrow to yellow marrow (Figure 4) but no osteomyelitis.

Diagnosis

Anorexia nervosa complicated by severe bony demineralization, pathological fractures, and pneumatosis intestinalis with pneumoperitoneum.

Discussion

Anorexia nervosa is a unique psychological disorder that leads to severe physiologic derangements across nearly every body system. The sequelae of such alterations can present with a variety of radiographic findings.

The neurological system is quarterbacked by the brain, whose main fuel source is glucose. Without adequate carbohydrate intake, the brain is starved of glucose, leading to overall decreased brain volume. Multiple MRI studies have demonstrated that gray matter volumes are primarily affected in AN; this volume

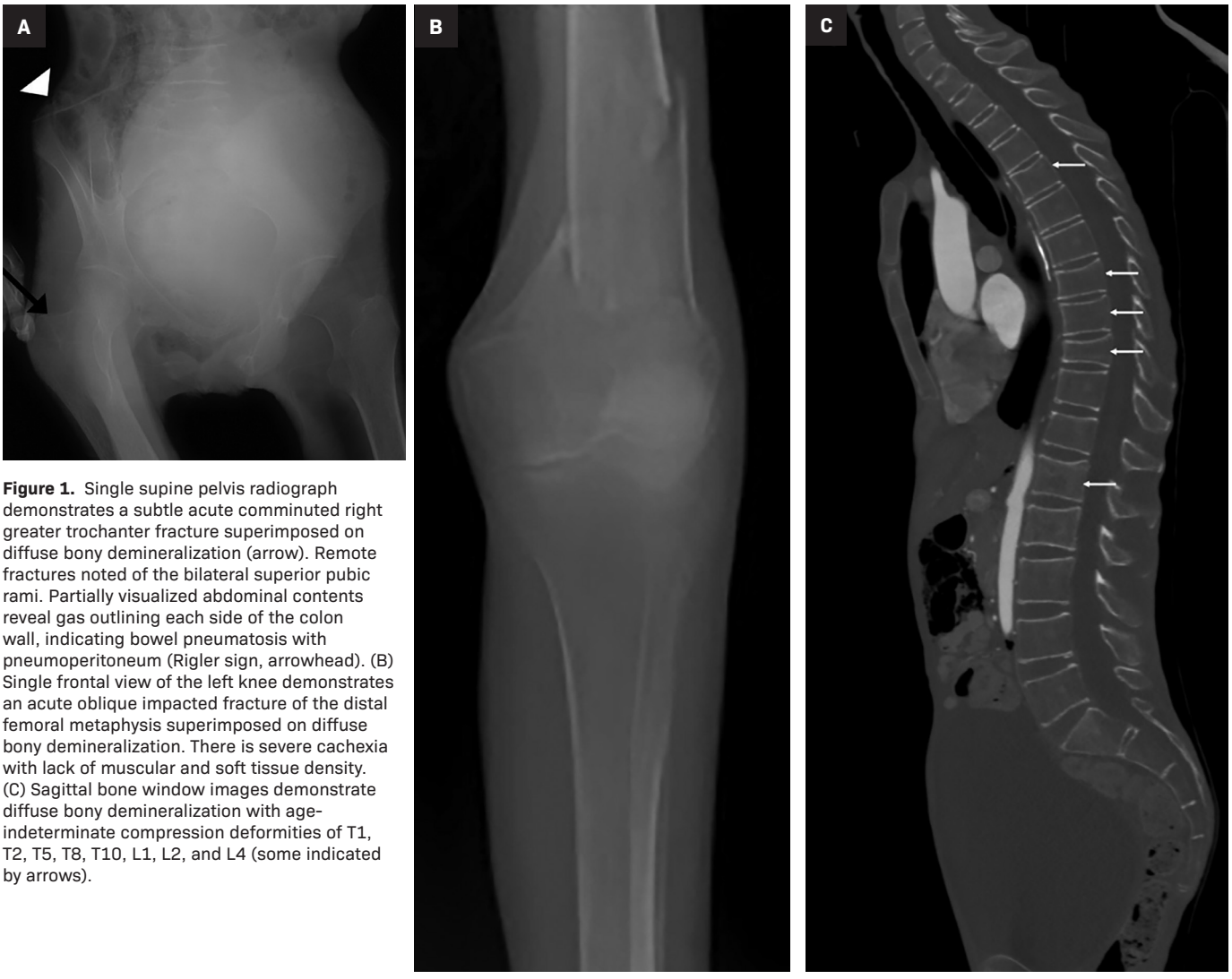

Figure 1. Single supine pelvis radiograph demonstrates a subtle acute comminuted right greater trochanter fracture superimposed on diffuse bony demineralization (arrow). Remote fractures noted of the bilateral superior pubic rami. Partially visualized abdominal contents reveal gas outlining each side of the colon wall, indicating bowel pneumatosis with pneumoperitoneum (Rigler sign, arrowhead). (B) Single frontal view of the left knee demonstrates an acute oblique impacted fracture of the distal femoral metaphysis superimposed on diffuse bony demineralization. There is severe cachexia with lack of muscular and soft tissue density. (C) Sagittal bone window images demonstrate diffuse bony demineralization with age-indeterminate compression deformities of T1, T2, T5, T8, T10, L1, L2, and L4 (some indicated by arrows).

Figure 2. Axial noncontrast CT of the head demonstrates significant ventricular and sulcal prominence out of proportion for the patient's age.

loss has been shown to be reversible with weight restoration..

In cases of AN, malnutrition leaves the body in a constant "fight or flight" state, leading to excessive and continuous release of cortisol. This blocks calcium absorption and disrupts calcium homeostasis, causing decreased bone cell growth and ultimately leading to bone reabsorption and decreased bone mineral density. The earlier the onset of disease before peak bone density is achieved, the more severe the osteoporosis.[2] This leads to increased incidence of pathologic fractures. Our patient reportedly fell from a height of no more than three feet and developed multiple acute left lower extremity fractures with more age-indeterminate vertebral compression fractures.

Anorexia nervosa has also been linked to abnormalities in osteoblast and osteoclast progenitor cells in bone marrow. Hormonal alterations with disruption of the hypothalamic-pituitary axis and amenorrhea leads to adipocyte over osteoblast differentiation within the mesenchymal stem cell pool.[3] This results in fat deposition and premature conversion from red marrow to yellow marrow.

Severe protein and electrolyte derangements lead to impaired synthetic liver function, which can result in coagulopathy and abnormally low albumin levels. This causes large fluid shifts from intravascular to extravas-

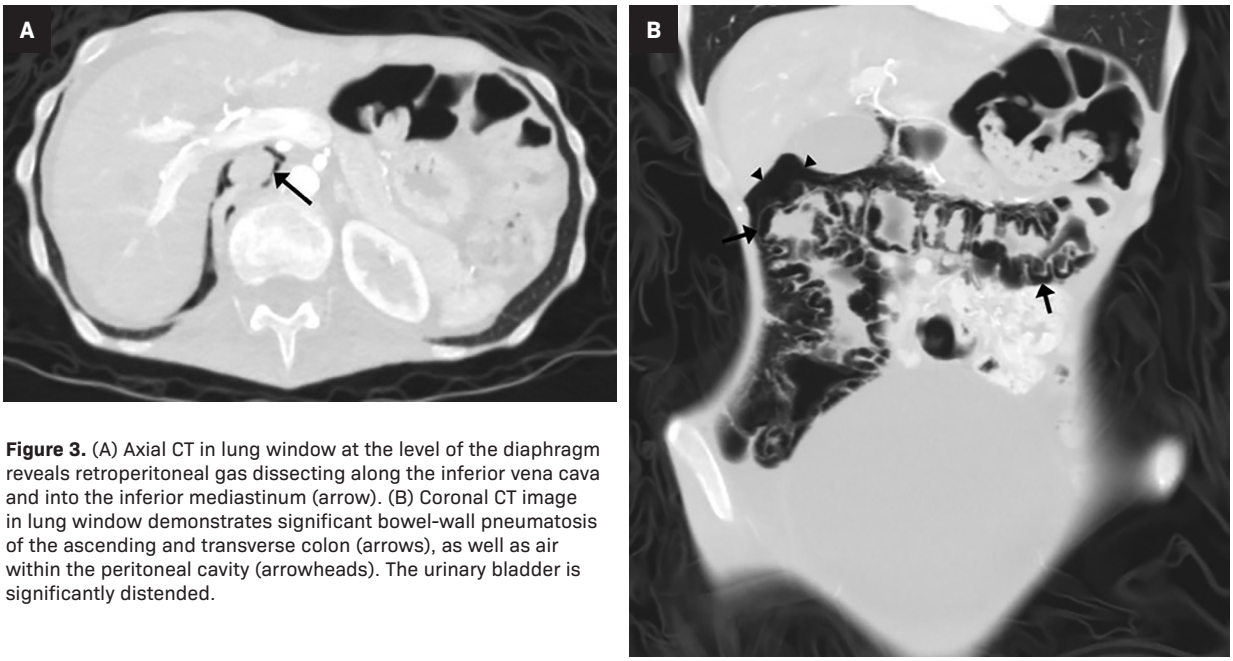

Figure 3. (A) Axial CT in lung window at the level of the diaphragm reveals retroperitoneal gas dissecting along the inferior vena cava and into the inferior mediastinum (arrow). (B) Coronal CT image in lung window demonstrates significant bowel-wall pneumatosis of the ascending and transverse colon (arrows), as well as air within the peritoneal cavity (arrowheads). The urinary bladder is significantly distended.

Figure 4. Sagittal MR images of the foot in proton density, T1, and T2 demonstrate bright osseous marrow signal, indicating the premature conversion of red marrow to yellow marrow. The evaluation is limited secondary to lack of fat suppression; however, no gross findings for osteomyelitis are seen.

cular spaces, resulting in anasarca, ascites, and pleural effusions, all of which this patient experienced during their hospital stay.

Very few cases of pneumatosis intestinalis have been reported in the setting of AN. As in this patient, the condition is typically found incidentally. It is theorized that the combination of electrolyte imbalance, anasarca, and large fluid shifts in the setting of a low-flow mesenteric circulation state causes nonocclusive bowel ischemia and eventually pneumatosis intestinalis and pneumoperitoneum.[4]

Conclusion

The images presented in this case demonstrate the unique and multisystem sequelae of extreme AN. Knowledge of such findings form a link behind the body's physiological response to severe malnourishment and the downstream consequences, some of which are reversible, such as bony demineralization. Careful attention must be paid in identifying such findings to help these patients receive the most appropriate care.

References

1) Biller B M, Saxe, V, Herzog D B, Rosenthal, D I, Holzman S, Klibanski A. Mechanisms of osteoporosis in adult and adolescent women with anorexia nervosa. *J Clin Endocrinol Metab.* 1989; *68*(3): 548-554. doi:10.1210/jcem-68-3-548

2) Clarke B. Bone marrow changes in adolescent girls with anorexia nervosa. *Yearbook of Endocrinology. 2010:* 238-240. doi:10.1016/s0084-3741(10)79490-7

3) Diagnostic and Statistical Manual of Mental Disorders, Fourth Edition, Text Revision (DSM-IV-TR). (2000). doi:10.1176/appi.books.9780890423349

4) Hudson J L, Hiripi E, Pope H G, Kessler R C. The prevalence and correlates of eating disorders in the National Comorbidity Survey Replication. *Biological Psych.* 2012*; 72*(2): 164. doi:10.1016/j.biopsych.2012.05.016

5) Neychev V, Borruso J. Bowel ischemia and necrosis in anorexia nervosa: a case report and review of the literature. *Intl J Surg Case Rep.* 2015; 8:141-143. doi:10.1016/j.ijscr.2015.01.035

6) Roberto, C A, Mayer L E, Brickman A M, et al. Brain tissue volume changes following weight gain in adults with anorexia nervosa. 2010; *Intl J Eating Dis. 44*(5): 406-411. doi:10.1002/eat.20840

7) Sachs K V, Harnke B, Mehler P S, Krantz M. J. Cardiovascular complications of anorexia nervosa: A systematic review. *Intl J Eating Dis.* 2015; *49*(3): 238-248. doi:10.1002/eat.22481

Neonatal Adrenal Hemorrhage

Hanna Tolson; Richard B. Towbin, MD; Carrie M. Schaefer, MD; Alexander J. Towbin, MD

Case Summary

A newborn with tracheoesophageal fistula, imperforate anus, and tethered cord underwent abdominal ultrasound to evaluate the solid organs for further anomalies.

Imaging Findings

Ultrasound (Figure 1) showed a 1.2 cm asymptomatic hypoechoic mass within the right adrenal gland. The lesion had no internal color Doppler flow, and it was not present on earlier ultrasound. It decreased in size on subsequent ultrasound (Figure 2) before later resolving. Abdominal ultrasounds were repeated at two weeks, one month, and four months. Throughout this time, the mass decreased in size, remained adreniform in configuration, and appeared hypoechoic to anechoic, consistent with the suspected diagnosis of adrenal hemorrhage.

Affiliations: University of Arizona College of Medicine—Phoenix (Ms Tolson), Department of Radiology, Phoenix Children's Hospital (Drs Schaefer, R Towbin), Department of Radiology Cincinnati Children's Hospital, University of Cincinnati College of Medicine, (Dr A Towbin)

Diagnosis

Adrenal hemorrhage.

The differential diagnosis for a suprarenal mass in a neonate includes neuroblastoma, mesoblastic nephroma, and subdiaphragmatic extralobar pulmonary sequestration[1] risk factors and clinical presentations of neonatal adrenal haemorrhage (NAH

Discussion

Adrenal hemorrhage is a relatively uncommon condition in neonates, occurring in just 0.2-0.55% of live births.[1] The vascular architecture of the adrenal gland is unique and particularly vulnerable to arteriolar rupture and bleeding. Three arteries supply the gland, dividing into fifty to sixty small branches, forming a subcapsular plexus. A relatively small number of venules drain the subcapsular plexus. This intrinsically vulnerable network, termed a vascular dam, is sensitive to vasoconstriction from catecholamines released by the adrenal medulla resulting in increased intravascular pressure.[2,3]

Adrenal hemorrhage is more common on the right side (70%) of cases, with bilateral involvement occurring in 10% of cases. The greater incidence of right adrenal hemorrhage is thought to occur because the veins drain directly into the inferior vena cava. This configuration makes the gland more susceptible to pressure changes, which ultimately lead to arteriolar rupture. Neonates are at risk for adrenal hemorrhage owing to the relatively large size of their adrenal glands and their resultant increased vascularity.[4] Other factors that increase the risk of hemorrhage in neonates include the hormone release during the antenatal period and changing pressures as the neonate passes through the vaginal canal.[5]

Though some risk factors for adrenal hemorrhage have been reported, the etiology of bleeding in many cases remains unknown. As previously mentioned, physiologic stress predisposes neonates to adrenal hemorrhage. Thus, acidemia, asphyxia, septicemia, prolonged labor, hypotension, and difficult delivery all increase the risk of adrenal hemorrhage.[5] Additionally, male gender and macrosomia have been identified as risk factors, likely owing to increased size of the newborn and potential for stress during delivery.[6]

The presentation of neonatal adrenal hemorrhage is variable and nonspecific. Many neonates are as-

Figure 1. (A) Longitudinal ultrasound (US) shows a 1.2 cm hypoechoic suprarenal mass (arrow). (B) Transverse US (arrow) shows no internal color Doppler blood flow.

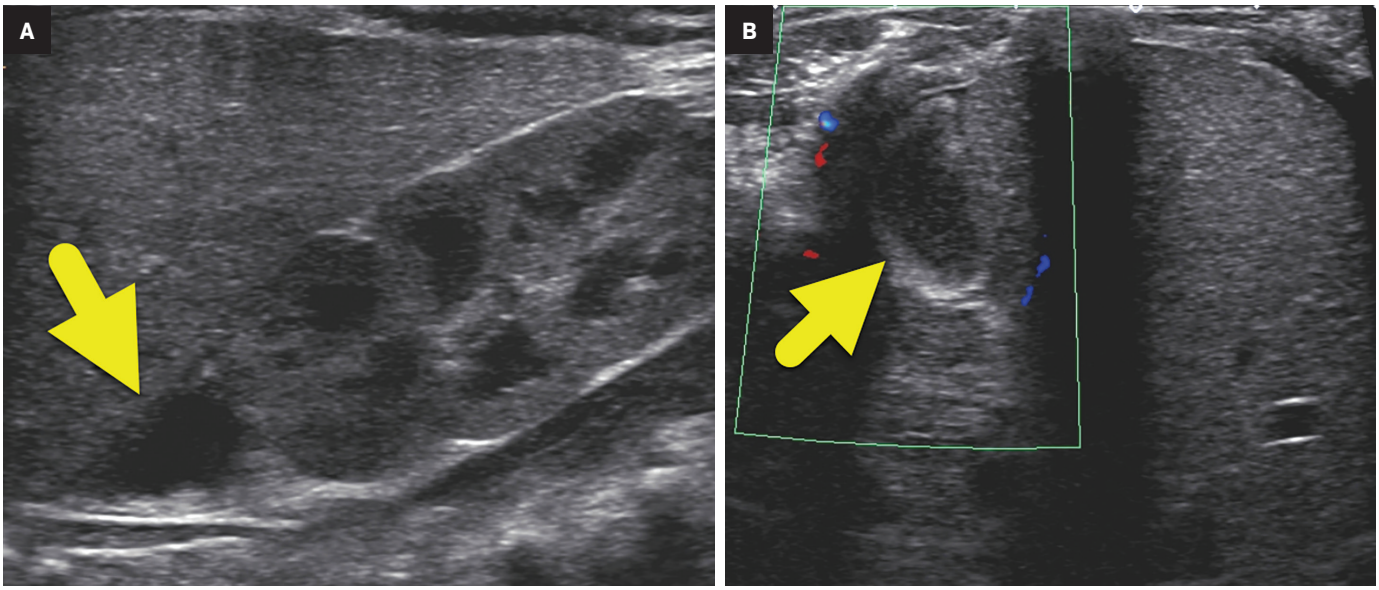

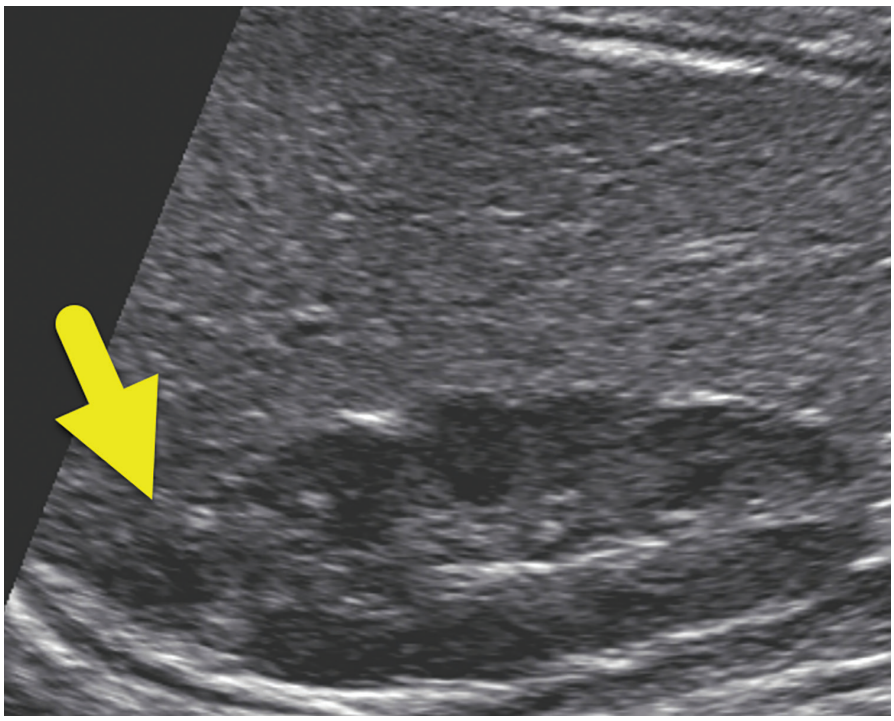

Figure 2. Longitudinal US performed 6 months later shows that the hypoechoic suprarenal mass (arrow) decreased in size, measuring 9 mm in its longest diameter.

ymptomatic. The most common presenting symptom in neonatal adrenal hemorrhage is indirect hyperbilirubinemia, resulting in jaundice. Other common features include anemia, pallor, flank mass, and lethargy/hypotonia.[1] Scrotal discoloration has been reported, with an incidence of about 0.2%, and occurs either by dissection along the tissue planes of the retroperitoneum outside the processus vaginalis or by rupture of the posterior peritoneum, resulting in intraperitoneal hemorrhage and descending within the patent processes vaginalis.[5] As the adrenal gland has significant regenerative capacity, hemorrhage is typically not associated with adrenal insufficiency.[4]

Abdominal ultrasound generally serves as the initial diagnostic modality. Findings vary with the age of the hemorrhage. Initially the adrenal hemorrhage appears solid and hyperechoic. As the clot lyses, the echogenicity becomes mixed with a central echogenic region

that becomes cystic in appearance. Calcification can develop as early as 1-2 weeks after onset of the bleeding. The hemorrhage usually resolves by about 2 months of age. Calcifications remain visible on radiograph and CT. The conspicuity of the calcification on radiographs likely decreases as the child grows into adulthood.

In the neonatal period, distinguishing neuroblastoma from adrenal hemorrhage is important. Imaging is not always conclusive, since neuroblastoma can also present as a solid, cystic, or mixed lesion exerting mass effect on the upper pole of the kidney. Doppler ultrasound can help distinguish the lesions. Neonatal adrenal hemorrhage is often hypovascular or has no blood flow, while neuroblastoma may have increased blood flow. The shape of the lesions may also help to distinguish neuroblastoma from hemorrhage. Neuroblastoma often appears mass-like, while the adrenal gland may maintain its triangular shape with hemorrhage.

There is no treatment for neonatal adrenal hemorrhage, as most cases spontaneously resolve. Standard practice is watchful waiting with serial sonography performed at follow-up to check for regression of the lesion. If the lesion does not regress as expected or increases in size, it may be biopsied to exclude malignancy.[8] Alternatively, neuroblastoma could be confirmed with MIBG scan or the presence of urine or serum catecholamine levels.

Conclusion

Ultrasound remains the primary modality for assessing and following neonates with suspected adrenal hemorrhage. Regression of the adrenal mass and absence of vascular flow on color Doppler are the main differentiating features of neonatal adrenal hemorrhage from neuroblastoma. Though the symptoms of neonatal adrenal hemorrhage are variable and non-specific, the index of suspicion should increase when a neonate presents with unexplained jaundice, anemia, or hypotonia.

References

1) Mutlu M, Karagüzel G, Aslan Y, Cansu A, Ökten A. Adrenal hemorrhage in newborns: A retrospective study. *World J Pediatr*. 2011;7(4):355-357. doi:10.1007/s12519-011-0259-7

2) Kawashima A, Sandler CM, Ernst RD, et al. Imaging of nontraumatic hemorrhage of the adrenal gland. *Radiographics*. Published online 1999. doi:10.1148/radiographics.19.4.g99jl13949

3) Jordan E, Poder L, Courtier J, Sai V, Jung A, Coakley F V. Imaging of nontraumatic adrenal hemorrhage. *Am J Roentgenol*. Published online 2012. doi:10.2214/AJR.11.7973

4) Toti MS, Ghirri P, Bartoli A, et al. Adrenal hemorrhage in newborn: How, when and why- from case report to literature review. *Ital J Pediatr*. 2019;45(1):1-8. doi:10.1186/s13052-019-0651-9

5) Roupakias S, Papoutsakis M, Mitsakou P. Blunt adrenal gland trauma in the pediatric population. *Asian J Surg*. Published online 2011. doi:10.1016/j.asjsur.2011.08.003

6) Gyurkovits Z, Maróti Á, Rénes L, Németh G, Pál A, Orvos H. Adrenal haemorrhage in term neonates: A retrospective study from the period 2001-2013. *J Matern Neonatal Med*. Published online 2015. doi:10.3109/14767058.2014.976550

7) Dorai CRT, Smith AJ, Dewan PA. Adrenal haemorrhage: Presenting as acute scrotal swelling in a neonate. *J Paediatr Child Health*. Published online 1994. doi:10.1111/j.1440-1754.1994.tb00571.x

8) Wang CH, Chen SJ, Yang LY, Tang R Bin. Neonatal adrenal hemorrhage presenting as a multiloculated cystic mass. *J Chinese Med Assoc*. Published online 2008. doi:10.1016/S1726-4901(08)70153-9

Bilateral Branchial Cleft Fistulae

PJ Preethi Philomina, MBBS; Vishwanath Vijay Joshi, MBBS; Jyotirmay Shyamsundar Hegde, MBBS

Case Summary

A young adult presented with complaint of intermittent discharge from small openings located over both lateral aspects of the lower neck since childhood. On examination, two small openings were noted, one on each side of the lateral aspect of lower third of the neck along the anterior border of sternocleidomastoid, along with mildly inflamed margins and mucopurulent discharge. No opening was found in the oropharyngeal cavity.

Imaging Findings

Intravenous contrast-enhanced CT with additional 10 ml of diluted contrast introduced through both openings revealed bilateral linear fistulous tracts in the neck with the external opening in the skin at the lower one-third of the sternocleidomastoid muscle, at the level of C7-T1 (Figure 1). The tracts coursed cranially along the anterior borders of the sternocleidomastoid muscles, anterior to the carotid spaces with medial bends at the C3 level and passed between the internal and external carotid arteries (Figure 2,3). The internal openings were within the tonsillar fossae of the oropharynx with contrast seen pooling in the oropharyngeal lumen (Figure 4). There was no abscess formation. The patient underwent surgery of complete excision of the tracts (Figure 5).

Diagnosis

Bilateral second branchial cleft fistulae. The differential diagnoses include thyroglossal duct fistulae and acquired fistulae secondary to infection.

Discussion

Mesodermal condensations present in the side wall of the embryological pharynx give rise to branchial arches and their pouches. Second branchial arch and pouch anomalies are common anomalies of the branchial apparatus.[1] The anomalies of branchial apparatus were first described by Von Ascheron.[2]

During embryological development, the branchial arch grows caudally, enveloping the third, fourth, and sixth arches and forming the cervical sinus by fusing with skin caudal to these arches. Normally the edges of cervical sinus fuse and the ectoderm within it regresses. Abnormal persistence of this ectoderm gives rise to a cyst. The fistula results from the breakdown of endoderm internally; most commonly this occurs in the second pouch.[1,3]

While anomalies of the second branchial cleft account for 90% of all developmental abnormalities of the branchial apparatus, complete second arch fistulae are rare and comprise only 2%.[4] Branchial cysts and simple sinus openings ending blindly after a variable distance are more common than branchial fistulae.[5]

Complete branchial fistulae with an internal opening are very rare. They are usually present at birth with the tiny external opening often going initially unnoticed and commonly presenting in childhood or the second decade.

Intermittent or continuous mucoid discharge and recurrent infection, particularly following an upper respiratory tract infection are common presenting symptoms. Abscess with cellulitis may also be a complication. Owing to variability in the course of the tracts and the need for complete excision, preoperative radiologic visualization of the tract is a prerequisite to successful treatment.

Radiographic fistulograms show a smoothly marginated tract with variable width along the usual anatomic course. Neck CT with administration

Affiliations: Department of Radiodiagnosis, Manipal Hospitals, Bangalore, India (Drs Philomina, Joshi); Department of Otorhinolaryngology, Manipal Hospitals, Bangalore, India (Dr Hegde). Disclosures: None.
Keywords: Branchial cleft, fistulae, CT, Fistulogram, Branchial anomalies

Figure 1. CT axial section fistulogram images in bone window showing bilateral external openings (arrows).

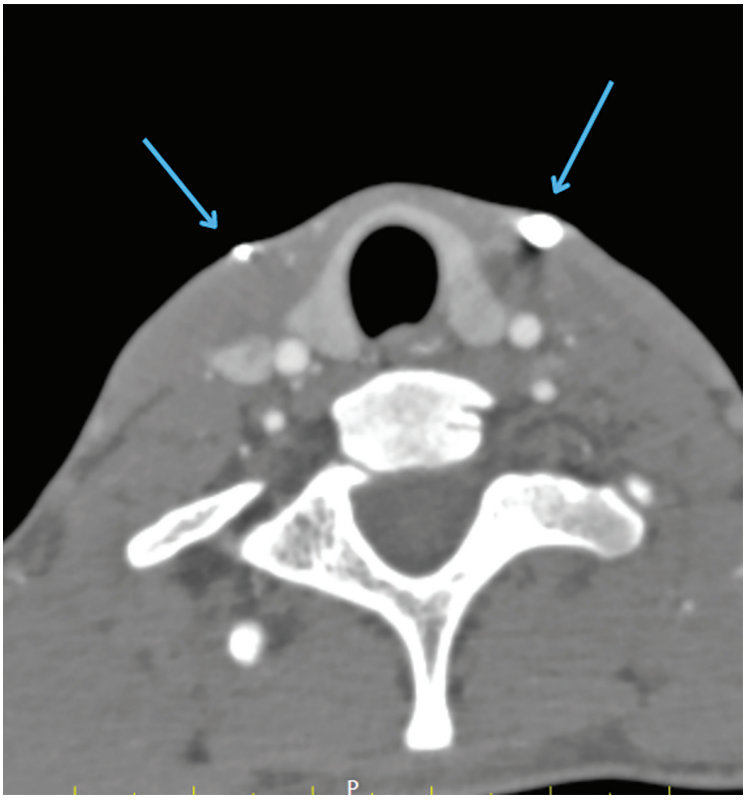

Figure 2. CT fistulogram coronal reformatted image in bone window delineating course of bilateral fistulous tracts (arrows).

Figure 3. CT axial section fistulogram images in soft tissue window at the level of the bifurcation of the common carotid arteries showing bilateral tracts passing between the internal and external carotid arteries (arrows).

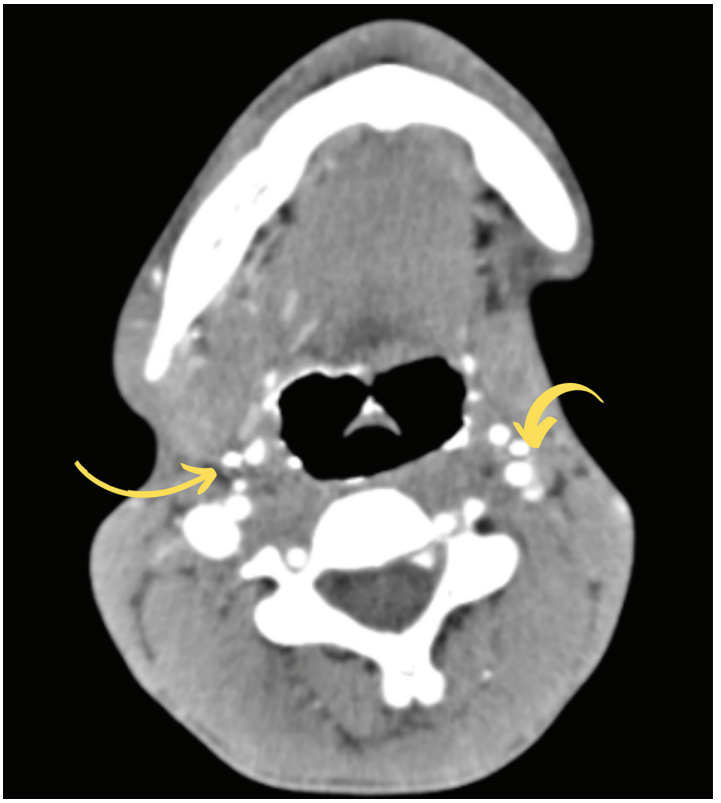

Figure 4. CT axial section fistulogram images in bone window at the level of tonsils showing bilateral internal openings (arrows).

Figure 5. Clinical images showing (A) left external opening (circle) preoperatively, (B) intraoperative procedure showing transcervical approach with stepladder dissection, and (C) postoperative excised tracts.

of contrast through cutaneous openings has been shown to be superior for fistula demonstration, over non-contrast or intravenous contrast-only CT and conventional fistulogram.[6,7] However, contrast injected into the fistula may not flow freely when the tract is blocked by secretions or granulation tissue.

The advantages of contrast-enhanced CT with a sinogram or fistulogram over conventional imaging include the ability to reconstruct images in multiple planes, including curved reformations, to offer better delineation of the tract in relation to other neck structures; and accurate depiction of the tract course to help guide the surgeon.

A fistulogram can help confirm the clinical diagnosis, to estimate the length and course of the tract, to look for an associated cyst.

The typical course of a second branchial cleft fistula begins at the external opening in the middle or lower third of the neck along the anterior border of the sternocleidomastoid muscle, runs deep to the platysma across the carotid sheath, taking a medial bend, and passes between the internal and external carotid arteries before finally opening into the tonsillar fossa.[9]

Surgery is the treatment of choice, as these entities will not regress spontaneously and there is increased incidence of recurrent infections due to the external communication. Imaging assists in surgical planning to facilitate complete excision of the tract to prevent recurrence. Sclerosing agents carry the risk of necrosis and perforation.

Recurrence, secondary infection, hematoma, and injury to traversing nerves or the internal jugular vein and are examples of potential surgical complications.[10]

Conclusion

Lateral cutaneous openings with discharge should raise suspicion for branchial fistulae and radiologic investigation. A CT fistulogram may be valuable to guide surgery.

References

1) Ford GR, Balakrishnan A, Evans IN, et al. Branchial cleft and pouch anomalies. *J Laryngol Otol*. 1992;106:137-143.

2) De PR, Mikhail T. A combined approach excision of branchial fistula. *J Laryngol Otol*. 1995;109:999-1000.

3) Shinde K. Complete second branchial fistula: a study of four cases. *Int J Head Neck Surg*. 2013; 4 (3):129-132.

4) Ismail Y, Ozcan C, Nuri O, Fatih B, Beyhan D. Complete fistula of the second branchial cleft: case report of catheter aided total excision. *Int J Ped Otorinolaryngol*. 2004;68:1109-1113.

5) Kamal NR, Simi R, Dheeraj P, Joginder SG, Samar Pal Singh Y. Second branchial cleft fistula. Is fistulogram necessary for total excision. *Int J Ped Otorinolaryngol*. 2006;70:1027-1030.

6) Burton MG. Second branchial cleft cyst and fistula. *Am J Radiol*. 1980 May;134:1067-1069.

7) Ryu CW, Lee JH, Lee HK, Lee DH, Choi CG, Kim SJ. Clinical usefulness of multidetector CT fistulography of branchial cleft fistula. *Clin Imaging*. 2006; 30(5):339-342. doi: 10.1016/j.clinimag.2006.05.001. PMID: 16919556.

8) Sun Z, Fu K, Zhang Z, Zhao Y, Ma X. Multidetector computerized tomographic fistulography in the evaluation of congenital branchial cleft fistulae and sinuses. *Oral Surg Oral Med Oral Pathol Oral Radiol*. 2012;113(5):688-694. doi: 10.1016/j.oooo.2011.08.015. Epub 2012 Apr 12. PMID: 22668628.

9) Talaat M. Pull-through branchial fistulectomy: Technique for the otolaryngologist. *Ann Otol Rhino Laryngol*. 1992;101:501-502.

10) Francisco C, Agaton B, Cosmay GE. Diagnosis and treatment of branchial cleft cysts and fistulae. A retrospective study of 183 patients. *Int J Oral Maxillofac Surg*. 1996;25: 449-452.

Epidural Lipomatosis

Faiz Syed; Mitchel Whorton, MD; Steven Lev, MD

Case Summary

An adult with a history of type II diabetes mellitus, hypothyroidism, COPD, asthma, and cervical cancer presented with lower back pain exacerbated by walking and relieved with rest. The patient described the pain as 7/10 and associated with numbness and tingling that radiated down both legs but was more pronounced in the right leg. Physical examination revealed tenderness to palpation of the lumbar paraspinal musculature with muscle spasms. Pain was elicited with 60 degrees of flexion of the hips bilaterally. There was decreased sensation to light touch in the right lower extremity in an L3-L5 dermatomal distribution. Patellar reflexes were 1+ bilaterally.

Imaging Findings

Magnetic resonance imaging of the lumbosacral spine (Figures 1,2) demonstrated prominent epidural fat surrounding the thecal sac, from approximately the L3 level and inferiorly. Axial images, particularly at the L4-L5 level (Figure 3), revealed the fat causing deformation and significant stenosis of the thecal sac. The polygonal deformation of the dural sac was a pathognomonic sign of the condition.

Affiliations: New York Institute of Technology College of Osteopathic Medicine, Old Westbury, New York (Mr Syed); Department of Radiology, Nassau University Medical Center, East Meadow, New York (Dr Lev)

Diagnosis

Epidural lipomatosis**.** Clinical differential diagnoses for typical symptoms include herniated disc, narrowing of the spinal canal, spondylolysthesis, and distal polyneuropathy.

Discussion

Spinal epidural lipomatosis is caused by an overgrowth of adipose tissue in the epidural space. This leads to narrowing of the spinal canal and compression of neural structures.[1] Patients may be asymptomatic in the early stages of disease. However, with progression and compression of different regions of the spinal canal, patients may present with back pain, weakness, paresthesias, claudication, radiculopathy, sensory disturbances, and/or ataxia.[2]

Epidural lipomatosis is most often associated with exogenous steroid use. It is less common in patients without steroid use secondary to obesity or endogenous steroid excess. It may also be idiopathic. Men are more commonly affected than women.[3]

The most sensitive test for the condition is MRI, particularly T1 where the fat will be white. The pathognomonic "Y" shape polygonal deformation of the dural sac is caused by compression due to excess fat.[2] The "Y" sign does not become apparent until the disease is severe. Grading of epidural lipomatosis (I, II, III) is based on the epidural fat-to-spinal-column index, with normal values being less than 40%. The condition is designated as Grade III when the "Y" sign is first seen on MRI and the epidural fat-to-spinal-column ratio is greater than 75%.[4]

Epidural lipomatosis can be managed with steroid taper and discontinuation or with laminectomy and epidural fat resection. Approximately 90% of cases are managed surgically, which is considered in severe cases or where conservative treatment has failed.[5] Weight reduction strategies can be beneficial in alleviating patients with epidural lipomatosis secondary to obesity.[6] Clinical trials have not been conducted to compare outcomes of conservative and surgically managed cases.[2]

Conclusion

Epidural lipomatosis has the potential to cause spinal stenosis, which can be diagnosed with MRI. Imaging determines extent to which epidural lipomatosis has affected the spinal canal and can facilitate surgical planning.

References

1) Kim K, Mendelis J, Cho W. Spinal epidural lipomatosis: a review of pathogenesis, characteristics, clinical presentation, and management. *Global Spine J*. 2019; 9(6):658-665. doi: 10.1177/2192568218793617. Epub 2018 Aug 13. PMID: 31448201; PMCID: PMC6693071.

2) Walker PB, Sark C, Brennan G, Smith T, Sherman WF, Kaye AD. Spinal epidural lipomatosis: a comprehensive review. *Orthop Rev* (Pavia). 2021;13(2): 25571.doi: 10.52965/001c.25571. PMID: 34745483; PMCID: PMC8567763.

Figure 1. Sagittal T1 (A) and T2 (B) MRI of the lumbosacral spine demonstrate prominent epidural fat (arrow) surrounding the thecal sac and cauda equina and extending inferiorly beginning at approximately L3 level.

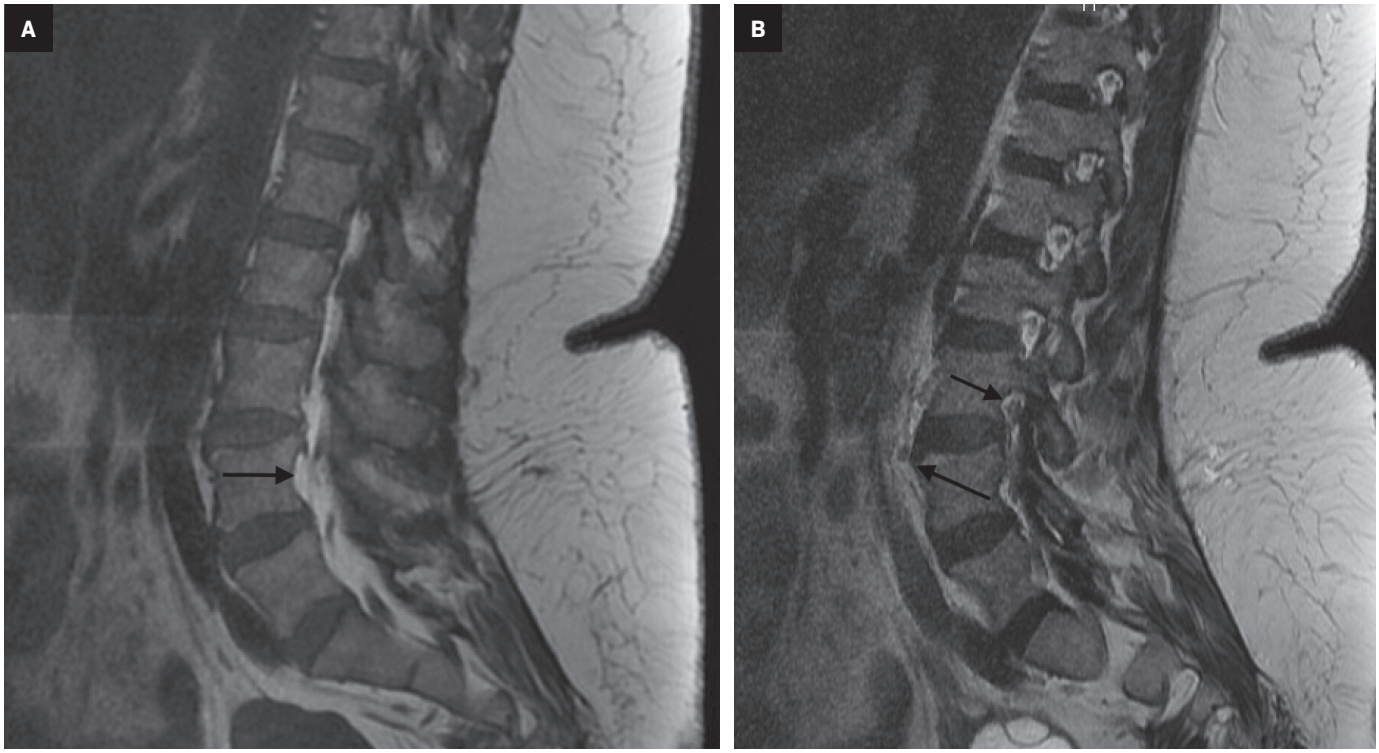

Figure 2. Axial T1 MRI at the L4-5 level demonstrates prominent fat in the epidural space surrounding the spinal column (arrow). There is resultant compression with polygonal deformation of the thecal sac, characteristic of this entity.

3) Lévy-Weil FE, Feldmann JL. Lipomatose épidurale [Epidural lipomatosis]. *Presse Med*. 2000; 29(9): 469-475. French. PMID: 10745936.

4) Borré DG, Borré GE, Aude F, Palmieri GN. Lumbosacral epidural lipomatosis: MRI grading. *Eur Radiol*. 2003; 13(7):1709-1721. doi: 10.1007/s00330-002-1716-4. Epub 2002 Dec 13. PMID: 12835988.

5) Koch CA, Doppman JL, Patronas NJ, Nieman LK, Chrousos GP. Do glucocorticoids cause spinal epidural lipomatosis? When endocrinology and spinal surgery meet. *Trends Endocrinol Metab*. 2000; 11(3):86-90. doi:10.1016/s1043-2760(00)00236-8. PMID: 10707048.

6) Kniprath K, Farooque M. Drastic weight reduction decrease in epidural fat and concomitant improvement of neurogenic claudicatory symptoms of spinal epidural lipomatosis. *Pain Med*. 2017;18(6):1204-1206. doi:10.1093/pm/pnw313. PMID: 28108643.

CT Suite | MR Suite | Injectors and Digital Solutions

SmartInject
SOLUTIONS FROM BRACCO

Point-of-care imaging solutions that help promote patient safety and streamline workflow

NEXO®
Contrast management system

Advance patient care with smart injectors and digital solutions from Bracco.

Learn more at **SmartInject.com**

Bracco Diagnostics Inc.
259 Prospect Plains Road, Building H
Monroe Township, NJ 08831 USA

Phone: 609-514-2200
Toll Free: 1-877-272-2269 (U.S. only)
Fax: 609-514-2446

BRACCO
LIFE FROM INSIDE

Committed to Science,
Committed to You.™